

**UNIVERSITY OF GAZİANTEP  
GRADUATE SCHOOL OF  
NATURAL & APPLIED SCIENCES**

**DEVELOPMENT OF NEURO-FUZZY  
MODELS FOR HOLE DRILLING ON  
TI-6AL-4V AND INCONEL 718 USING  
ELECTRICAL DISCHARGE MACHINING**

**M. Sc. THESIS  
IN  
MECHANICAL ENGINEERING**

**BY  
FATİH ALAN  
JANUARY 2011**

**Development of Neuro-Fuzzy Models for Hole  
Drilling on Ti-6Al-4V and Inconel 718 using  
Electrical Discharge Machining**

**M.Sc. Thesis  
in  
Mechanical Engineering  
University of Gaziantep**

**Supervisor  
Assist. Prof. Dr. A. Tolga BOZDANA**

**by  
Fatih ALAN  
January 2011**

T.C.  
UNIVERSITY OF GAZIANTEP  
GRADUATE SCHOOL OF NATURAL & APPLIED SCIENCES  
DEPARTMENT OF MECHANICAL ENGINEERING

**Name of the thesis:** Development of Neuro-Fuzzy Models for Hole Drilling on Ti-6Al-4V and Inconel 718 using Electrical Discharge Machining


**Name of the student:** Fatih ALAN

**Exam date:** January 25, 2011


Approval of the Graduate School of Natural and Applied Sciences

  
Prof. Dr. Ramazan KOÇ  
**Director**

I certify that this thesis satisfies all the requirements as a thesis for the degree of Master of Science.

  
Prof. Dr. L. Canan DÜLGER  
**Head of Department**

This is to certify that we have read this thesis and that in our opinion it is fully adequate, in scope and quality, as a thesis for the degree of Master of Science.

  
Assist. Prof. Dr. A. Tolga BOZDANA  
**Supervisor**

**Examining Committee Members**

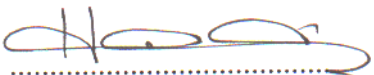
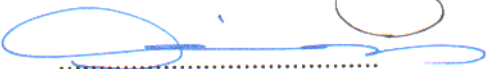
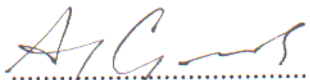


Prof. Dr. İ. Hüseyin FİLİZ

Prof. Dr. Ömer EYERCİOĞLU

Assoc. Prof. Dr. Abdulkadir ÇEVİK

Assist. Prof. Dr. A. Tolga BOZDANA

Assist. Prof. Dr. Oğuzhan YILMAZ

  
.....  
  
.....  
  
.....  
  
.....  
  
.....

# **ABSTRACT**

## **DEVELOPMENT OF NEURO-FUZZY MODELS FOR HOLE DRILLING ON TI-6AL-4V AND INCONEL 718 USING ELECTRICAL DISCHARGE MACHINING**

**ALAN, Fatih**

**M.Sc. in Mechanical Engineering**

**Supervisor: Assist. Prof. Dr. A. Tolga BOZDANA**

**January 2011, 86 Pages**

The aim of this study is to develop ANFIS models for prediction of input-output relationships in hole drilling EDM process. It is a nontraditional machining process preferred to produce holes on difficult-to-cut materials, particularly aerospace alloys, in a fast and accurate way with a good surface finish. There are many parameters in this process, and their effects on the process outputs are very complicated. It is usually not possible to define such complex relationships by means of conventional modeling techniques. Fuzzy logic and neural networks are intelligent modeling techniques to predict the response of a process in accordance with the given inputs.

For this purpose, an Adaptive Neuro-Fuzzy Inference System (ANFIS) has been implemented to develop neuro-fuzzy models. The experimental data were obtained by making several holes on specimens of Ti-6Al-4V and Inconel 718 using copper and brass electrodes ( $\varnothing 2$  mm) with input parameters of current, pulse-on and pulse-off times, and capacitance. The output parameters were material removal rate, electrode wear rate, and surface roughness. The comparison between experimental and ANFIS results reveal that developed models can predict the values of process outputs for given input parameters within the lowest error range.

**Key Words:** Hole Drilling EDM, Ti-6Al-4V, Inconel 718, ANFIS

## ÖZET

### **TI-6AL-4V VE INCONEL 718 MALZEMELERİNDE ELEKTRİKSEL EROZYON YÖNTEMİYLE DELİK DELME İŞLEMİ İÇİN SINIRSEL BULANIK MODELLER GELİŞTİRİLMESİ**

**ALAN, Fatih**

**Yüksek Lisans Tezi, Makine Mühendisliği Bölümü**

**Tez Yöneticisi: Yrd. Doç. Dr. A. Tolga BOZDANA**

**Ocak 2011, 86 Sayfa**

Bu çalışmada amaç, elektriksel erozyon prosesi ile delik delme işleminde girdi-çıkıtı parametre ilişkilerinin Adaptif Ağ Tabanlı Bulanık Mantık Çıkarım Sistemi (ANFIS) sayesinde belirlenmesidir. Bu proses; uzay ve havacılık malzemeleri gibi işlenmesi zor malzemelerde iyi yüzey kalitesine sahip deliklerin hızlı ve doğru şekilde delinebilmesi için kullanılır. Bu proste, girdi parametrelerinin (akım, vuru ve nefes alma süreleri, kapasitans) çıkıtı parametrelerine (iş parçası işleme hızı, elektrot aşınma hızı, yüzey pürüzlülüğü) etkisi oldukça karmaşıktır. Bu karmaşık ilişkileri geleneksel modelleme teknikleri ile ortaya koymak mümkün değildir. Yapay zeka teknikleri olarak bilinen bulanık mantık ve yapay sinir ağları kullanılarak belirli girdi parametrelerine göre çıkıtı parametrelerinin sonuçları tahmin edilebilmektedir.

Bu amaçla; Ti-6Al-4V ve Inconel 718 malzemelerinde 2mm çapında pirinç ve bakır elektrotlar kullanılarak farklı girdi parametreleri ile belirli sayıda delikler delinmiş ve çıkıtı parametreleri elde edilmiştir. Deneysel veriler doğrultusunda geliştirilen ANFIS modellerinin sonuçları gözönüne alındığında; bu modeller kullanılarak istenen girdi parametreleri için çıkıtı parametreleri en düşük hata oranı ile tahmin edilebilmektedir.

**Anahtar Kelimeler:** Elektriksel Erozyon Prosesi ile Delik Delme, Ti-6Al-4V, Inconel 718, ANFIS

## **ACKNOWLEDGMENT**

My sincere thanks go to my supervisor, Assist. Prof. Dr. A. Tolga BOZDANA, for his guidance throughout this study and his suggestions on the preparation of this manuscript.

The experimental data used in this study were taken from the research project (108M022) in University of Gaziantep that has been supported by Scientific and Technological Research Council of Turkey (TUBITAK). I would like to thank the principal investigator of this project, Assist. Prof. Dr. Oğuzhan YILMAZ, for his permission and help in use of this information.

I also wish to express my thanks to Assist. Prof. Dr. Necip Fazıl YILMAZ who has been supporting me throughout my educational background. I am very thankful to my valuable wife, Süheyla ALAN, for her support and motivation during the work.

Finally, many thanks to others I have overlooked here for their support and encouragement in every way. This study will provide remarkable benefits to my educational and professional life in the future.

# CONTENTS

<b>ABSTRACT .....</b>	<b>II</b>
<b>ÖZET .....</b>	<b>III</b>
<b>ACKNOWLEDGMENT .....</b>	<b>IV</b>
<b>CONTENTS .....</b>	<b>V</b>
<b>LIST OF FIGURES.....</b>	<b>VII</b>
<b>LIST OF TABLES.....</b>	<b>IX</b>
<b>CHAPTER 1: INTRODUCTION .....</b>	<b>1</b>
<b>CHAPTER 2: LITERATURE SURVEY .....</b>	<b>4</b>
2.1 INTRODUCTION .....	4
2.2 LITERATURE ON PROCESS MODELING AND PREDICTION.....	5
2.3 LITERATURE ON PROCESS CONTROL .....	6
2.4 LITERATURE ON PROCESS OPTIMIZATION .....	7
2.5 DISCUSSIONS AND SUMMARY .....	9
<b>CHAPTER 3: FUZZY LOGIC AND NEURO-FUZZY SYSTEMS.....</b>	<b>10</b>
3.1 INTRODUCTION .....	10
3.2 ARTIFICIAL INTELLIGENCE.....	10
3.3 THEORY OF FUZZY LOGIC .....	11
3.4 STRUCTURE OF FUZZY LOGIC.....	12
3.5 A FUZZY LOGIC APPLICATION – AIR CONDITIONER .....	13
3.5.1 Stage I: Fuzzification .....	13
3.5.2 Stage II: Rule Evaluation .....	16
3.5.3 Stage III: Fuzzy Inference and Aggregation of Rule Outputs .....	16
3.5.4 Stage IV: Defuzzification.....	18
3.6 ADVANTAGES AND DISADVANTAGES OF FUZZY LOGIC.....	19
3.7 ADAPTIVE NEURO-FUZZY INFERENCE SYSTEM (ANFIS) .....	21
3.8 SUMMARY.....	22
<b>CHAPTER 4: ELECTRICAL DISCHARGE MACHINING.....</b>	<b>23</b>
4.1 INTRODUCTION .....	23
4.2 ELECTRICAL DISCHARGE MACHINING (EDM) .....	24
4.3 HOLE DRILLING EDM PROCESS.....	25
4.4 PROCESS PARAMETERS .....	26
4.4.1 Controllable Parameters.....	26
4.4.2 Uncontrollable Parameters.....	28
4.4.3 Process Outputs.....	28
<b>CHAPTER 5: DEVELOPMENT OF ANFIS MODELS .....</b>	<b>29</b>
5.1 INTRODUCTION .....	29
5.2 EXPERIMENTAL WORK.....	29

5.2.1 Workpiece and Electrode Materials.....	29
5.2.2 Experimental Setup .....	30
5.2.3 Design of Experiments and Machining Conditions.....	33
5.2.4 Uncontrollable Parameters.....	35
5.2.5 Measurement of Output Parameters .....	36
5.3 DEVELOPMENT OF ANFIS MODELS .....	36
5.3.1 Step I: Loading Data Files into System.....	39
5.3.2 Step II: Generating FIS.....	40
5.3.3 Step III: Structure of FIS.....	42
5.3.4 Step IV: Training FIS.....	43
5.3.5 Step V: Checking (Validating) FIS.....	44
5.3.6 Structure and Properties of Developed Models .....	47
5.4 ANALYSIS OF MODELS FOR TRAINING RESULTS.....	49
5.5 ANALYSIS OF MODELS FOR CHECKING RESULTS.....	53
5.6 SUMMARY.....	56
<b>CHAPTER 6: DISCUSSION AND CONCLUSIONS.....</b>	<b>57</b>
6.1 DISCUSSIONS .....	57
6.2 CONCLUSIONS.....	58
6.3 FUTURE STUDIES .....	59
<b>REFERENCES .....</b>	<b>60</b>
<b>APPENDIX A: TRIALS FOR D2NIBR_MRR.....</b>	<b>65</b>
<b>APPENDIX B: TRIALS FOR D2NIBR_EWR.....</b>	<b>71</b>
<b>APPENDIX C: TRIALS FOR D2NIBR_SR.....</b>	<b>77</b>
<b>APPENDIX D: VALIDATION RESULTS FOR OTHER ANFIS MODELS .....</b>	<b>83</b>



## LIST OF FIGURES

Figure 2.1 Summary of related literature on use of AI techniques on EDM processes .....	4
Figure 3.1 Range of logical values in Boolean and fuzzy logic (Negnevitsky, 2005).....	12
Figure 3.2 Schematic view of Fuzzy Logic process (adapted from Jang, 1993) .....	12
Figure 3.3 Representation of crisp and fuzzy sets for variable X (Negnevitsky, 2005) .....	13
Figure 3.4 MFs in fuzzy logic (Fuzzy Logic Toolbox in Matlab) .....	14
Figure 3.5 Air-conditioner example: crisp vs. fuzzy sets for temperature .....	15
Figure 3.6 Air-conditioner example: crisp vs. fuzzy sets for fan speed.....	15
Figure 3.7 Air-conditioner example: determination of rule outputs in Mamdani-style .....	17
Figure 3.8 Air-conditioner example: aggregation of rule outputs in Mamdani-style .....	17
Figure 3.9 Air-conditioner example: determination of rule outputs in Sugeno-style .....	18
Figure 3.10 Air-conditioner example: defuzzification in Mamdani-style.....	19
Figure 3.11 Structure of ANFIS (adapted from Jang, 1993).....	21
Figure 4.1 Principle of sparking in EDM process (Jameson, 2001) .....	24
Figure 4.2 Hole drilling EDM process (adapted from Leao et al., 2005) .....	25
Figure 4.3 Peak current versus pulse-on and pulse-off times (Kumar et al., 2009).....	27
Figure 4.4 RC discharge pulse generation circuit (Jung et al., 2007) .....	27
Figure 5.1 Sketch of specimens and drilled holes.....	31
Figure 5.2 Specifications of JS AD-20 EDM machine .....	31
Figure 5.3 Components of JS AD-20 EDM machine .....	32
Figure 5.4 Close-up view of EDM process.....	32
Figure 5.5 Control panel of JS AD-20 EDM machine.....	33
Figure 5.6 Screenshot of ANFIS editor .....	37
Figure 5.7 The experimental data used for D2NiBr_MRR.....	39
Figure 5.8 Training and checking data loaded into the system.....	40
Figure 5.9 Specifying the properties of model using grid partitioning method .....	41
Figure 5.10 Structure of developed model.....	42
Figure 5.11 Training and checking of the model for MRR.....	43
Figure 5.12 Training error of the model for MRR .....	44
Figure 5.13 Checking error of the model for MRR .....	45
Figure 5.14 Training and checking of the model for EWR.....	46
Figure 5.15 Training and checking of the model for SR.....	47

Figure 5.16 Schematic view of structure of the model for MRR.....	48
Figure 5.17 Obtaining results using Rule Viewer.....	48
Figure 5.18 Experimental versus ANFIS results for training data of MRR.....	51
Figure 5.19 Experimental versus ANFIS results for training data of EWR.....	51
Figure 5.20 Experimental versus ANFIS results for training data of SR.....	51
Figure 5.21 Regression analysis for training data of MRR.....	52
Figure 5.22 Regression analysis for training data of EWR.....	52
Figure 5.23 Regression analysis for training data of SR.....	53
Figure 5.24 Experimental versus ANFIS results for checking data of MRR.....	54
Figure 5.25 Experimental versus ANFIS results for checking data of EWR.....	54
Figure 5.26 Experimental versus ANFIS results for checking data of SR.....	54
Figure 5.27 Regression analysis for checking data of MRR.....	55
Figure 5.28 Regression analysis for checking data of EWR.....	55
Figure 5.29 Regression analysis for checking data of SR.....	56

## LIST OF TABLES

Table 3.1 Air-conditioner example: fuzzy rules .....	16
Table 3.2 Layers in ANFIS structure .....	21
Table 4.1 Controllable and uncontrollable EDM parameters .....	26
Table 5.1 Chemical composition of Ti64 and IN718 (wt. %)... ..	30
Table 5.2 Material properties of tool electrodes .....	30
Table 5.3 Machine settings and the corresponding values of input parameters.....	34
Table 5.4 The experiments used for training data.....	34
Table 5.5 The experiments used for checking data.....	35
Table 5.6 The list of uncontrollable parameters.....	35
Table 5.7 Experimental data used for training the model D2NiBr .....	38
Table 5.8 Experimental data used for checking (validating) the model D2NiBr.....	38
Table 5.9 Repeatability errors in experimental data for D2NiBr .....	39
Table 5.10 The properties of developed models for D2NiBr.....	49
Table 5.11 Experimental versus ANFIS results for training data for D2NiBr.....	50
Table 5.12 Experimental versus ANFIS results for checking data for D2NiBr.....	53

# CHAPTER 1

## INTRODUCTION

Electrical Discharge Machining (EDM) is a nontraditional machining process for removal of metal that is associated with the erosive effects (Tsai and Wang, 2001). Such effects occur under a series of successive electrical sparks generating with the tool electrode and the workpiece. There is a small gap between tool and workpiece, and the process takes place in a dielectric fluid with constant electric field. The process is widely used for manufacturing tools, dies and other difficult-to-cut parts and materials in automotive, aerospace and medical applications. There are different type of EDM processes such as die-sinking EDM in which electrode is made with a desired shape of machining, Wire-cut EDM (WEDM) in which a continuous wire cuts the workpiece, and hole drilling EDM to produce small holes on the parts.

Hole drilling EDM process is a special type in which a rotating tubular electrode is used through which the dielectric fluid flows with a high pressure (Leao et al., 2005). This technique can be used for making holes in a fast and accurate way with a good surface finish. There are many controllable and uncontrollable parameters in hole drilling EDM process. The effects of these parameters on the process outputs are very complicated. The effect of a single parameter on an output parameter can be different than that of multiple parameters. Moreover, the effect of certain parameters may be significant while the effect of others may be negligible. As a result, it is usually not possible to define these complex relationships between input and output parameters by means of conventional modeling techniques.

In recent years, Artificial Intelligence (AI) techniques have been used to represent nonlinear and complicated modeling of manufacturing processes including EDM process. These techniques are imitating the abilities of humans and their way of

thinking, resulting in advanced modeling techniques (Bozdana, 1999). Among them, fuzzy logic is at the forefront in modeling the systems involving an input-output data set. Fuzzy logic can predict the response of a process or system in accordance with the given inputs. However, such models do not have the capability of tuning (i.e. the effectiveness of models cannot be improved with respect to the errors occurring due to inconsistent or imprecise data). Neural network has been adapted recently into fuzzy logic to obtain a hybrid modeling approach. This enables to construct neuro-fuzzy models that can learn from the known data sets so that the response of models for unknown data can be predicted. Despite of many research on the use of AI techniques for modeling, optimization and/or intelligent control of different manufacturing processes, neuro-fuzzy modeling of hole drilling EDM process is not existent in the related literature.

In this study, an Adaptive Neuro-Fuzzy Inference System (ANFIS) has been implemented for developing neuro-fuzzy models in order to predict the values of process outputs in hole drilling EDM process for the given input parameters. The input parameters were Current (I), Pulse-on Time ( $t_{on}$ ), Pulse-off Time ( $t_{off}$ ), and Capacitance (C). Accordingly, Material Removal Rate (MRR), Electrode Wear Rate (EWR), and Surface Roughness (SR) were process outputs. The experimental data used in this study was taken from a research project recently completed in University of Gaziantep, Turkey (Yılmaz et al. 2010). This was done by producing several holes on specimens made of two aerospace alloys (Ti-6Al-4V and Inconel 718) using copper and brass electrodes having diameter of  $\text{Ø}2$  mm. The number experiments as well as the values of input parameters in such experiments were specified using Central Composite Design (CCD) technique. The corresponding values of process outputs were measured and/or calculated accordingly. In addition to the data used in developing the models, additional holes with completely different input values were also produced to validate the efficiency and reliability of models.

The related literature on the use of AI techniques for modeling EDM processes are summarized in Chapter 2 with particular applications of fuzzy logic and neural networks. Chapter 3 presents the theory of fuzzy logic and a brief description of ANFIS method. The structure of fuzzy logic is explained in detail on a case study, and is compared with the structure of ANFIS. Chapter 4 introduces the principle of

hole drilling EDM process with brief description of controllable and uncontrollable parameters. The experimental work and Design of Experiments (DOE) for obtaining experimental data are included in Chapter 5. The procedure for developing neuro-fuzzy models using ANFIS is explained in detail on a case study with a selected data set. The predicted results obtained from developed models are also discussed and compared with the experimental results. Finally, the concluding remarks and highlights of this study as well as the suggestions for potential future works are given in Chapter 6. The details of several trials with different modeling options as well as the properties of all developed models with the results of their validation are also reported in Appendices.

# CHAPTER 2

## LITERATURE SURVEY

### 2.1 Introduction

Artificial intelligence techniques such as Fuzzy Logic (FL), Artificial Neural Networks (ANNs), Genetic Algorithms (GAs), and so on have been applied by many researches to modeling for prediction, control and optimization of die-sinking EDM, WEDM and hole drilling EDM processes. In addition to these techniques, other advanced methods (for instance Taguchi and Grey Fuzzy Logic) have also been implemented. Besides, hybrid approaches with the use of multiple techniques have been found in the literature for significant applications. This chapter presents a comprehensive literature survey on the use of such techniques on different type of EDM processes. The summary of related literature is given in Fig. 2.1. The details of research works are reported in the following sections.

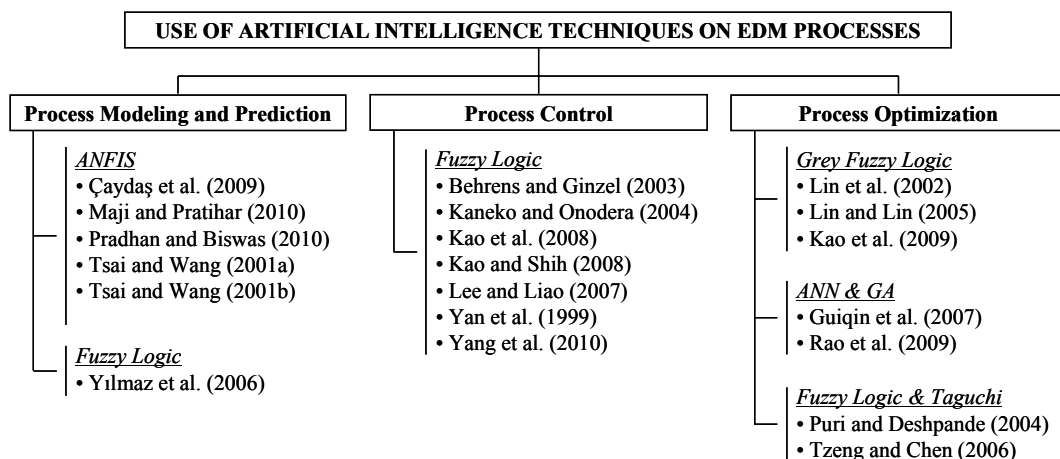


Figure 2.1 Summary of related literature on use of AI techniques on EDM processes

## 2.2 Literature on Process Modeling and Prediction

Çaydaş et al. (2009) have developed an adaptive neuro-fuzzy inference system (ANFIS) model for WEDM process. In this study, 24 experiments were performed on AISI D5 tool steel using Ø0.25 mm CuZn37 brass wire electrode with tap water as dielectric fluid. Then, the effect of input parameters (pulse duration, open circuit voltage, wire speed and dielectric flushing) on WEDM outputs (surface roughness and white layer thickness) were modeled.

Maji and Pratihari (2010) have focused on forward and reverse mappings of die-sinking EDM process using ANFIS. In this study, mild steel workpiece (diameter of Ø30 mm and thickness of 6 mm) and copper electrode together with dielectric fluid of paraffin oil were used. The relationships between input parameters (peak current, pulse-on time, pulse-duty factor) and output parameters (MRR, SR) have been determined by means of regression analysis. ANFIS models using triangular and bell-shape membership functions were then developed and the results from these models were compared.

Neuro-fuzzy and neural network-based prediction in die-sinking EDM process of AISI D2 steel was performed by Pradhan and Biswas (2010). The experiments were done with copper tool electrode using commercial grade EDM oil. ANOVA analyses were done based on input (discharge current, pulse duration, duty cycle, voltage) and output (MRR, tool wear rate, radial overcut) parameters. According to the results of such analyses, the models for outputs were developed based on ANN as well as Mamdani and Sugeno type neuro-fuzzy inference systems.

Predictions on surface finish of aluminum and iron parts after die-sinking EDM process have been done by Tsai and Wang (2001a) based upon several neural network models including ANFIS. The experimental data were obtained by using copper electrode and SPE oil on a CNC EDM machine. ANFIS models were trained and validated by means of a number of experiments. Then, the surface roughness results of models were evaluated. The same methodology has also been applied by the authors in order to obtain the predictions on MRR (Tsai and Wang, 2001b).



Yılmaz et al. (2006) have developed a user-friendly fuzzy-based system for the selection of die-sinking EDM process parameters. AISI 4340 tool steel was machined using copper electrode ( $\text{\O}8$  mm) with dielectric fluid of kerosene. In this study, input parameters were discharge current, pulse duration and pulse interval whereas MRR, EWR and SR were output parameters.

### **2.3 Literature on Process Control**

Behrens and Ginzel (2003) presented a control system for die-sinking EDM process consisting of a fuzzy gap-width controller adapted by a neural network. The parts made of 56NiCrMoV7 steel were machined using electrolytic copper electrodes having different tip shapes. Experimental results showed the working efficiency of developed neuro-fuzzy system.

Kaneko and Onodera (2004) have studied the improvement of machining performance of die-sinking EDM process using self-adjusting fuzzy control. The system has been implemented on steel workpiece using cylindrical copper electrode with diameter of  $\text{\O}4$  mm. Remarkable improvements in machining speed and maximum depth of cut were achieved by use of a simplified fuzzy inference with only two input signals (i.e. a frequency of short circuit and a frequency of arcing).

Micro-hole EDM system with adaptive fuzzy logic control has been developed by Kao et al. (2008). For fuzzy-logic control, a high-speed monitoring system was implemented to measure gap voltage, current, and ignition delay time to derive input parameters of average gap voltage, deviation in spark ratio, and change in the deviation in spark ratio during machining of AISI 1010 steel. Effects of single and multiple input parameters on the performance and speed of drilling process were experimentally studied. The results showed that the fuzzy-logic control system yields more stable and efficient process. In other study of authors (Kao and Shih, 2008), the design and tuning of a three-input fuzzy logic controller for EDM of diesel injector spray holes were presented. The input parameters were selected as gap voltage, spark ratio, and change of spark ratio for drilling hardened AISI 52100 steel workpiece at different thicknesses using  $\text{\O}75$   $\mu\text{m}$  and  $\text{\O}150$   $\mu\text{m}$  wire electrodes. The tuned fuzzy logic controller is comparable with the gain scheduling controller in drilling time and

demonstrates its advantages on different EDM drilling configurations, including deep-hole and small-diameter micro-hole drilling.

An adaptive self-tuning fuzzy-logic control of WEDM process with grey prediction was accomplished by Lee and Liao (2007). For this purpose, experiments on SKD11 alloy steel using brass wire electrode ( $\text{\O}0.25$  mm) were conducted with process parameters of pulse-on and pulse-off time, arc-on and arc-off time, wire speed and tension, flushing pressure, and voltage. Their effect on SR was measured via RS485 card connection.

The design of a fuzzy controller for servo feed control in WEDM was presented by Yan et al. (1999) from the viewpoint of industrial application and implementation. The proposed controller contains two control loops: the main loop employs fuzzy logic as a rule-based control strategy for the gap voltage control whereas a secondary loop is used to maintain machining stability by adjusting the reference voltage. The developed control system was tested on SKD11 tool steel using brass wire ( $\text{\O}0.25$  mm) under the conditions of approach machining, rough machining, and cutting a part with a corner working path. Experimental results showed that the developed fuzzy controller was more feasible and effective than a proportional controller.

Yang et al. (2010) recently proposed a discharge state detection method in micro-hole EDM process based on fuzzy control technique using Matlab. Based on the rules that were obtained using different levels of voltage and current, a number of experiments were performed on copper workpiece with 300  $\mu\text{m}$  thick using brass electrodes of  $\text{\O}200$   $\mu\text{m}$  in the environment of kerosene dielectric fluid. Compared with the traditional detection methods, the proposed method gained better results by using the discharge state of fuzzy controller, and significantly shortens the machining time and improves the machining efficiency.

## **2.4 Literature on Process Optimization**

Grey fuzzy logic has recently been used for process optimization. The outputs of hole drilling EDM process were optimized by Lin et al. (2002) and Lin and Lin (2005) based on Grey FL technique. The input parameters were pulse on time, duty

factor and discharge current while MRR, EWR and SR were taken as output parameters. A number of holes were drilled using cylindrical copper electrode ( $\text{\O}8$  mm) with dielectric fluid of kerosene on SKD11 alloy steel.

Kao et al. (2009) have also studied the optimization of hole drilling EDM parameters on machining of Ti-6Al-4V with multiple quality characteristics. Electrolytic copper electrode with  $\text{\O}10$  mm was used to drill several holes of different input parameters, and kerosene was used as dielectric fluid. Grey fuzzy logic approach has been applied with input parameters of discharge current, open voltage, pulse duration and duty factor. The output parameters were MRR, EWR and SR.

The use of ANN and GA were also found in the literature. Guiqin et al. (2007) have studied neuro-fuzzy modeling and genetic optimization of WEDM process. Several experiments using input parameters of workpiece thickness pulse-on time, peak and mean current were conducted, and the output parameters of MRR and SR were predicted. Rao et al. (2009) have developed a hybrid model to optimize the surface roughness in die-sinking EDM process using neural networks and genetic algorithm. Four types of workpiece materials (i.e. Ti-6Al-4V, HE15, 15CVD6, M-250) were machined using copper electrode and kerosene dielectric fluid. A number of experiments were done by using input factors (current, voltage, and machining time) in order to predict SR.

Taguchi optimization of EDM processes were also integrated with fuzzy logic approach. Multiple quality characteristics of WEDM process has been optimized by Puri and Deshpande (2004) based on fuzzy logic and Taguchi techniques. High-Carbon-High-Chromium (HCHC) die steel plate ( $\text{\O}30$  mm) has been machined using cylindrical hard copper wire ( $\text{\O}0.25$  mm) in dielectric fluid of tap water. Several experiments have been done with input parameters (gap voltage and current, wire feed, and duty factor) and output parameters (MRR and SR). Tzeng and Chen (2006) have also studied multi-objective optimization of die-sinking EDM process using a taguchi fuzzy-based approach. SKD11 tool steel and electrolytic copper was selected as workpiece and electrode materials while dielectric fluid was kerosene. The effects of pulse time, duty cycle, and peak current have been predicted on MRR and SR.

## **2.5 Discussions and Summary**

As reported in the previous sections of this chapter, there are a number of applications of AI techniques on the prediction of relationships between process parameters and outputs of process as well as intelligent control and optimization of process outputs. Beside the use of a single technique, hybrid approaches with use of multiple techniques have also been implemented.

On the other hand, although some applications of AI methods on EDM processes exist in the literature, the modeling of hole drilling EDM process for machining of aerospace alloys (Ti-6Al-4V and Inconel 718) with implementation of ANFIS technique have not been conducted in the related literature. This is a key gap from the viewpoint of research and industrial applications for predicting the response of process (i.e. the values of process outputs) in accordance with the desired values of certain input parameters. Therefore, neuro-fuzzy models have been developed in this study in order to define the input-output relationships in hole drilling EDM process for the case of drilling aerospace alloys under different machining conditions.

## **CHAPTER 3**

### **FUZZY LOGIC and NEURO-FUZZY SYSTEMS**

#### **3.1 Introduction**

This chapter presents ANFIS systems which integrate neural networks into fuzzy logic technique. The structure of fuzzy logic, which is the core of ANFIS, is described in detail by presenting an industrial example of air conditioner. The methodology used in ANFIS is also described followed by fuzzy logic.

#### **3.2 Artificial Intelligence**

Artificial Intelligence (AI) is the science and engineering of making intelligent machines, especially intelligent computer programs. It is related to the similar task of using computers to understand human intelligence. In other words, it is a tool used in intelligent manufacturing associated with human behavior. The aim of implementing AI is to simulate human behavior on computers such as learning, reasoning, complex problem solving, thinking and understanding, etc. (Bozdana, 1999). In recent years, AI tools have been designed and used for capturing, representing, organizing and utilizing knowledge by computers. There are several AI techniques with applications in different engineering fields such as Expert Systems (ESs), Artificial Neural Networks (ANNs), Genetic Algorithm (GA), Fuzzy Logic (FL).

ES is an intelligent computer program that uses knowledge techniques to solve problems that are difficult enough, requiring significant human expertise for their solution. Unlike conventional programs, ESs can explain their actions, justify their conclusions and provide end users with details of the knowledge they contain. They are widely used in design, process planning and scheduling, material handling, quality

control, machine diagnosis, machine layout, and so on. ANN is a hardware or software that attempts to emulate the processing patterns of the biological brain. These systems are capable of high-level functions, such as adaptation or learning, and lower level functions such as data pre-processing for different kinds of inputs. There are numerous applications of ANNs in data analysis, pattern recognition and control. GAs are search algorithms based on the mechanics of neural selection and genetics. They are one of the best ways to solve a problem for which limited knowledge is available. Many of the real world problems involved finding optimal parameters would be ideal for GAs.

### **3.3 Theory of Fuzzy Logic**

Fuzzy logic is a powerful problem-solving methodology with many applications in embedded control and information processing. This technique provides a simple way to reach definite conclusions from vague, ambiguous or imprecise information. In a sense, fuzzy logic resembles human decision making with its ability to work from approximate data and find precise solutions. Classical logic requires a deep understanding of a system, exact equations, and precise numeric values. On the other hand, fuzzy logic incorporates an alternative way of thinking, which allows modeling complex systems using a higher level of abstraction originating from our knowledge and experience. Fuzzy logic allows expressing this knowledge with subjective concepts (such as *very hot*, *bright red*, *long time*, etc.) which is mapped into exact numeric ranges.

As an extension of classical set theory, the theory of fuzzy logic was first presented in 1965 by Prof. Lotfi Zadeh at University of California in Berkley (Zadeh, 1965). He defined the fuzzy logic as a set of mathematical principles for knowledge representation based on degrees of membership rather than on crisp membership of classical binary logic. As given in Fig. 3.1, unlike two-valued Boolean logic (i.e. either 0 or 1), fuzzy logic is multi-valued (i.e. a value between 0 and 1). Fuzzy logic deals with degrees of membership and degrees of truth. In other words, it uses the continuum of logical values between 0 (completely false) and 1 (completely true). Therefore, instead of just black and white, fuzzy logic employs the spectrum of colors, accepting that things can be partly true and partly false at the same time.

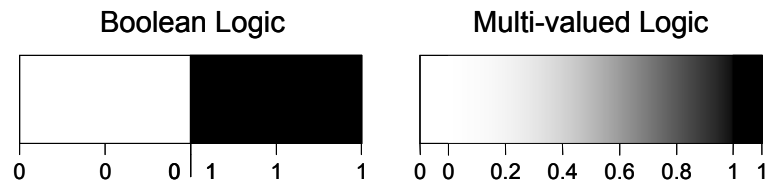


Figure 3.1 Range of logical values in Boolean and fuzzy logic (Negnevitsky, 2005)

Fuzzy logic has been applied into many different fields by engineers, philosophers, psychologists, and sociologists. In recent years, it has widely been used in parameter selection, modeling and control of manufacturing processes and machine elements, electronic and mechatronic systems, automobile and aerospace industries, and so on. Exclusive applications of fuzzy logic can be found in elevator control, handheld computers, TV and sound systems, washing machines, air-conditioners, vacuum cleaners, antilock braking system (ABS) in vehicles, subway train systems, etc.

### 3.4 Structure of Fuzzy Logic

The structure of fuzzy logic is illustrated in Fig. 3.2. The first stage is fuzzification of crisp values of input parameters into fuzzified values (i.e. fuzzy inputs). The fuzzy inputs are then implemented in a fuzzy inference engine working together with IF-THEN type of fuzzy rules to obtain fuzzified values of output parameters. Finally, the fuzzified values of output parameters are defuzzified into crisp output values. Each stage is described in the following sections.

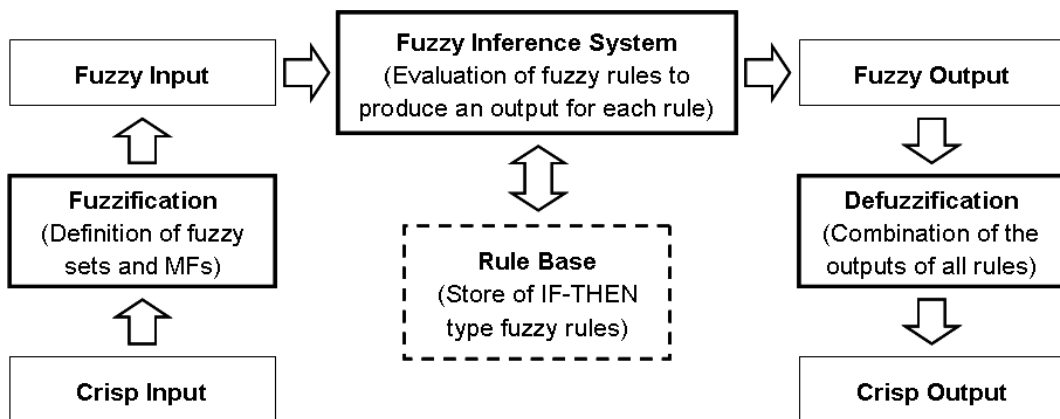


Figure 3.2 Schematic view of Fuzzy Logic process (adapted from Jang, 1993)

### 3.5 A Fuzzy Logic Application – Air Conditioner

In this section, the methodology of fuzzy logic is explained in detail on an example application of air conditioner. Air conditioner is used for controlling temperature and humidity of an enclosed space. It has a fan which blows/cool/circulates fresh air and has a cooler under thermostatic control. Generally, the amount of air being compressed is proportional to the ambient temperature. Consider that the range (i.e. domain) of input parameter (i.e. temperature) is between 0 and 30 °C whereas the range of output parameter (i.e. fan speed) varies from 0 to 100 rpm.

#### 3.5.1 Stage I: Fuzzification

At this stage, the fuzzy sets are defined and the degrees of membership for crisp inputs in appropriate fuzzy sets are determined. Crisp and fuzzy sets are presented in Fig. 3.3. Crisp sets can be fuzzified according to the requirements of tolerance.

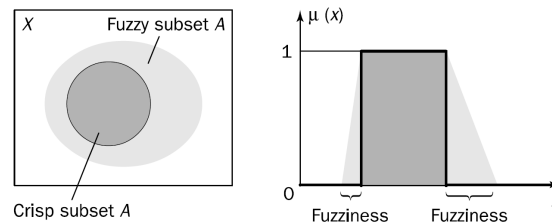


Figure 3.3 Representation of crisp and fuzzy sets for variable  $X$  (Negnevitsky, 2005)

Membership function is the mathematical representation of degree of membership for a variable in a fuzzy set. Membership functions characterize the fuzziness of variables in a fuzzy set. There are 11 different types of membership functions in fuzzy logic (Fig. 3.4). All membership functions have the letters *mf* at the end of their names. The simplest membership functions (*trimf* and *trapmf*) are formed using straight lines. Triangular function (*trimf*) consists of three points forming a triangle. Trapezoidal function (*trapmf*) is a truncated triangle curve with a flat top. These two functions have the advantage of simplicity.

Some membership functions are built on the Gaussian distribution curve: a simple Gaussian curve (*gaussmf*) and a two-sided composite of two different Gaussian curves (*gauss2mf*). Generalized bell membership function (*gbellmf*) has one more



parameter than *gaussmf* so that it can approach a non-fuzzy set if the free parameter is tuned. Both *gaussmf* and *gbellmf* functions have the advantage of being smooth and nonzero at all points. However, these functions are unable to specify asymmetric membership functions which may be required in certain applications.

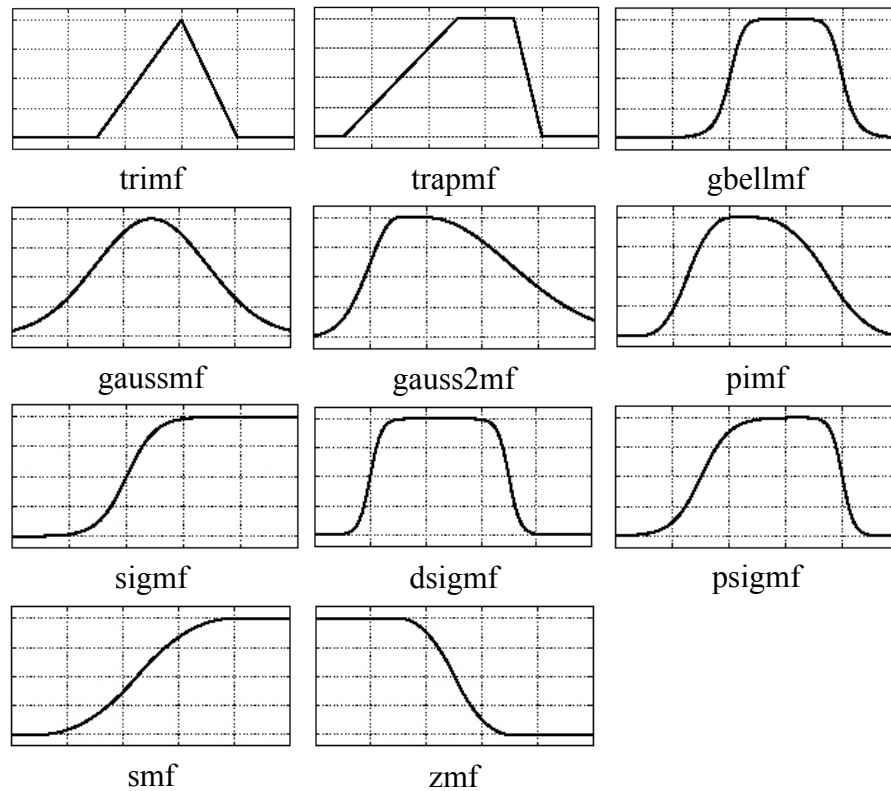


Figure 3.4 MFs in fuzzy logic (Fuzzy Logic Toolbox in Matlab)

There is also sigmoidal membership function (*sigmf*) that is either open left or open right. Asymmetric and closed *sigmf* functions can be synthesized the difference between two *sigmf* functions (*dsigmf*) or the product of two *sigmf* functions (*psigmf*). Polynomial based curves are named according to their shape. Z-shape function (*zmf*) is the asymmetrical polynomial curve open to the left, S-shape function (*smf*) is the mirror-image function that opens to the right, and P-shape function (*pimf*) is zero on both extremes with a rise in the middle.

Fuzzy set allows a continuum of possible choices. The *degree of membership* (also called membership value) of an element in a fuzzy set is represented by a value between 0 and 1. In our case, five control switches for temperature (i.e. COLD, COOL, PLEASANT, WARM, and HOT) and five corresponding speed settings (i.e.

MINIMAL, SLOW, MEDIUM, FAST, and BLAST) can be used. Fig. 3.5 and 3.6 show the crisp sets versus fuzzy sets defined for temperature and fan speed. The triangular membership function (*trimf*) is selected as an example.

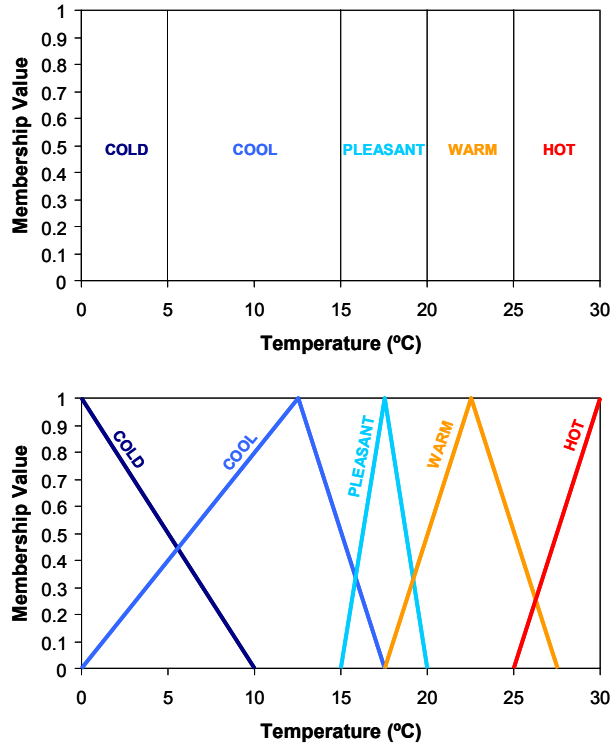


Figure 3.5 Air-conditioner example: crisp vs. fuzzy sets for temperature

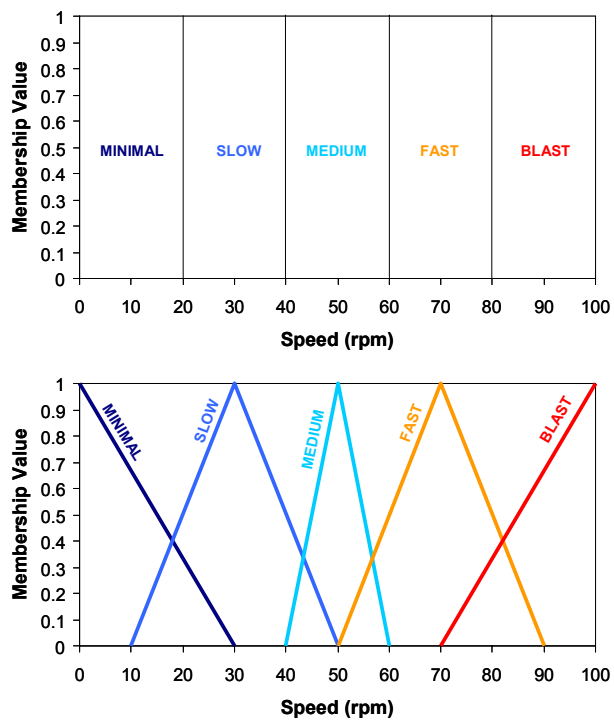


Figure 3.6 Air-conditioner example: crisp vs. fuzzy sets for fan speed

For instance, temperature of 16 °C in Fig. 3.5 belongs to crisp set of *pleasant* with a membership value of 1.0. On the other hand, it is a member of *cool* fuzzy set with a degree of membership of 0.3, and at the same time, it is also a member of *pleasant* fuzzy set with a degree of 0.4.

### 3.5.2 Stage II: Rule Evaluation

The fuzzy rules for this application are defined as given in Table 3.1. In fuzzy rules, both *antecedent* (i.e. IF part) and *consequent* (i.e. THEN part) are linguistic variables. In other words, the values of variables are expressed in linguistic form. However, the variables have numerical values in case of classical type of rules (e.g. Rule 1 in classical form: IF Temperature is < 5 °C THEN Speed is MINIMAL).

*Table 3.1 Air-conditioner example: fuzzy rules*

<i>Rule 1 :</i>	IF Temperature is COLD	THEN Speed is MINIMAL
<i>Rule 2 :</i>	IF Temperature is COOL	THEN Speed is SLOW
<i>Rule 3 :</i>	IF Temperature is PLEASANT	THEN Speed is MEDIUM
<i>Rule 4 :</i>	IF Temperature is WARM	THEN Speed is FAST
<i>Rule 5 :</i>	IF Temperature is HOT	THEN Speed is BLAST

### 3.5.3 Stage III: Fuzzy Inference and Aggregation of Rule Outputs

There are two common inference methods in fuzzy logic: Mamdani and Sugeno. The most commonly used technique is Mamdani method. In 1975, Professor Ebrahim Mamdani of London University built one of the first fuzzy systems to control a steam engine and boiler combination (Mamdani and Assilian, 1975). Mamdani inference requires finding the centroid of a two-dimensional shape by integrating across a continuously varying function. In general, this process is not computationally efficient. Instead of this approach, a single spike (i.e. a *singleton*) can be used as the membership function of the rule consequent. This method was first introduced by Michio Sugeno in 1985 (Sugeno, 1985). Singleton is a fuzzy set with a membership function that is unity at a single particular point on the domain and zero elsewhere.

As mentioned in Section 3.5.1, the related fuzzy sets for 16 °C are *cool* and *pleasant*. At the inference stage, *Rule 2* and *Rule 3* are fired as seen from Table 3.1. Hence, the

affected fuzzy sets for output variable (i.e. fan speed) are *slow* and *medium*. Fig. 3.7 shows the Mamdani-style inference process. Mamdani-style inference deals with the area of fuzzy sets, and hence the areas shaded in Fig. 3.7 are taken into consideration according to the membership values (i.e. 0.3 for *cool* fuzzy set, and 0.4 for *pleasant* fuzzy set) obtained from firing *Rule 2* and *Rule 3*. The corresponding areas in output fuzzy sets (namely *slow* and *medium* sets in fan speed) are determined based on the same membership values.

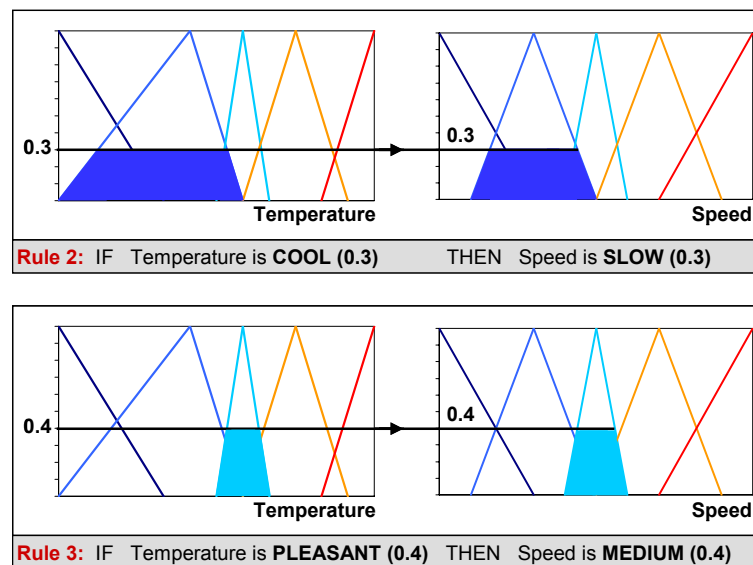


Figure 3.7 Air-conditioner example: determination of rule outputs in Mamdani-style

The next step is aggregation of the rule outputs (i.e. composition). Aggregation is the process of unification of the outputs of all rules. Fig. 3.8 shows the methodology of aggregation of rule outputs according to Mamdani-style inference. The areas from *slow* and *medium* fuzzy sets are composed (i.e. unified). In other words, the membership functions of all rule consequents are combined into a single fuzzy set.

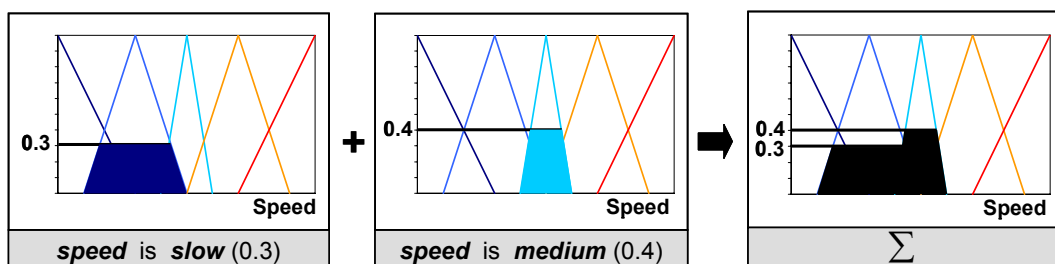


Figure 3.8 Air-conditioner example: aggregation of rule outputs in Mamdani-style

In contrast to Mamdani-style, Sugeno uses singleton fuzzy sets. This means that, instead of dealing with “area” as in case of Mamdani-style, “single crisp values” of outputs are calculated in consequent (i.e. THEN part of fuzzy rules) membership functions in Sugeno-style inference. Fig. 3.9 shows the Sugeno-style inference process. The output values are determined from each membership value of output fuzzy sets (i.e. 0.3 for *slow* fuzzy set, and 0.4 for *medium* fuzzy set) obtained from firing *Rule 2* and *Rule 3*. As a coincidence for this example, the crisp outputs from each rule are identical values (i.e. 44 rpm).

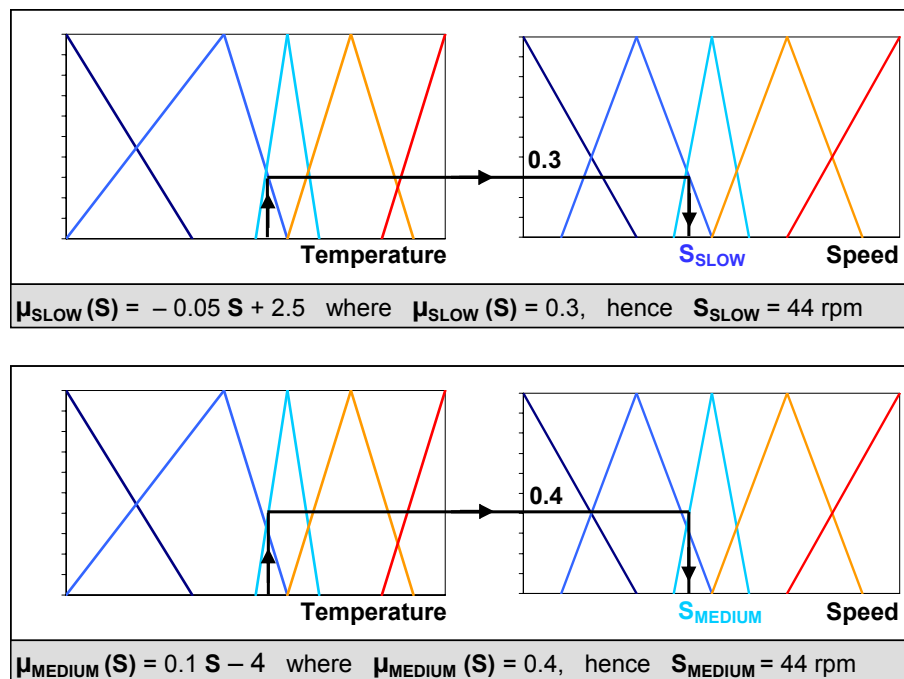


Figure 3.9 Air-conditioner example: determination of rule outputs in Sugeno-style

### 3.5.4 Stage IV: Defuzzification

The last stage is defuzzification. Fuzzification helps to evaluate the rules, but the final output of a fuzzy system has to be a crisp number. Therefore, in contrast to fuzzification, the fuzzy output is required to be converted into a crisp output. There are several defuzzification methods (Ross, 2009), but probably the most popular one is the centroid technique that is commonly used in Mamdani-style. This technique finds the centre of gravity (COG) of the unified area obtained in stage III. Fig. 3.10 shows the defuzzification (i.e. obtaining the crisp output value) by COG method.

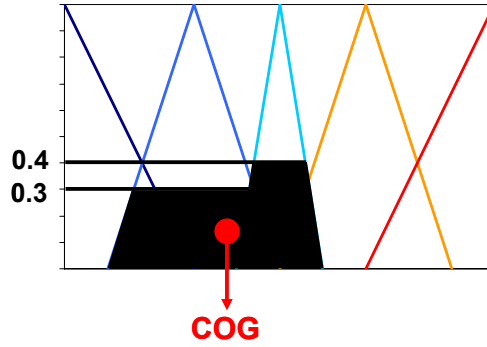


Figure 3.10 Air-conditioner example: defuzzification in Mamdani-style

Thus, the resulting crisp value for fan speed based on Mamdani-style inference is calculated as given in Eq. 3.1. The composition and defuzzification using Sugano-style inference gives a crisp value of speed as given in Eq. 3.2.

$$S = \frac{0.125(12.5) + 0.25(15) + 0.3(17.5 + 20 + \dots + 42.5) + 0.4(45 + 47.5 + \dots + 55) + 0.25(57.5)}{0.125 + 0.25 + 0.3(11) + 0.4(5) + 0.25} = 45.54 \text{ rpm} \quad \text{Eq. 3.1}$$

$$S = \frac{0.3(44) + 0.4(44)}{0.3 + 0.4} = 44 \text{ prm} \quad \text{Eq. 3.2}$$

As seen from results, the value of fan speed for 16 °C was found to be 45.54 rpm according to Mamdani-style inference. However, Sugeno-style inference determined the speed value as 44 rpm. The question may arise here that which technique should be used? Sugeno method is computationally effective and works well with optimization and adaptive techniques, which makes it very attractive in control problems, particularly for dynamic nonlinear systems. Therefore, Sugeno-style inference should be preferred in case of our example.

### 3.6 Advantages and Disadvantages of Fuzzy Logic

Here is a list of significant features of fuzzy logic (Fuzzy Logic Toolbox in Matlab):

- Fuzzy logic is conceptually easy to understand. The mathematical concepts behind fuzzy reasoning are very simple. Fuzzy logic is a more intuitive approach without high levels of complexity.
- Fuzzy logic is flexible. With any given system, it is easy to build-up more functionality without starting again from scratch.

- Fuzzy logic is tolerant of imprecise data. Everything is imprecise if you look closely enough, but more than that, most things are imprecise even on careful inspection. Fuzzy reasoning builds this understanding into the process.
- Fuzzy logic can model nonlinear functions of arbitrary complexity. A fuzzy system can be constructed to match any set of input-output data. This is made particularly easy by adaptive techniques like Adaptive Neuro-Fuzzy Inference Systems (ANFIS).
- Fuzzy logic can be built on top of the experience of experts. In contrast to complex and difficult-to-understand models developed by neural networks, fuzzy logic relies on the experience of people who already understand the system or problem.
- Fuzzy logic can be blended with conventional control techniques. Fuzzy systems do not necessarily replace conventional control methods. In many cases, fuzzy systems improve and simplify their implementation.
- Fuzzy logic is based on natural language. The basis for fuzzy logic is the basis for human communication. This observation supports many of other statements about fuzzy logic. Fuzzy logic is easy to use since it is built on the structures of qualitative description used in everyday language.

Despite these advantages of fuzzy logic over conventional techniques, there are some disadvantages of this technique as below:

- Fuzzy logic is not a cure-all. Fuzzy logic is a convenient way to map an input space to an output space. If a simpler solution already exists, that should be used.
- Fuzzy logic is the codification of common sense. For instance, many controllers do a fine job without using fuzzy logic.

As a conclusion, fuzzy logic can be a very powerful tool for dealing efficiently with imprecision and nonlinearity. This technique has been used in many applications as mentioned previously. In recent years, fuzzy logic has been used in combination with other AI techniques so that the disadvantages of these techniques can be eliminated. Hybrid systems with use of multiple AI techniques provide significant performance and efficiency in several engineering applications such as parameter selection, optimization, control, inspection, and so on. ANFIS is one of such systems in which neural networks is adapted into fuzzy logic, as explained in the following sections.

### 3.7 Adaptive Neuro-Fuzzy Inference System (ANFIS)

The acronym ANFIS derives its name from *adaptive neuro-fuzzy inference system*. Using a given input/output data set, ANFIS constructs a fuzzy inference system (FIS) whose membership function parameters are tuned (adjusted) using either a back propagation algorithm only or in combination with a least squares type of method. The structure of ANFIS is presented in Fig. 3.11, which is similar to that of fuzzy logic. Basically, six layers (Table 3.2) are used to construct ANFIS models. The function of each layer is very similar to that of each stage followed in fuzzy logic as described in the previous sections.

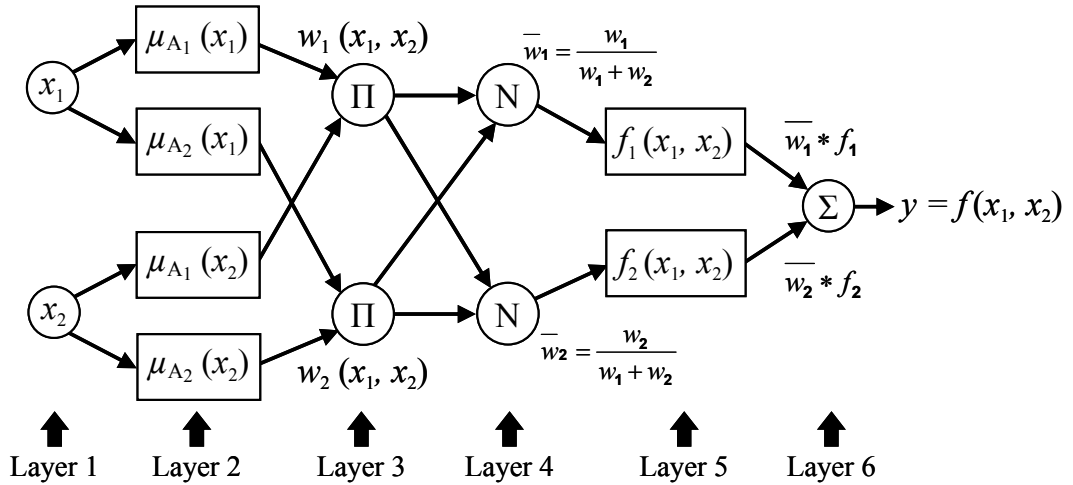


Figure 3.11 Structure of ANFIS (adapted from Jang, 1993)

Table 3.2 Layers in ANFIS structure

---

<i>Layer 1:</i> input layer that includes the input parameters ( $x_1$ and $x_2$ ).
<i>Layer 2:</i> fuzzification layer where type and number of the membership functions for input parameters ( $\mu_{A_1}$ and $\mu_{A_2}$ ) are specified.
<i>Layer 3:</i> rule layer that involves fuzzy rules ( $w_1$ and $w_2$ ) generated from the relationships between functions given in Layer 2.
<i>Layer 4:</i> normalization layer that normalizes values ( $\bar{w}_1$ and $\bar{w}_2$ ) obtained from each node in Layer 3.
<i>Layer 5:</i> defuzzification layer where the weighted output value from each rule, i.e. $y_1 = f_1(x_1, x_2)$ and $y_2 = f_2(x_1, x_2)$ , is calculated.
<i>Layer 6:</i> output layer that calculates the overall value for output parameter, i.e. $y = f(x_1, x_2)$ . There is only one node here into which the weighted values from all nodes in Layer 5 are added.

---



### **3.8 Summary**

The integration of neural networks into fuzzy logic allows the fuzzy systems to learn from the data that they are modeling. Such framework makes the ANFIS modeling more systematic and less reliant on expert knowledge. The methodology in development of ANFIS models are explained step-by-step in Chapter 5. *ANFIS editor* included within *Fuzzy Logic Toolbox in Matlab* has been used to develop models. Once the models were developed, they were trained and validated using experimental data. After that, the predicted results were obtained via *fuzzy logic rule viewer*, and they were compared with experimental results.

## CHAPTER 4

# ELECTRICAL DISCHARGE MACHINING

### 4.1 Introduction

The origin of EDM dates back to 1770 when English scientist Joseph Priestly discovered the erosive effect of electrical discharges. During 1930s, attempts were made for the first time to machine metals and diamonds with electrical discharges. Erosion was caused by intermittent arc discharges occurring in air between electrode and workpiece connected to a DC power supply. These processes were not very precise due to overheating of machining area and may be defined as *arc machining* rather than *spark machining* (Ho and Newman, 2003).

Pioneering work on electrical discharge machining was carried out in 1943 during World War II by two Russian scientists, B.R. and N.I. Lazarenko at the Moscow University (Lazarenko, 1943). The destructive effect of an electrical discharge was channelized, and a controlled process for machining materials was developed. RC (resistance–capacitance) relaxation circuit was introduced in 1950s, which provided the first consistent dependable control of pulse times and also a simple servo control circuit to automatically find and hold a given gap between electrode and workpiece.

In recent years, due to its unique features over traditional techniques, EDM process has been used in many applications, particularly for machining the difficult-to-cut materials. Also, numerous developments in EDM have focused on the production of micro-features (Pham et al., 2004). This has become possible due to the availability of new CNC systems and advanced spark generators that have helped to improve machined surface quality. This chapter presents the principle of EDM process and type of EDM machines used in industry, particularly focusing on hole drilling EDM.

The description of process parameters and their effects on Material Removal Rate (MRR), Electrode Wear Rate (EWR) and Surface Roughness (SR) are also reported.

## 4.2 Electrical Discharge Machining (EDM)

EDM is the process of machining electrically conductive materials by using precisely controlled sparks that occur between an electrode and a workpiece in the presence of a dielectric fluid (Jameson, 2001). This method is preferred to machine difficult-to-cut materials, particularly aerospace alloys, which cannot be machined easily by means of traditional techniques.

EDM is sometimes called "spark machining" as it removes material from workpiece by producing a rapid series of repetitive electrical discharges. The sparking principle is illustrated in Fig. 4.1. Such electrical discharges are built between the electrode and the workpiece. The small amount of material that is removed from the workpiece is flushed away with a continuously flowing fluid. The repetitive discharges create a set of successively deeper craters in the work piece until the final shape is produced.

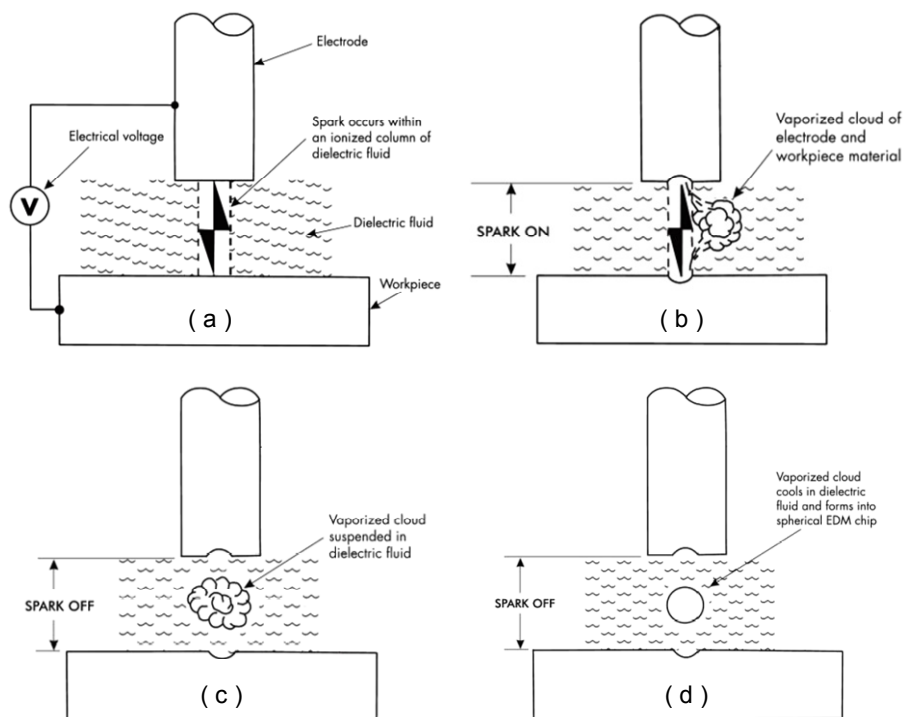


Figure 4.1 Principle of sparking in EDM process (Jameson, 2001)

EDM Process has been commonly used in tool and die-making industry. In recent years, EDM has also become an integral part of making prototypes and drilling small-scale cooling holes. Such applications are particularly seen in aerospace and electronics industries where production quantities remain low. For this purpose, there are different types of EDM machines for specific applications. Die-sinking (aka *ram-type*) EDM machines require an electrode having the exact opposite shape as the one in the workpiece. Wire (or *wire-cut*) EDM machines use a continuous wire as the electrode where the sparking takes place from the wire-side of electrode to the workpiece. Hole drilling EDM machines simply incorporate drilling of small-size holes using cylindrical hollow electrodes.

### 4.3 Hole Drilling EDM Process

Despite of using the same principle as other EDM techniques, hole drilling EDM process has two distinctive features (Fig. 4.2): a constantly rotated hollow-shape electrode and the pumping of dielectric fluid through this electrode. High flushing pressure of dielectric fluid flowing through the rotating electrode helps in flushing the particles away during machining. The electrode guider keeps the electrode on location and prevents drifting while the rotating electrode is cutting. With the aid of electrode guider and flushing effects on the electrode, this technique can be used for making holes in a fast and accurate way with a good surface finish.

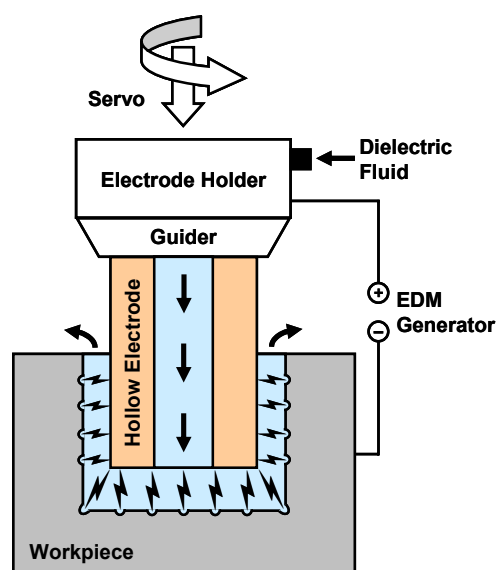


Figure 4.2 Hole drilling EDM process (adapted from Leao et al., 2005)

Use of traditional techniques in drilling holes on aerospace alloys cause problems of tool wear/breakage and slow machining rates, leading to inaccurate hole dimensions and unacceptable surface quality. Hole drilling EDM has been recently used to produce cooling holes on aeroengine components such as turbine blades and nozzle guide vanes. The combination of using high pressure (70-100 bar) dielectric pump, the rotation of tubular electrode and the high electrode feed rate (controlled by a fast response servo) make it possible to produce holes at a very fast rate. Drilling rates of 1 mm/s can be achieved, and the hole size is generally  $\text{Ø}0.15\text{-}3$  mm with a length-to-diameter ratio of over 150:1 (Leao et al., 2005).

#### 4.4 Process Parameters

The parameters in hole drilling EDM process can be grouped as controllable and uncontrollable parameters as given in Table 4.1. Controllable parameters, also called *machining parameters*, are the parameters which can be set or adjusted on EDM machine. Uncontrollable parameters can be selected or defined before the process.

*Table 4.1 Controllable and uncontrollable EDM parameters*

Controllable Parameters			Uncontrollable (Fixed) Parameters		
<i>Name</i>	<i>Unit</i>	<i>Symbol</i>	<i>Name</i>	<i>Unit</i>	<i>Symbol</i>
Peak current	A	I	Dielectric fluid	-	-
Pulse-on time	$\mu\text{s}$	$t_{\text{on}}$	Electrode rotation	rpm	N
Pulse-off time	$\mu\text{s}$	$t_{\text{off}}$	Polarity	-	-
Capacitance	$\mu\text{F}$	C	Voltage	volts	V
			Dielectric flushing pressure	bar	-

##### 4.4.1 Controllable Parameters

The controllable parameters in EDM process are as follows:

**Peak current:** This is the amount of power used in discharge machining, and it is the most important machining parameter in EDM. During each pulse-on time, the current increases until it reaches a preset level, which is expressed as the peak current as seen in Fig. 4.3. Higher currents will improve MRR, but at the cost of SR and EWR.

**Pulse-on and pulse-off time:** Each sparking cycle during EDM process has pulse-on time (aka *pulse duration*) and pulse-off time (aka *pulse interval*). Since all the work is done during pulse-on time, the duration of pulses and the number of cycles per second (frequency) are important. With longer pulse duration, more workpiece material will be melted away. The resulting crater will be broader and deeper than a crater produced by shorter pulse duration, which will cause a rougher surface finish. The cycle is completed when sufficient pulse interval is allowed before the start of the next cycle. Pulse interval will affect the speed and stability of the cut. In theory, the shorter the interval, the faster will be the machining operation. On the other hand, if the interval is too short the eroded workpiece material will not be swept away by the flow of dielectric fluid, which will cause the next spark to be unstable.

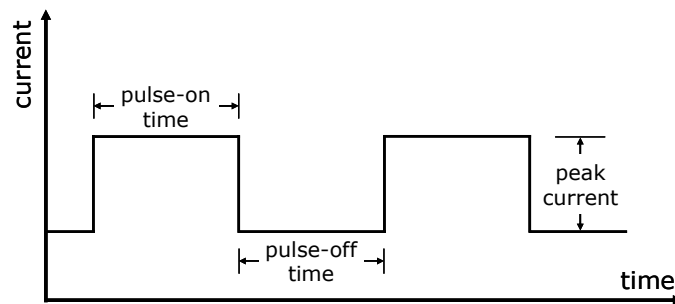


Figure 4.3 Peak current versus pulse-on and pulse-off times (Kumar et al., 2009)

**Capacitance:** In resistance-capacitor type discharge pulse generator (Fig. 4.4), the capacitor controls the action of charging and discharging as well as the frequency of discharging. An increase in capacitance results in higher material removal rate due to larger discharge energy. As capacitance becomes larger, peak current also increases. Therefore, deeper craters will be generated which causes an increase in MRR and SR as well as slight increase in EW.

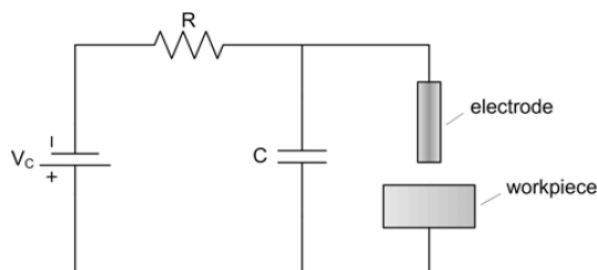


Figure 4.4 RC discharge pulse generation circuit (Jung et al., 2007)

#### 4.4.2 Uncontrollable Parameters

The following parameters can only be selected before the EDM operation:

**Voltage:** Discharge voltage in EDM is related to spark gap and breakdown strength of the dielectric. High voltage settings increase the gap, which improves the flushing conditions and helps to stabilize the cutting action. MRR, EWR, and SR increase by increasing open circuit voltage since the electric field strength increases.

**Dielectric fluid:** EDM process takes place in presence of a dielectric fluid. Basic characteristics of a dielectric are high dielectric strength and quick recovery after breakdown, effective quenching and flushing ability. EWR and MRR are affected by the type of dielectric and the method of its flushing. It is either a petroleum product or deionized water. Petroleum products are often referred to hydrocarbon fluids as they break down into hydrogen, carbon and other products when they are heated during sparking. Deionized water is free of impurities so that it is electrically conductive. The heat of sparking breaks down this water into hydrogen and oxygen. Deionized water is usually used in wire EDM, hole drilling EDM, and high precision die-sinking EDM machines due to its low viscosity and carbon-free characteristics.

**Polarity:** It can be either positive or negative. The spark creates high temperatures causing material evaporation at both electrode and workpiece. In general, the polarity is determined by experiments, and it is a matter of electrode material, workpiece material, current density and pulse length combinations.

#### 4.4.3 Process Outputs

Outputs of hole drilling EDM process are MRR, EWR, and SR. Among these, MRR and EWR are calculated based on the weight of workpiece, machining time and loss in electrode length. On the other hand, SR can be measured on the machined hole surfaces. Determination of EDM outputs are explained in detail in the next chapter.

## **CHAPTER 5**

### **DEVELOPMENT OF ANFIS MODELS**

#### **5.1 Introduction**

In this chapter, the methodology for development of ANFIS models for a selected application is presented. The experimental work including the description of EDM machine, the procedure of conducting experiments, and obtaining the experimental data are explained. After that, the development of ANFIS models for the selected data set is presented step-by-step. In each step, the findings are discussed by means of screenshots of ANFIS software. Finally, the results on training and validation capabilities of developed models are compared with experimental data.

#### **5.2 Experimental Work**

As mentioned previously in Chapter 1, the experimental data used in this study has been obtained from the research project (Yılmaz et al., 2010). This section presents the experimental work including the material properties for workpiece and electrode as well as the setup for conducting experiments. The design of experiments, the input parameters and the measurement of values of corresponding outputs are also described briefly in this section.

##### **5.2.1 Workpiece and Electrode Materials**

The workpiece materials used in this study were common aerospace super alloys:  $\alpha+\beta$  type Ti-6Al-4V (aka Ti64) and Inconel 718 (aka IN718). In spite of their poor machinability and low mechanical properties, these materials are preferred in



aerospace applications due to their specific thermal and physical properties (Bozdana et al., 2010). The chemical compositions of Ti64 and IN718 are given in Table 5.1.

*Table 5.1 Chemical composition of Ti64 and IN718 (wt. %)*

Ti-6Al-4V		Inconel 718	
Ti	89.464	Ni	50-55
Al	6.08	Si	0.35 (max)
V	4.02	Cr	17-21
Fe	0.22	Mn	0.35 (max)
O	0.18	Fe	Balanced
C	0.02	Nb	4.75-5.50
N	0.01	Mo	2.80-3.30
H	0.0053	C	0.08 (max)
		B	0.06 (max)
		Co	1.00 (max)
		Ti	0.65-1.15
		Al	0.20-0.80

Brass and copper electrodes with a tubular shape (single-channel) were used during experiments. These are commonly used tool electrode materials in EDM hole drilling applications due to their desirable thermal and electrical properties seen in Table 5.2.

*Table 5.2 Material properties of tool electrodes*

	Copper	Brass
Melting point (°C)	1084.62	900-940
Electrical resistivity (Ω-cm)	1.69	4.7
Thermal conductivity (W/m-°K)	391	159
Specific heat capacity (J/g-°C)	0.385	0.38

### 5.2.2 Experimental Setup

Several holes were produced at different machining conditions on Ti64 and IN718 specimens with dimensions of 6 x 11 x 35 mm. The flat surfaces of two specimens were aligned in order to ensure that the mating surfaces could be secured accurately using a specially designed and manufactured fixture as illustrated in Fig. 5.1. Upper and lower surfaces of specimens were ground prior to experiments. The holes were drilled on the line of mating interface to enable implementation of standardized experiments, easier handling of specimens after experiments, and performing reliable surface roughness measurements on the hole surfaces.

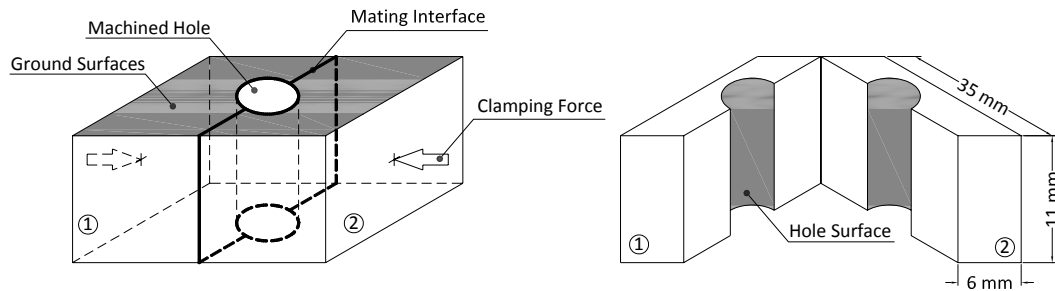


Figure 5.1 Sketch of specimens and drilled holes

The experiments were performed on JS EDM AD-20 hole drilling EDM machine manufactured by *Jiann Sheng Machinery and Electric Industrial Co. Ltd.* Specifications of this machine are given in Fig. 5.2.

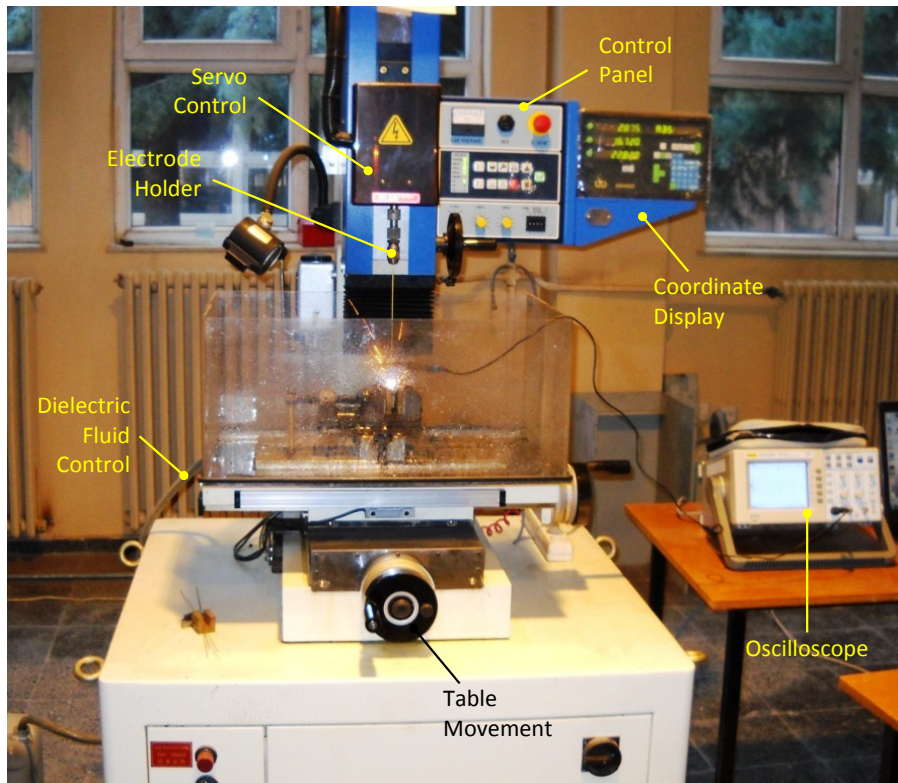
### JS AD-20 EDM



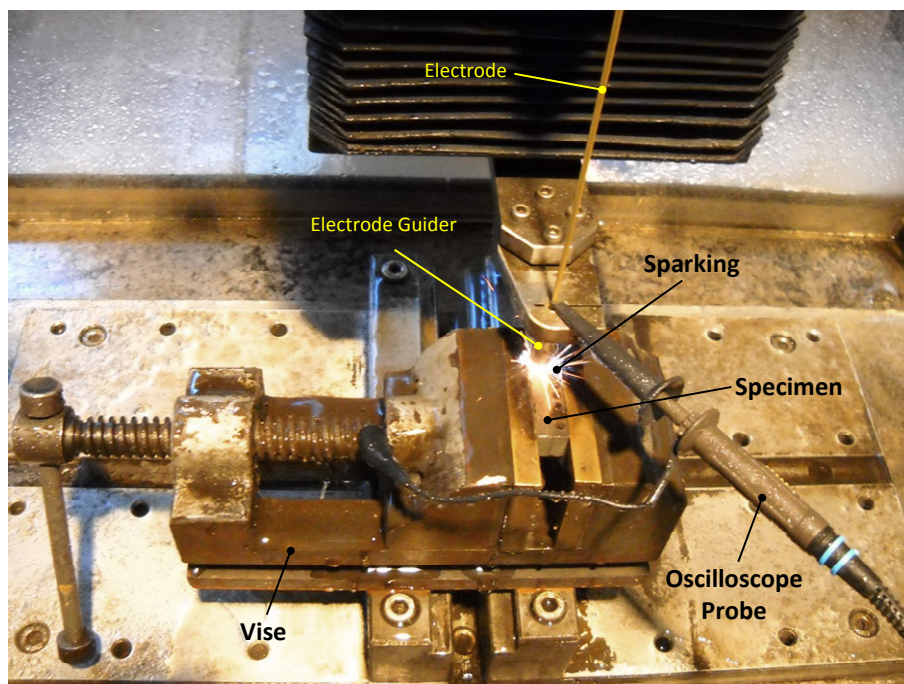
X / Y AXIS TRAVEL	300 x 200 mm (11.8" x 7.9")
Z1 / Z2 AXIS TRAVEL	345 mm (13.6")
WORK TABLE	480 x 210 mm (18.9" x 8.3")
X / Y / Z AXIS DRO RESOLUTION	0.005 mm (0.000196")
ELECTRODE GUIDE TRAVEL	150 mm (5.9")
HEIGHT OF WORK TABLE TO GUIDE	80 ~ 210 mm (3.1" ~ 8.3")
MAX. WORKPIECE WEIGHT	200 kg
MACHINE WEIGHT (N.W)	600 kg
OVERALL DIMENSIONS (L x W x H)	1000 x 1020 x 2070 mm (39.4" x 40.2" x 81.5")
MAX. MACHINING CURRENT	30 A
MAX. POWER CONSUMPTION	4 KVA
INPUT VOLTAGE	220 / 380 / 415 / 440 V

Figure 5.2 Specifications of JS AD-20 EDM machine

The components of experimental setup are shown in Fig. 5.3. The vertical movement of electrode is controlled by servo control whereas location of holes on the specimen is adjusted by means of table movement. Coordinates of corresponding movements are viewed on the coordinate display. The dielectric fluid is filtered, and it flows through hollow electrode during operation. The measurements of current and voltage were performed using an oscilloscope. On the other hand, the values of pulse-on time, pulse-off time, and capacitance were specified by the machine manufacturer. Fig. 5.4 shows a close-up view of the process with the occurrence of spark. The electrode guider holds the electrode and provides a stable electrode rotation.



*Figure 5.3 Components of JS AD-20 EDM machine*



*Figure 5.4 Close-up view of EDM process*

Machine settings are adjusted on the control panel, as seen in Fig. 5.5. The desired levels for controllable parameters can be chosen on this panel. The values of current

(A), pulse-on and pulse-off times ( $\mu\text{s}$ ), and capacitance ( $\mu\text{F}$ ) at selected settings are presented in the next section.



Figure 5.5 Control panel of JS AD-20 EDM machine

### 5.2.3 Design of Experiments and Machining Conditions

Design of Experiments (DOE) is a structured and organized method for determining the relationships between input parameters affecting the process outputs. The benefit of using this method is to obtain useful information about the process by conducting only minimum number of experiments (Montgomery, 2000). In this study, the minimum number of experiments was determined by method of Central Composite Design (CCD) that gives 31 experiments to be conducted in a specific order.

The experiments were performed using four input parameters (i.e.  $I$ ,  $t_{\text{on}}$ ,  $t_{\text{off}}$ , and  $C$ ). For each input parameter, five different settings on the machine (i.e. 5, 6, 7, 8, and 9) were selected. Table 5.3 shows the machine settings and the corresponding values of input parameters. This means that  $5^4 = 625$  experiments in total was required if all machine settings were used. However, CCD method requires only 31 experiments to be conducted in a specific order so that the effect of input parameters at different machine settings can be analyzed. The results of these 31 experiments, as given in Table 5.4, were used for training the ANFIS models in this study.

Table 5.3 Machine settings and the corresponding values of input parameters

Machine Setting	Real Values of Input parameters			
	I (A)	t <sub>on</sub> (μs)	t <sub>off</sub> (μs)	C (μF)
5	8.2	27	16	1100
6	8.8	30	18	1217
7	10.2	35	20	1316
8	11.5	38	23	1422
9	12.0	44	26	1476

Table 5.4 The experiments used for training data

Exp. No.	Machine Settings				Corresponding Values			
	I	t <sub>on</sub>	t <sub>off</sub>	C	I (A)	t <sub>on</sub> (μs)	t <sub>off</sub> (μs)	C (μF)
1	6	6	6	6	8.8	30	18	1217
2	7	7	5	7	10.2	35	16	1316
3	8	8	8	8	11.5	38	23	1422
4	8	6	8	8	11.5	30	23	1422
5	7	7	7	7	10.2	35	20	1316
6	7	7	7	7	10.2	35	20	1316
7	7	7	7	7	10.2	35	20	1316
8	7	7	7	9	10.2	35	20	1476
9	8	8	6	8	11.5	38	18	1422
10	6	8	6	8	8.8	38	18	1422
11	6	6	8	6	8.8	30	23	1217
12	7	7	7	7	10.2	35	20	1316
13	6	8	8	8	8.8	38	23	1422
14	8	6	8	6	11.5	30	23	1217
15	8	8	6	6	11.5	38	18	1217
16	9	7	7	7	12.0	35	20	1316
17	6	8	6	6	8.8	38	18	1217
18	6	6	6	8	8.8	30	18	1422
19	7	7	9	7	10.2	35	26	1316
20	7	9	7	7	10.2	44	20	1316
21	8	6	6	6	11.5	30	18	1217
22	7	7	7	7	10.2	35	20	1316
23	7	7	7	7	10.2	35	20	1316
24	7	5	7	7	10.2	27	20	1316
25	6	8	8	6	8.8	38	23	1217
26	8	8	8	6	11.5	38	23	1217
27	6	6	8	8	8.8	30	23	1422
28	8	6	6	8	11.5	30	18	1422
29	5	7	7	7	8.2	35	20	1316
30	7	7	7	5	10.2	35	20	1100
31	7	7	7	7	10.2	35	20	1316

As highlighted in Table 5.4, seven experiments with the same settings (exp. no. 5, 6, 7, 12, 22, 23, and 31) were repeated to check the consistency of results for experiments conducted at machine settings of  $I = 7$ ,  $t_{on} = 7$ ,  $t_{off} = 7$ , and  $C = 7$ . It is expected that the results obtained from these experiments would be different due to the irregularities within microstructure of electrode and workpiece materials, and also variations in the environmental factors (i.e. temperature, vibration, dielectric fluid, etc). This causes a repeatability error during the experiments that was also introduced into training capabilities of the developed models, as discussed in the following sections.

In addition to 31 experiments used for training data, the experimental data obtained from 5 additional experiments having different values of input parameters were used for validation of the system, as given in Table 5.5. The machine settings in these 5 experiments were selected randomly among possible 625 experiments.

*Table 5.5 The experiments used for checking data*

Exp. No.	Machine Settings				Corresponding Values			
	I	$t_{on}$	$t_{off}$	C	I (A)	$t_{on}$ ( $\mu$ s)	$t_{off}$ ( $\mu$ s)	C ( $\mu$ F)
V1	7	8	7	8	10.2	38	20	1422
V2	8	7	7	6	11.5	35	20	1217
V3	6	8	8	7	8.8	38	23	1316
V4	6	7	8	9	8.8	35	23	1476
V5	7	9	5	8	10.2	44	16	1422

#### 5.2.4 Uncontrollable Parameters

There are some uncontrollable parameters on EDM machine as listed in Table 5.6. These parameters were kept constant during experiments.

*Table 5.6 The list of uncontrollable parameters*

Name of parameter	Value
Voltage	27 V
Dielectric fluid	Deionized water
Dielectric flushing pressure	75 bar
Electrode rotational speed	150 rpm
Polarity of electrode	Negative (-)

### 5.2.5 Measurement of Output Parameters

The drilling time for each hole was recorded using an electronic timer. The test pieces were weighed before and after drilling using a digital precision scale. Based on these measurements, Material Removal Rate (MRR) for each experiment was calculated by the following formula:

$$\text{MRR (mg/min)} = \frac{\text{initial weight} - \text{final weight}}{\text{drilling time}} \quad \text{Eq. 5.1}$$

Electrode Wear Rate (EWR) was determined according to the drilling time of hole and the corresponding amount of electrode consumption (i.e. the variation in electrode length):

$$\text{EWR (mm/min)} = \frac{\text{electrode consumption in length}}{\text{drilling time}} \quad \text{Eq. 5.2}$$

Surface Roughness (SR) of machined surfaces was measured using optical surface measurement tool. For this purpose, photos of machined hole surfaces were taken using SEM and the roughness values ( $R_a$ ,  $\mu\text{m}$ ) were measured on these photos by means of a special-purpose software *3D Mex* produced by *Alicona*. For obtaining reliable results, the roughness values at the entrance, the middle, and the exit locations of holes were measured, and the average of these values was taken.

### 5.3 Development of ANFIS Models

In this study, ANFIS editor (Fig. 5.6) within the *Fuzzy Logic Toolbox of Matlab* was used for development of models. As stated in previous sections, the aim was to achieve ANFIS models for  $\text{Ø}2$  mm holes drilled on Inconel 718 and Ti-6Al-4V workpiece materials using brass and copper electrodes. As numbered in Fig. 5.6, the methodology to develop models is explained step-by-step in this section. For this purpose; Inconel 718 workpiece material and brass electrode were chosen as a case study, and this model was named as “D2NiBr”. Other models were also named in a similar way (i.e. D2NiCu, D2TiBr, and D2TiCu) as given in Appendix D.

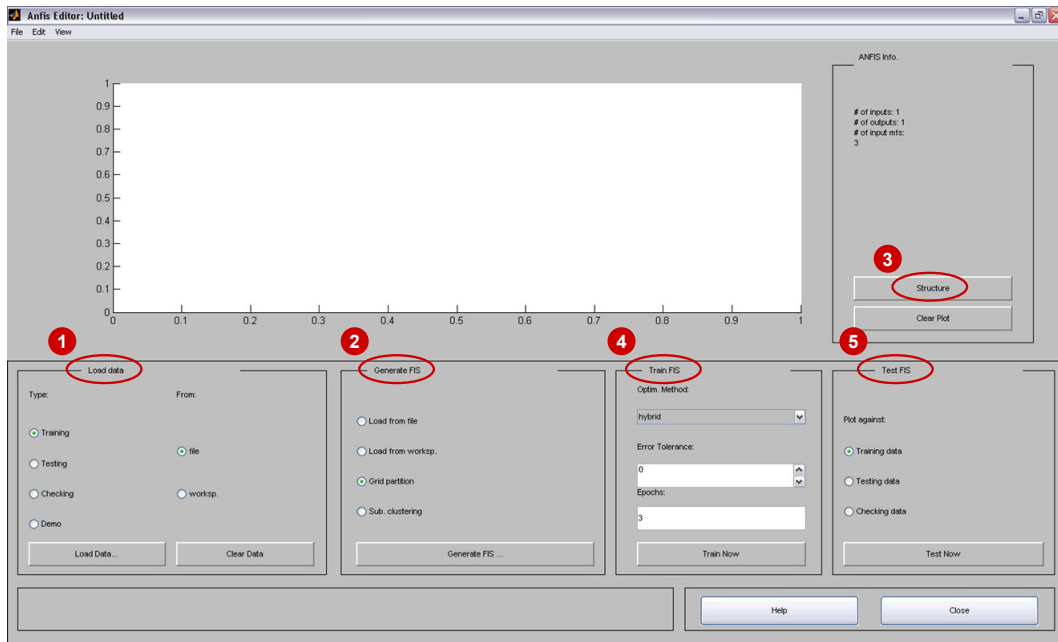


Figure 5.6 Screenshot of ANFIS editor

Table 5.7 and 5.8 present the experimental data used for training and checking the model D2NiBr, respectively. The experiments used for validation were named as V1, V2, V3, V4, and V5 in order to prevent confusion throughout the report. As mentioned in Section 5.2.3, the repeated experiments with the same input values, shaded in Table 5.7, have different output values. Such differences in values are evaluated as repeatability error, which shows the precision of EDM machine in producing consistent outputs with respect to the identical machining conditions. Table 5.9 shows the repeatability errors for outputs MRR, EWR, and SR for repeated experiments in set of D2NiBr. The average of values for repeated experiments is calculated, and then the deviation of each value from the average is determined.

As seen from Table 5.9, the deviations are within  $\pm 20\%$ , which means that the repeatability error in experimental data for D2NiBr is acceptable. The experimental data used for validation of the models for other sets of data (i.e. D2NiCu, D2TiBr, and D2TiCu) are given in Appendix D. The following sections describe the methodology of developing ANFIS models for outputs of MRR, EWR and SR for the case of D2NiBr using these training and checking data.



Table 5.7 Experimental data used for training the model D2NiBr

Exp. No.	Input Parameters				Output Parameters		
	I (A)	t <sub>on</sub> (μs)	t <sub>off</sub> (μs)	C (μF)	MRR (mg/min)	EWR (mm/min)	SR (μm)
1	8.8	30	18	1217	61.869	0.384	10.941
2	10.2	35	16	1316	92.841	0.866	12.054
3	11.5	38	23	1422	128.193	1.825	3.982
4	11.5	30	23	1422	107.012	1.655	3.771
5	10.2	35	20	1316	80.847	0.814	12.809
6	10.2	35	20	1316	80.200	0.722	11.608
7	10.2	35	20	1316	78.600	0.702	12.305
8	10.2	35	20	1476	103.575	1.341	3.858
9	11.5	38	18	1422	136.235	2.118	3.863
10	8.8	38	18	1422	118.510	1.612	4.357
11	8.8	30	23	1217	69.042	0.701	11.483
12	10.2	35	20	1316	88.828	0.814	10.513
13	8.8	38	23	1422	117.843	1.498	4.037
14	11.5	30	23	1217	83.322	0.779	12.086
15	11.5	38	18	1217	102.023	0.827	10.659
16	12.0	35	20	1316	147.381	1.962	3.545
17	8.8	38	18	1217	89.486	0.742	10.630
18	8.8	30	18	1422	93.032	1.194	4.672
19	10.2	35	26	1316	81.371	0.941	10.690
20	10.2	44	20	1316	102.987	0.930	11.728
21	11.5	30	18	1217	93.832	0.822	12.277
22	10.2	35	20	1316	88.068	0.736	10.462
23	10.2	35	20	1316	84.444	0.736	11.592
24	10.2	27	20	1316	75.478	0.623	10.312
25	8.8	38	23	1217	82.187	0.675	11.633
26	11.5	38	23	1217	95.830	0.870	11.871
27	8.8	30	23	1422	94.277	1.219	3.810
28	11.5	30	18	1422	113.766	1.812	4.447
29	8.2	35	20	1316	62.807	0.611	11.105
30	10.2	35	20	1100	84.804	0.850	10.767
31	10.2	35	20	1316	73.941	0.576	10.005

Table 5.8 Experimental data used for checking (validating) the model D2NiBr

Exp. No.	Input Parameters				Output Parameters		
	I (A)	t <sub>on</sub> (μs)	t <sub>off</sub> (μs)	C (μF)	MRR (mg/min)	EWR (mm/min)	SR (μm)
V1	10.2	38	20	1422	152.679	1.821	3.294
V2	11.5	35	20	1217	134.000	1.247	10.737
V3	8.8	38	23	1316	117.943	0.881	8.672
V4	8.8	35	23	1476	135.652	1.604	5.090
V5	10.2	44	16	1422	154.951	2.196	2.917

Table 5.9 Repeatability errors in experimental data for D2NiBr

Exp. No.	MRR (mg/min)		EWR (mm/min)		SR ( $\mu\text{m}$ )	
	Value	Deviation	Value	Deviation	Value	Deviation
5	80.847	1.56	0.814	-11.68	12.809	-13.08
6	80.200	2.35	0.722	0.89	11.608	-2.47
7	78.600	4.30	0.702	3.64	12.305	-8.63
12	88.828	-8.15	0.814	-11.71	10.513	7.19
22	88.068	-7.23	0.736	-1.08	10.462	7.64
23	84.444	-2.81	0.736	-0.97	11.592	-2.33
31	73.941	9.97	0.576	20.90	10.005	11.67
<b>Ave.</b>	<b>82.133</b>		<b>0.729</b>		<b>11.328</b>	

### 5.3.1 Step I: Loading Data Files into System

At the first step, training and checking data that will be used for training and checking (validation) of the model are loaded into system. For instance, the input parameters and the corresponding MRR values used for training of the model are recorded in “D2NiBr\_Trndata\_MRR.dat” file as shown in Fig. 5.7a. Similarly, the checking data for validation of model are recorded in “D2NiBr\_Chkdata\_MRR.dat” file (Fig. 5.7b). In these files, the first four columns represent the values of input parameters whereas the values of output parameter (MRR) are given in the last column. The screenshot of the system after loading these files is given in Fig. 5.8.

Dosya	Düzen	Biçim	Görünüm	Yardım
8.8	30	18	1217	61.869
10.2	35	16	1316	92.841
11.5	38	23	1422	128.193
11.5	30	23	1422	107.012
10.2	35	20	1316	80.847
10.2	35	20	1316	80.200
10.2	35	20	1316	78.600
10.2	35	20	1476	103.575
11.5	38	18	1422	136.235
8.8	38	18	1422	118.510
8.8	30	23	1217	69.042
10.2	35	20	1316	88.828
8.8	38	23	1422	117.843
11.5	30	23	1217	83.322
11.5	38	18	1217	102.023
12.0	35	20	1316	147.381
8.8	38	18	1217	89.486
8.8	30	18	1422	93.032
10.2	35	26	1316	81.371
10.2	44	20	1316	102.987
11.5	30	18	1217	93.832
10.2	35	20	1316	88.068
10.2	35	20	1316	84.444
10.2	27	20	1316	75.478
8.8	38	23	1217	82.187
11.5	38	23	1217	95.830
8.8	30	23	1422	94.277
11.5	30	18	1422	113.766
8.2	35	20	1316	62.807
10.2	35	20	1100	84.804
10.2	35	20	1316	73.941

a. Training data

Dosya	Düzen	Biçim	Görünüm	Yardım
10.2	38	20	1422	152.679
11.5	35	20	1217	134.000
8.8	38	23	1316	117.943
8.8	35	23	1476	135.652
10.2	44	16	1422	154.951

b. Checking (Validation) data

Figure 5.7 The experimental data used for D2NiBr\_MRR

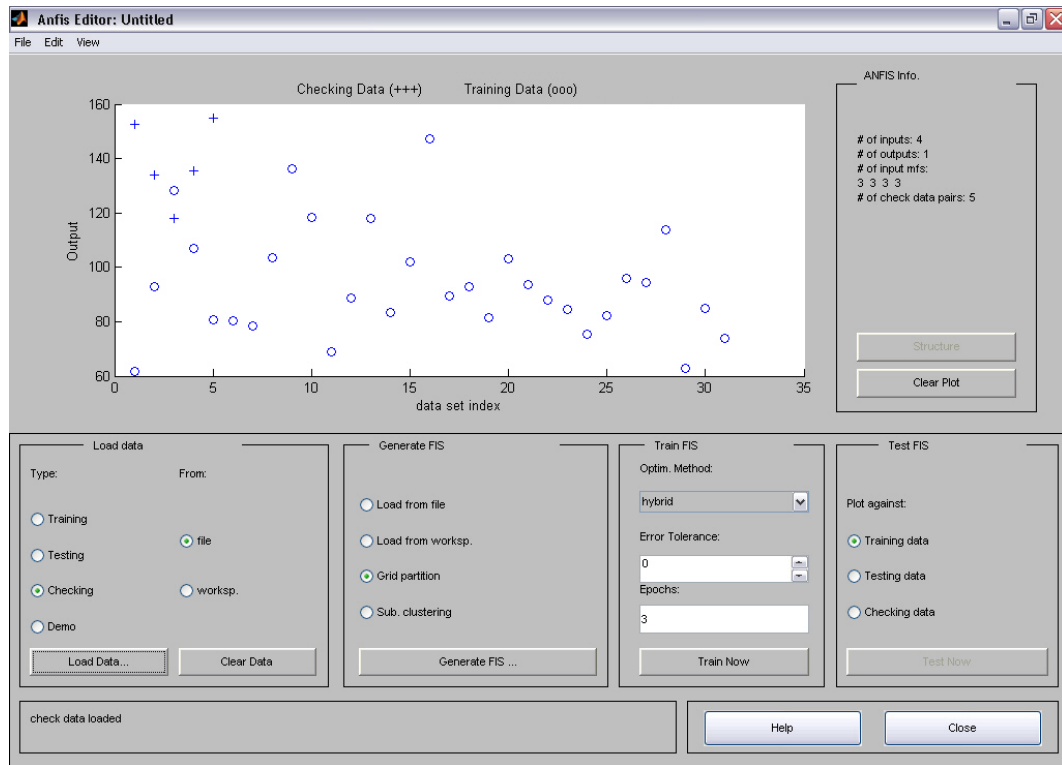


Figure 5.8 Training and checking data loaded into the system

In ANFIS, it is possible to define multiple input parameters. However, only one output parameter can be defined. This is due to the fact that Sugeno approach is used as inference methodology in ANFIS. Therefore, training and checking data for EWR and SR were also introduced into the system, and the corresponding ANFIS models were developed separately.

### 5.3.2 Step II: Generating FIS

The membership functions for input and output parameters as well as IF-THEN type of fuzzy rules that define the relationships between such functions are specified at this step. For this purpose, there are two common methodologies in ANFIS: “*grid partitioning*” and “*subtractive clustering*”. In grid partitioning method, the relationships between input and output parameters are analyzed one-by-one and the fuzzy rules for specifying such relationships are generated. On the other hand, in subtractive clustering method, similar relationships between input and output parameters are grouped and added into clusters, and the corresponding fuzzy rules are generated based on such clusters.

The number of rules generated in the first method is usually higher than that in the second method. This is due to the fact that the first method generates a rule for each relationship whereas the rules for clusters only are generated in the second method. Therefore, training time for the models developed based on the first method is longer due to large number of rules. However, such models present more accurate and reliable results as compared to those in the second method. Grid partitioning method is suggested when there are less than six input parameters and limited number of training data (Jang). Thereby, grid partitioning method was chosen in this study and all models were developed based on this method.

As seen in Fig. 5.9, type and number of membership functions for input parameters as well as type of membership function for output parameter are specified in grid partitioning method. For each input parameter, different number of membership function can be specified. Total number of fuzzy rules generated within the system depends upon number of input parameters and number of membership function for each input parameter (Eq. 5.3).

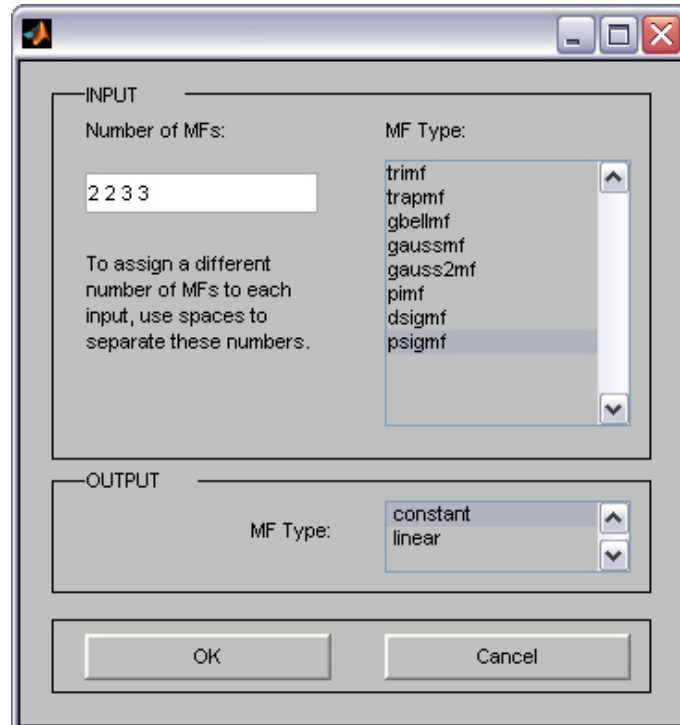


Figure 5.9 Specifying the properties of model using grid partitioning method

$$\text{Total number of fuzzy rules} = [\text{number of MFs}]^{(\text{number of input parameters})} \quad \text{Eq. 5.3}$$

Therefore, the number of rules will increase accordingly with higher number of membership functions. This will cause the system to be trained in a longer time. Due to this reason, several trials were performed in training the models using different number of membership functions, and the most suitable number of membership function for each input parameter was found to be “2 2 3 3”. This means that the total number of fuzzy rules in the models is defined as  $2 * 2 * 3 * 3 = 36$  rules.

The membership functions available in ANFIS were given previously in Fig. 3.4. It is quite difficult to make a choice among these functions since the efficiency of each function will vary according to certain applications. In this study, the models were built using different membership functions and the obtained results revealed that the most suitable function is “*psigmf*”. This function was chosen over other functions due to its smoothness and ability of being used for asymmetrical data. Besides, the type of membership function for output parameter was selected as “*constant*” that has provided better performance than “*linear*” option during training of models.

### 5.3.3 Step III: Structure of FIS

Each model has four input parameters (i.e. I,  $t_{on}$ ,  $t_{off}$ , and C) and one output parameter (i.e. MRR, EWR, or SR) with 36 fuzzy rules (as given in Fig. 5.10).

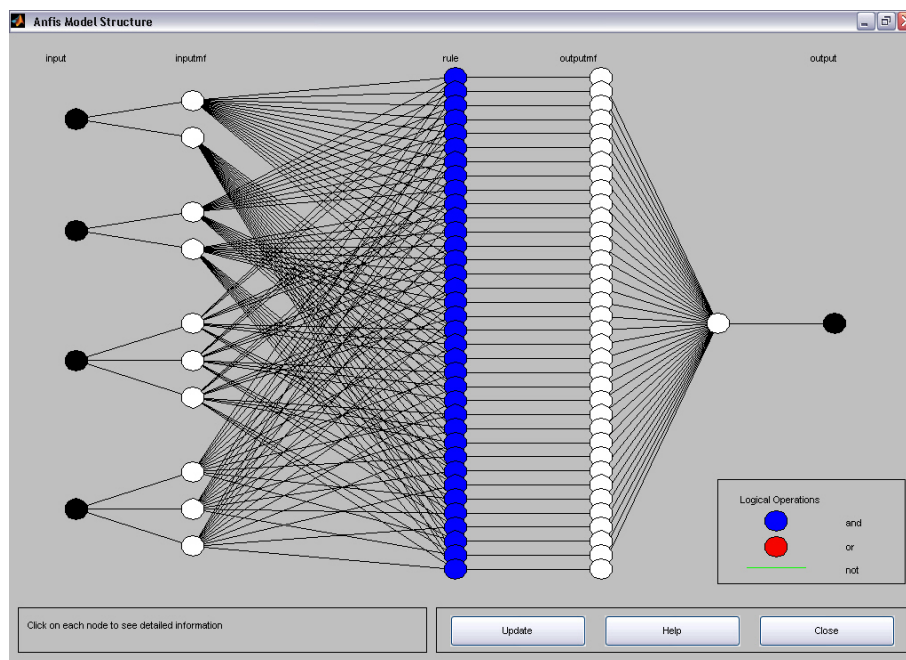


Figure 5.10 Structure of developed model

### 5.3.4 Step IV: Training FIS

In this section, the model having the FIS structure is supposed to be trained. Fig. 5.11 shows the procedure of training the model for MRR output and obtaining the training error. In this study, “*hybrid learning algorithm*” was used as optimization method in training. This algorithm uses the combined effect of “minimum square algorithm” and “back propagation algorithm” to obtain the optimum training performance. The error obtained by hybrid algorithm is the Root Mean Square Error (RMSE) value (i.e. standard deviation) of the output MRR values. The target for error tolerance was not specified (i.e. error tolerance was set to zero) so that the possible minimum error value could be achieved. The epoch number for all models was defined as 500 by default. However, the most appropriate epoch number for each model was defined after obtaining the error curves.

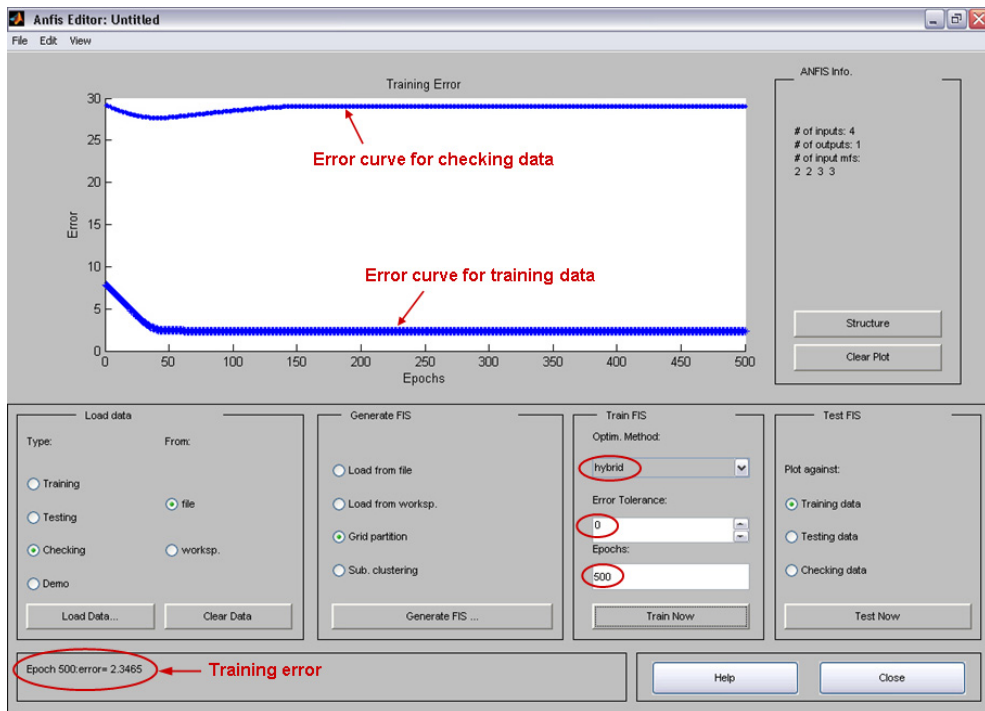


Figure 5.11 Training and checking of the model for MRR

As seen in Fig. 5.11, the error curve for training data decreases until a specific value (i.e. 2.3465) and continues horizontally after 100 epochs. Therefore, the most appropriate epoch number for this model can be accepted as 100 since the error value beyond this epoch number is constant. However, this should not be decided based on only observing training error curve.

Considering the checking error curve; the checking error first decreases until a specific value and increases as the training continues, and finally reaches a constant value after about 200 epochs. This means that selecting 200 epochs for this model would be more appropriate. As a conclusion, both training and error curves should be observed for determining the most appropriate epoch number, which is explained in detail in the next section.

### 5.3.5 Step V: Checking (Validating) FIS

The last step is validating the model. Average training and checking errors of the model for MRR are shown in Fig. 5.12 and 5.13. In these figures, the experimental data for training and checking are represented by circle (o) and plus (+) signs, respectively. The outputs from the model (i.e. FIS outputs) are denoted by star (\*) sign. The fitness of developed model in terms of training and checking capabilities are measured by the arithmetic mean of corresponding errors between experimental data and outputs of the system.

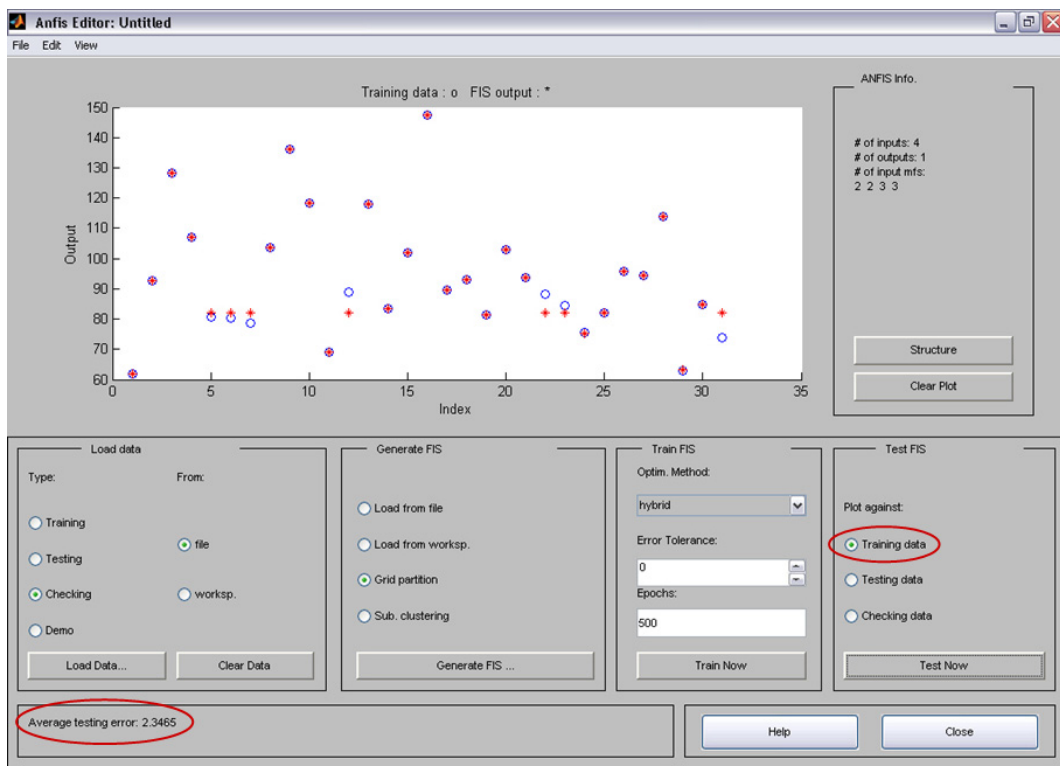


Figure 5.12 Training error of the model for MRR

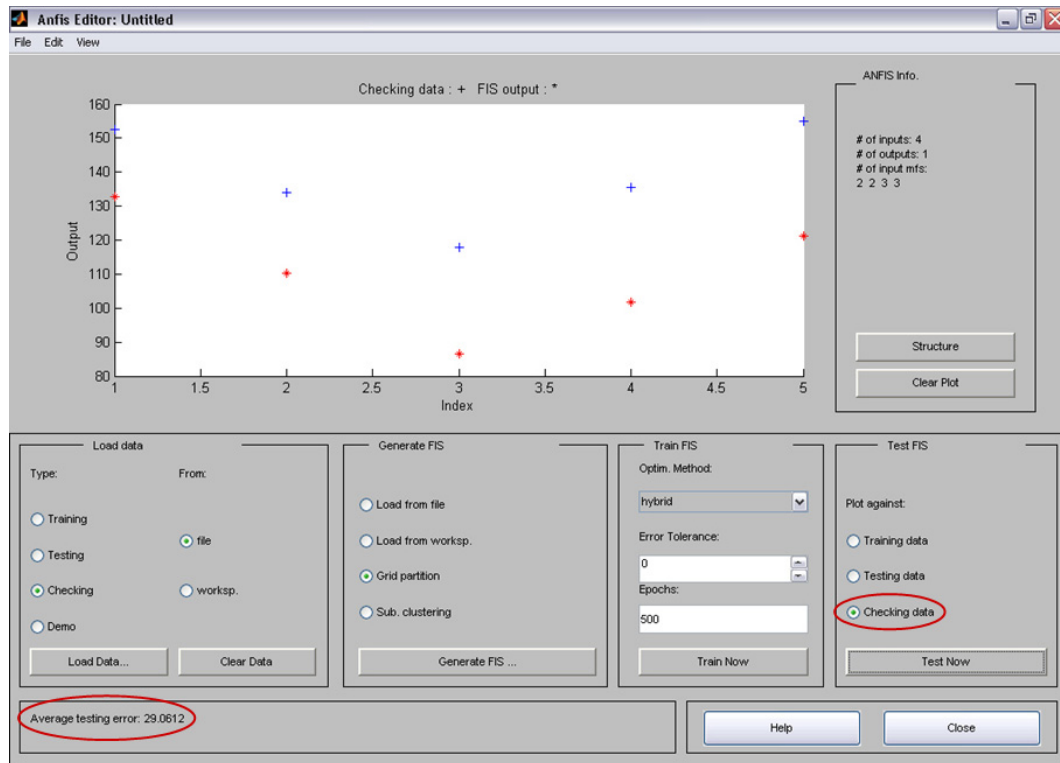


Figure 5.13 Checking error of the model for MRR

Despite the model after training exhibits very good fitness in Fig. 5.12, there are differences between experimental data and FIS outputs in repeated experiments (i.e. 5, 6, 7, 12, 22, 23, 31). This is due to repeatability error between such experiments. FIS output for these experiments has a single value although the experimental values differ from each other, which causes an increase in the average training error.

At this stage, the aim is to obtain the minimum values for training and checking of the models. In other words, the model should be trained as good as possible with the lowest validation error. Therefore, in all models, the most appropriate epoch number must be selected in order to achieve the optimum results for both training and checking data. In general, the most appropriate epoch number is chosen at the epoch where the training is complete (i.e. the training error curve is stabilized). This means that the minimum training error is obtained when the training procedure is complete. On the other hand, this may not apply to the case in checking (validation) error, as stated in the previous section.



For instance, in case of training and checking error curves of the model for EWR (Fig. 5.14), different error values were obtained at epoch #1 and epoch #100. The training error curve decreases and stabilizes after certain epoch number. The checking error curve gradually increases, then exhibits a small drop, and finally continues horizontally after certain epoch number. The checking error value at epoch #1 is determined as 0.19877 while its value is 0.276 at epoch #100.

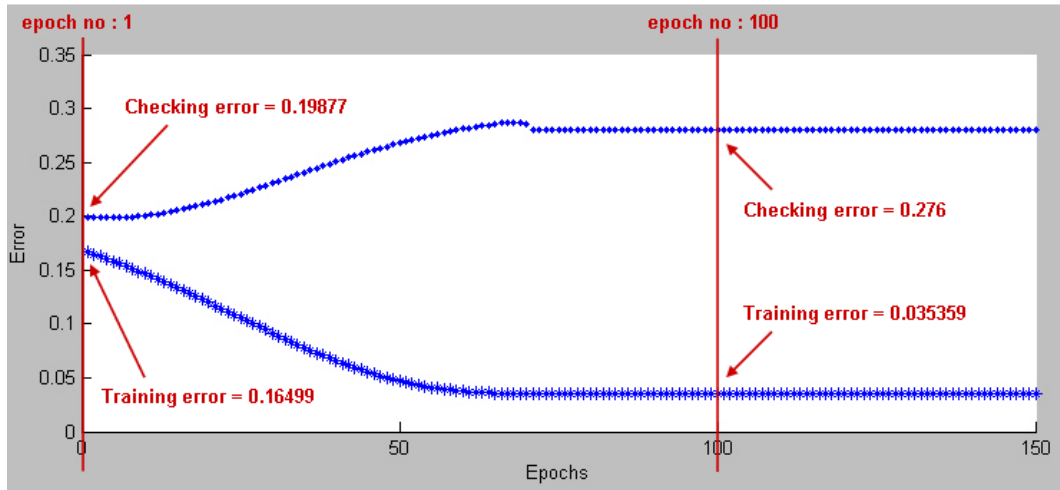


Figure 5.14 Training and checking of the model for EWR

In this case, it seems that using the model for EWR at epoch #1 is reasonable. However, there is a great difference in training error values at epoch #1 (i.e. 0.16499) and epoch #100 (i.e. 0.035359). This means that training procedure was incomplete at epoch #1 whereas epoch #100 refers to a completely trained model. Therefore, epoch #100 should be selected due to the completed training procedure with the lowest training error although the checking error at this epoch number is the highest.

The error curves of the model for SR are also examined in Fig. 5.15. Similar to the case of models for MRR and EWR, the training error curve decreases until a certain error value and stabilizes after about epoch #150. However, the checking error curve exhibits unstable progress with falls and rises at different epoch numbers. Therefore, the most appropriate epoch number for this model was found to be #125 for obtaining the optimum training and checking error levels.

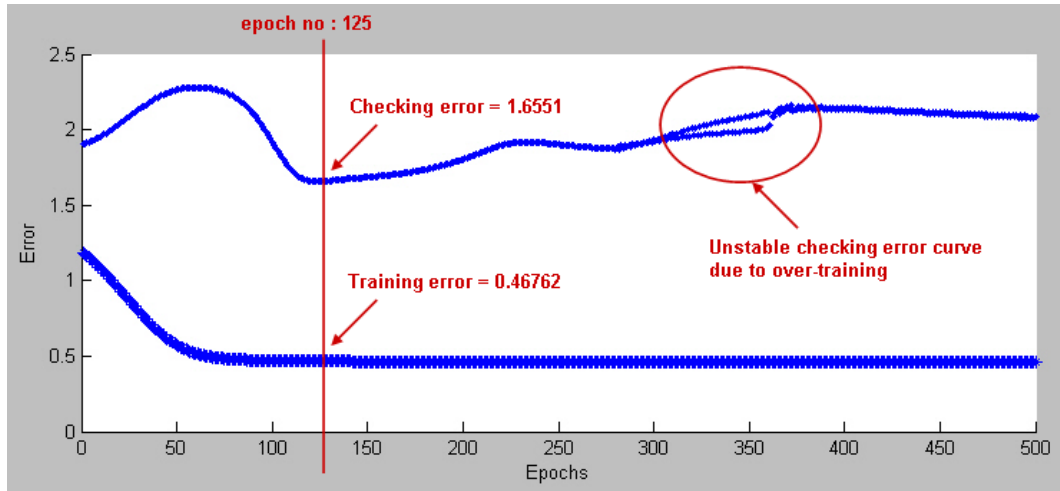


Figure 5.15 Training and checking of the model for SR

In some cases, although the training procedure is complete (i.e. the training error curve is stabilized), training the model in a continuous way may cause over-training. For instance, there is an unstable region in the checking error curve between epoch #300 and #375 (Fig. 5.15). In such cases, a stabilized checking error curve cannot be achieved due to small leaps in up and down manner. For reliable results, the epoch numbers within the unstable region in checking error curve should not be used.

### 5.3.6 Structure and Properties of Developed Models

Schematic structure of the models developed by means of ANFIS can be presented using FIS editor of Matlab. Fig. 5.16 shows the structure of model for MRR trained at epoch #200 as explained in the previous section. In this structure, the input parameters ( $I$ ,  $t_{on}$ ,  $t_{off}$ ,  $C$ ) having membership function of *psigmf* appear on the left side whereas the output parameter (MRR) having singleton (i.e. crisp) function is on the right side. The relationships between input and output parameters are defined using Sugeno type inference system.

Fig. 5.17 shows the rule editor where the output value for MRR is obtained by entering the input parameters. For instance, the value of MRR was found to be 82.1 mg/min when the values of input parameters were entered as  $I = 10.2$  A,  $t_{on} = 35$   $\mu$ s,  $t_{off} = 20$   $\mu$ s, and  $C = 1316$   $\mu$ F.

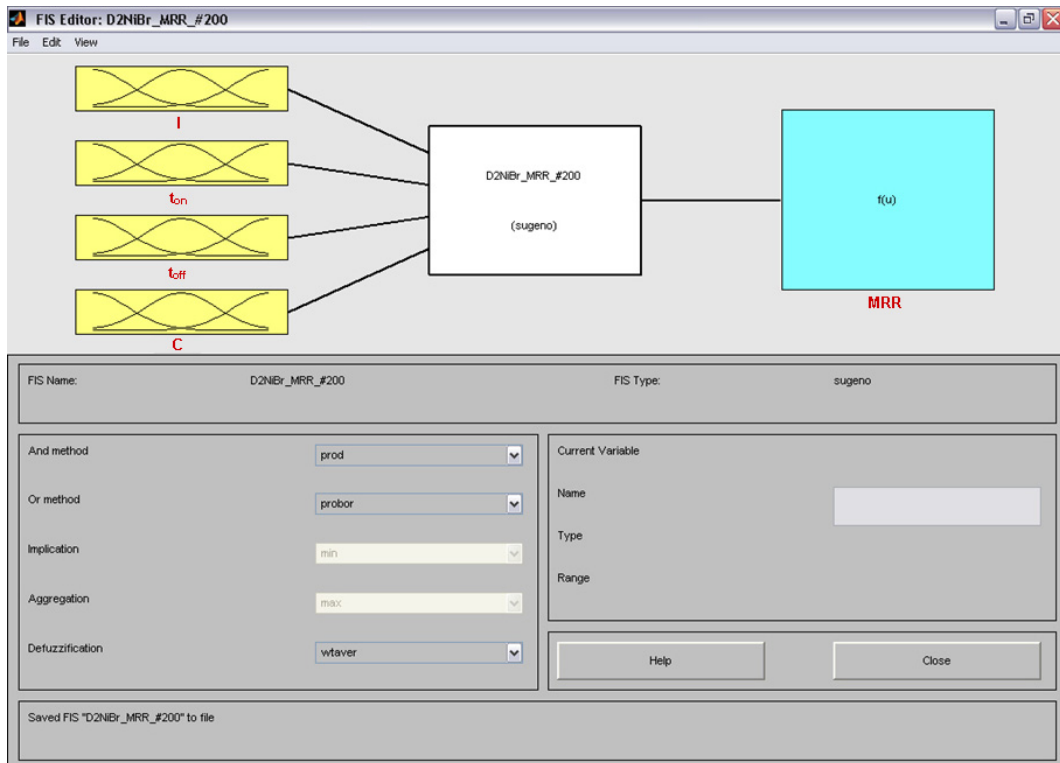


Figure 5.16 Schematic view of structure of the model for MRR

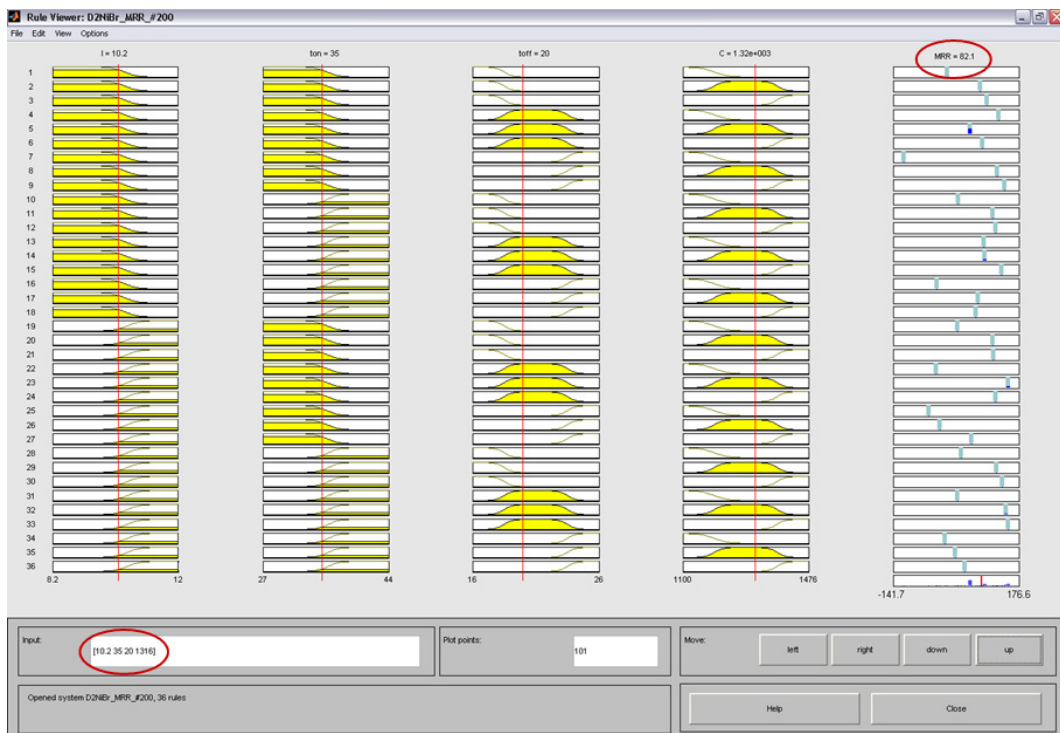


Figure 5.17 Obtaining results using Rule Viewer

As mentioned in the previous sections, many trials for MRR, EWR, and SR models of D2NiBr have been done using different MF types and various numbers of MFs.

The training and checking error curves for MRR, EWR and SR obtained after these trials are given in Appendix A, B and C, respectively. As seen from the results, the most appropriate combination was found to be **2 2 3 3** with *psigmf*. Therefore, in all models for case of D2NiBr, there are 36 *psigmf* MFs assigned to input parameters, and hence all models consist of 36 fuzzy rules. The output parameter in each model is defined by singleton type of MF since Sugeno inference system is used in ANFIS.

However, different epoch numbers were used for training the models for EWR and SR. Table 5.10 presents the properties of developed models for all output parameters (i.e. MRR, EWR and SR) for D2NiBr. The properties of models (i.e. selected epoch number, training and checking error values, and so on.) for other data sets (namely D2NiCu, D2TiBr, and D2TiCu) are also reported in Appendix D.

*Table 5.10 The properties of developed models for D2NiBr*

<b>Property name</b>	<b>MRR</b>	<b>EWR</b>	<b>SR</b>
Fuzzification method	Grid partitioning		
MF type for input parameters	psigmf		
Number of MFs for input parameters	2 2 3 3		
MF type for output parameter	Constant		
Total number of fuzzy rules	36		
Target error tolerance	0		
Number of epochs in training	200	100	125
Training error value	2.3465	0.035359	0.46762
Checking error value	29.0612	0.276	1.6551

## **5.4 Analysis of Models for Training Results**

The experimental values used for training the models and the corresponding values obtained from models are compared in Table 5.11. Their visual comparisons are also given in Fig. 5.18, 5.19, and 5.20. As seen from the results, the percentage errors between experimental and ANFIS values are nearly zero. This proves that the models for MRR, EWR, and SR in case of D2NiBr were trained very well. On the other hand, the errors in repeated experiments (i.e. experiment no. 5, 6, 7, 12, 22, 23, 31) are prominent due to the repeatability errors in experimental data. The output of

models corresponding to such experiments is a single value so that the adverse effect of repeatability error arising from experimental data can be compensated.

*Table 5.11 Experimental versus ANFIS results for training data for D2NiBr*

Exp. No.	MRR (mg/min)			EWR (mm/min)			SR ( $\mu\text{m}$ )			
	Exp.	ANFIS	Err. (%)	Exp.	ANFIS	Err. (%)	Exp.	ANFIS	Err. (%)	
1	61.869	61.900	0.051	0.384	0.384	0.015	10.941	10.900	0.375	
2	92.841	92.800	0.044	0.866	0.866	0.010	12.054	12.100	0.379	
3	128.193	128.000	0.151	1.825	1.820	0.265	3.982	3.980	0.042	
4	107.012	107.000	0.011	1.655	1.650	0.320	3.771	3.770	0.018	
5	80.847	82.100	1.549	0.814	0.730	10.271	12.809	11.200	12.561	
6	80.200	82.100	2.369	0.722	0.730	1.108	11.608	11.200	3.512	
7	78.600	82.100	4.453	0.702	0.730	3.989	12.305	11.200	8.980	
8	103.575	104.000	0.410	1.341	1.340	0.058	3.858	3.860	0.043	
9	136.235	136.000	0.173	2.118	2.120	0.111	3.863	3.860	0.069	
10	118.510	119.000	0.414	1.612	1.610	0.109	4.357	4.360	0.069	
11	69.042	69.000	0.060	0.701	0.701	0.055	11.483	11.500	0.151	
12	88.828	82.100	7.574	0.814	0.730	10.297	10.513	11.200	6.535	
13	117.843	118.000	0.133	1.498	1.500	0.131	4.037	4.040	0.066	
14	83.322	83.300	0.027	0.779	0.779	0.052	12.086	12.100	0.116	
15	102.023	102.000	0.022	0.827	0.827	0.034	10.659	10.700	0.388	
16	147.381	147.000	0.258	1.962	1.960	0.097	3.545	3.550	0.141	
17	89.486	89.500	0.015	0.742	0.742	0.030	10.630	10.600	0.282	
18	93.032	93.000	0.034	1.194	1.190	0.303	4.672	4.670	0.043	
19	81.371	81.400	0.036	0.941	0.941	0.036	10.690	10.700	0.090	
20	102.987	103.000	0.013	0.930	0.928	0.201	11.728	12.000	2.322	
21	93.832	93.800	0.034	0.822	0.822	0.013	12.277	12.300	0.190	
22	88.068	82.100	6.777	0.736	0.730	0.864	10.462	11.200	7.051	
23	84.444	82.100	2.776	0.736	0.730	0.755	11.592	11.200	3.382	
24	75.478	75.100	0.500	0.623	0.620	0.470	10.312	10.700	3.759	
25	82.187	82.200	0.016	0.675	0.675	0.035	11.633	11.600	0.284	
26	95.830	95.800	0.032	0.870	0.870	0.037	11.871	11.900	0.247	
27	94.277	94.300	0.025	1.219	1.220	0.070	3.810	3.810	0.009	
28	113.766	114.000	0.205	1.812	1.810	0.093	4.447	4.450	0.075	
29	62.807	63.100	0.466	0.611	0.609	0.365	11.105	11.300	1.753	
30	84.804	84.800	0.005	0.850	0.850	0.000	10.767	10.800	0.306	
31	73.941	82.100	11.035	0.576	0.730	26.684	10.005	11.200	11.940	
<i>Average Error (%):</i>			<b>1.280</b>				<b>1.835</b>			

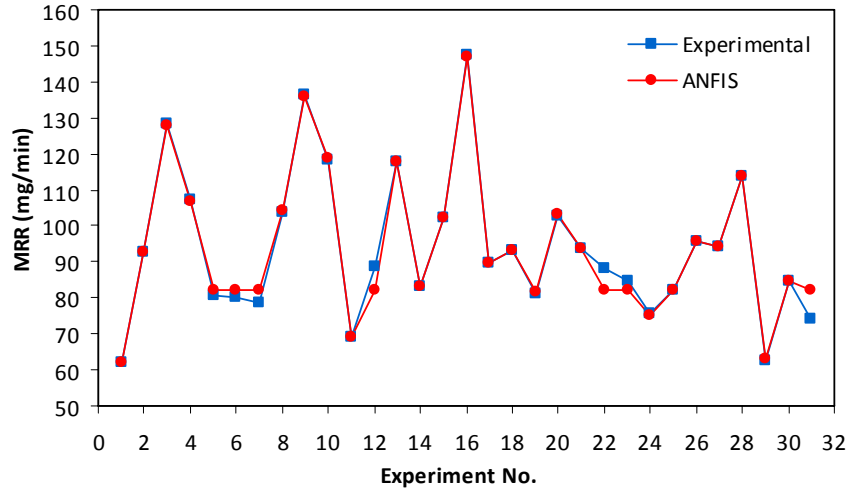


Figure 5.18 Experimental versus ANFIS results for training data of MRR

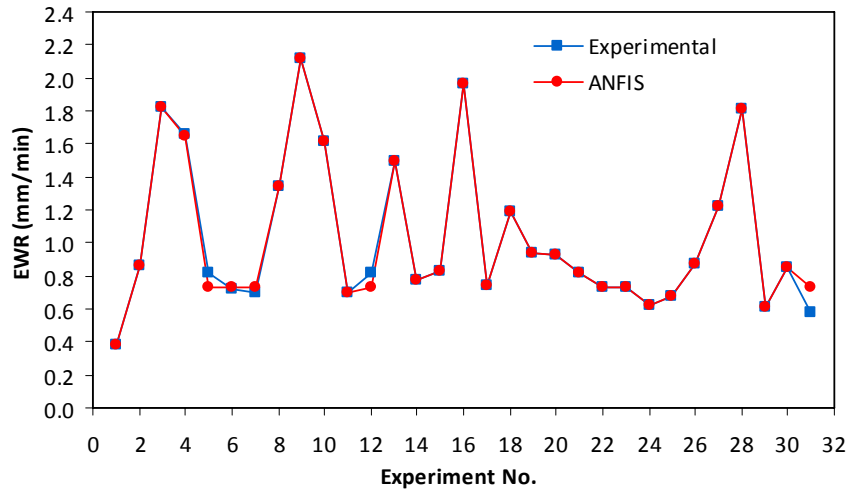


Figure 5.19 Experimental versus ANFIS results for training data of EWR

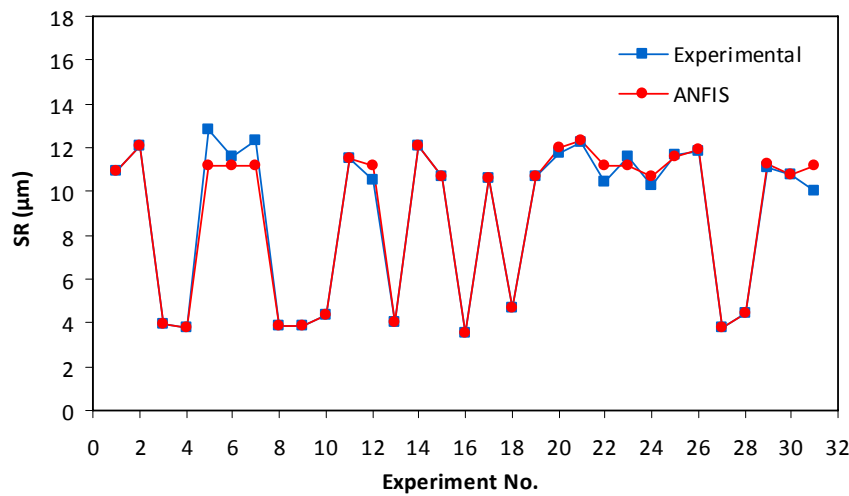
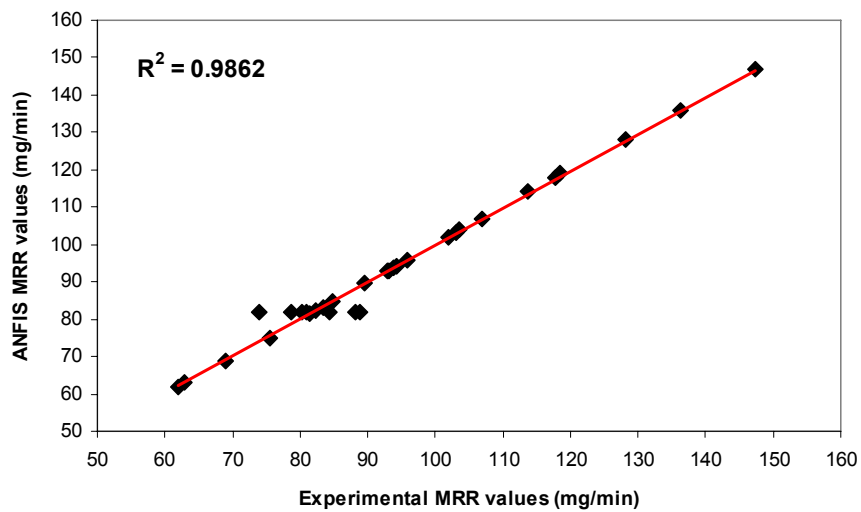
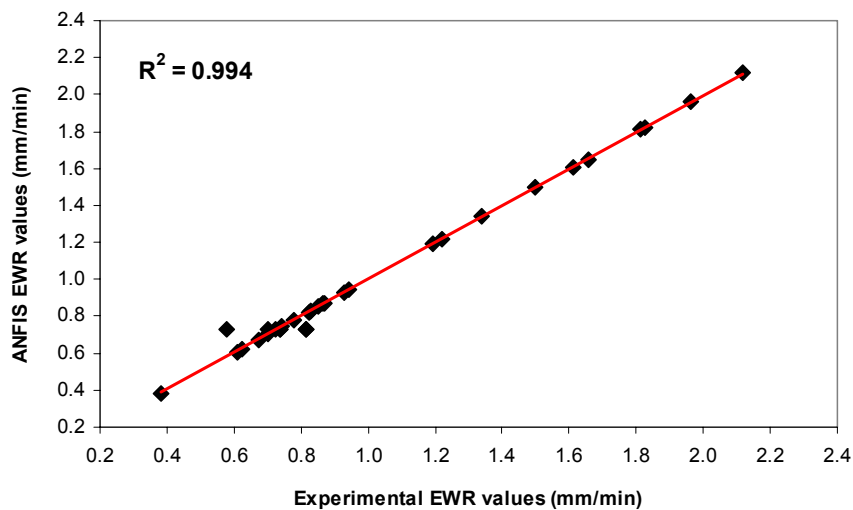


Figure 5.20 Experimental versus ANFIS results for training data of SR

Fig. 5.21, 5.22 and 5.23 presents the results of linear regression analysis for MRR, EWR and SR respectively. Regression analysis, denoted by  $R^2$ , is a measure of fitness (i.e. efficiency) of a model. Its value varies between 0 and 1. Higher values of  $R^2$  refer to well fitting models with high confidence levels whereas the models with poor fitness usually have lower  $R^2$  values. The developed models for MRR, EWR and SR exhibit very high  $R^2$  values when training data are taken into consideration. This means that the training of models was quite successful, and hence reliable results can be achieved using these models.



*Figure 5.21 Regression analysis for training data of MRR*



*Figure 5.22 Regression analysis for training data of EWR*

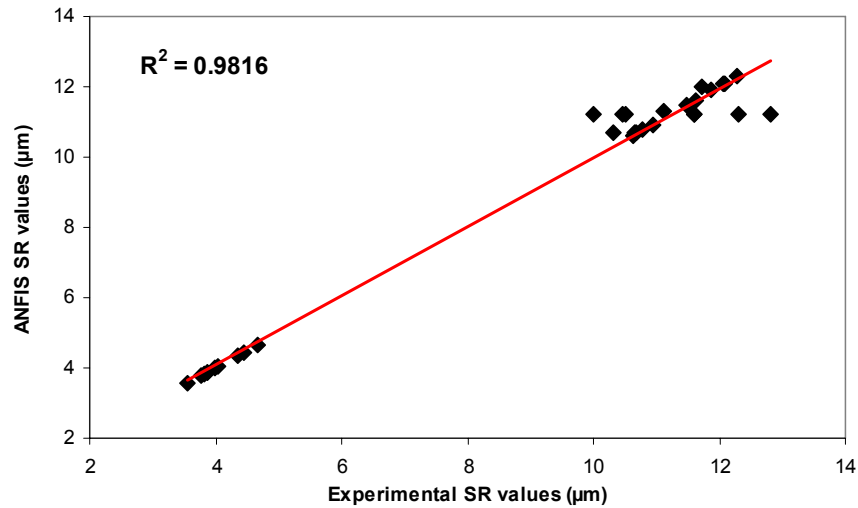


Figure 5.23 Regression analysis for training data of SR

### 5.5 Analysis of Models for Checking Results

The efficiency (i.e. the reliability) of developed models was also tested using checking data. The experiments included within checking data were not known by the models (i.e. such data were not used during the training of models). This way, response of models for experiments that are not recognized by the system can be predicted. Table 5.12 present the experimental values used for validation of the models and the corresponding values obtained from models.

Table 5.12 Experimental versus ANFIS results for checking data for D2NiBr

Exp. No.	MRR (mg/min)			EWR (mm/min)			SR (µm)		
	Exp.	ANFIS	Err. (%)	Exp.	ANFIS	Err. (%)	Exp.	ANFIS	Err. (%)
1	152.679	133.00	12.889	1.821	1.61	11.608	3.294	4.38	32.982
2	134.000	110.00	17.910	1.247	1.30	4.278	10.737	10.90	1.518
3	117.943	86.60	26.575	0.881	0.78	11.479	8.672	11.60	33.764
4	135.652	102.00	24.808	1.604	1.35	15.854	5.090	3.59	29.465
5	154.951	121.00	21.911	2.196	1.69	23.046	2.917	4.32	48.097
			<b>20.819</b>			<b>13.253</b>			<b>29.165</b>

Fig. 5.24, 5.25 and 5.26 compare the experimental and ANFIS results for validation of models. Predicted results are generally similar to experimental results although some results have relatively higher error values. The possible reasons for such errors may arise from repeatability errors, the errors due to operator and/or measurements, etc. which are discussed in Chapter 6.



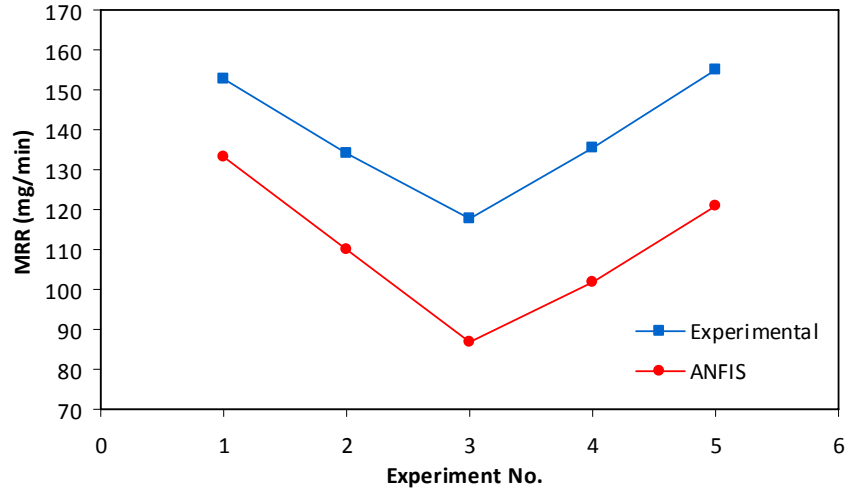


Figure 5.24 Experimental versus ANFIS results for checking data of MRR

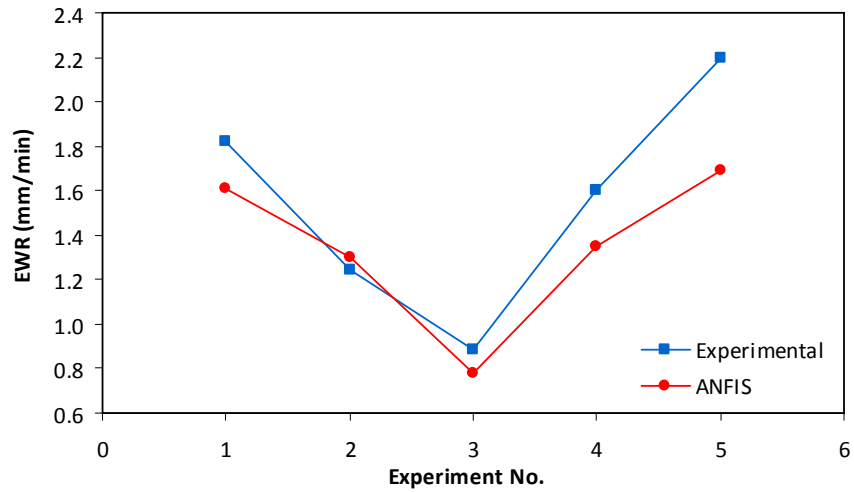


Figure 5.25 Experimental versus ANFIS results for checking data of EWR

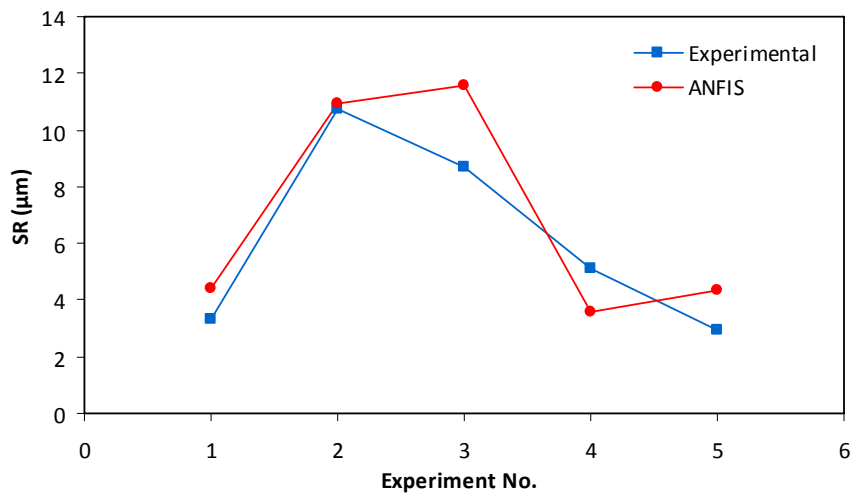


Figure 5.26 Experimental versus ANFIS results for checking data of SR

Regression analyses of checking data results for MRR, EWR and SR are given in Fig. 5.27, 5.28 and 5.29, respectively. Similar to regression results obtained for training data as reported previously, the models also exhibit relatively high fitness levels (i.e. high  $R^2$  values) for testing the efficiency of models using checking data. This proves that the developed models for D2NiBr were successfully trained and validated with a high level of fitness. Regarding the other data sets given in Appendix D, this may not be possible in all cases, particularly for validation of models, due to the fact that the models may always be trained well whereas the effectiveness in their validation may not be satisfactory.

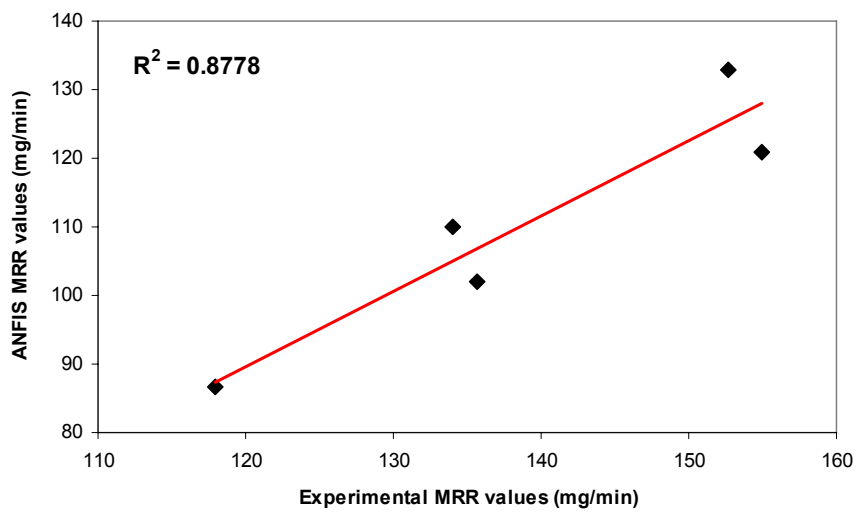


Figure 5.27 Regression analysis for checking data of MRR

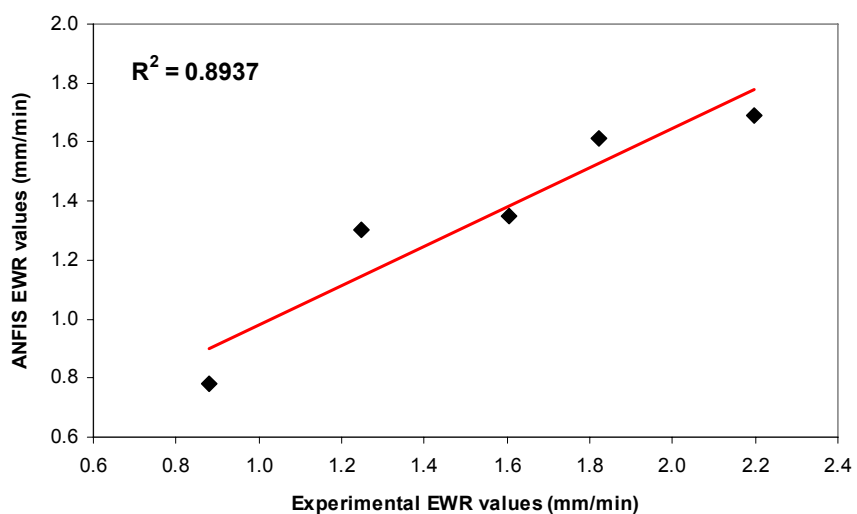


Figure 5.28 Regression analysis for checking data of EWR

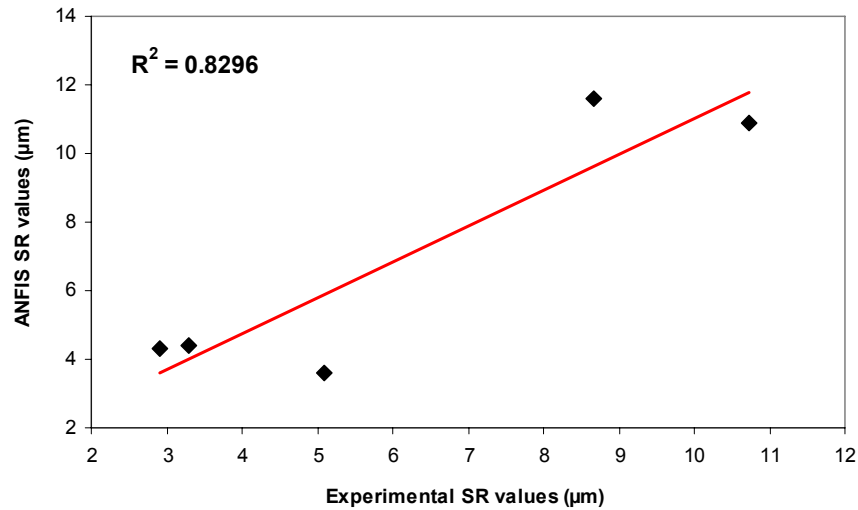


Figure 5.29 Regression analysis for checking data of SR

## 5.6 Summary

In case of D2NiBr, the models for MRR, EWR, and SR were developed using the identical modeling options in ANFIS. The models were trained and validated successfully by means of training and checking data. The results reveal that the applied methodology was appropriate and effective.

The same methodology was also applied to other sets of Ø2 mm (namely D2Nicu, D2TiBr, and D2TiCu); and the validation results are reported in Appendix D. In particular with validation of models, the results show that the models with high  $R^2$  values generally exhibit lower validation errors. This means that the models would present better prediction if their fitness level was higher.

## CHAPTER 6

### DISCUSSION AND CONCLUSIONS

#### 6.1 Discussions

The relationships between input and output parameters in hole drilling EDM process are very complicated and difficult to model using conventional approaches. Neuro-fuzzy models have been developed in this study by means of ANFIS technique within Matlab software. For this purpose, a number of holes ( $\text{\O}2$  mm) with input parameters (current, pulse-on and pulse-off time, and capacitance) have been conducted on two commonly used aerospace alloys (Ti-6Al-4V and Inconel 718) using two different electrode materials (brass and copper) in an environment of dielectric fluid (deionized water). The corresponding process outputs (MRR, EWR, and SR) have been determined. These data have been obtained from a research project recently completed in University of Gaziantep Yılmaz et al. (2010).

In this study, the aim was to predict the response of process (i.e. output values) under certain machining conditions (i.e. given values of inputs). This was accomplished by developing models for each process output using different data sets with a combination of each workpiece and electrode material. In other words, using  $\text{\O}2$  mm electrodes, 12 models in total have been developed separately in order to predict the values of MRR, EWR, and SR for case of drilling holes on both workpiece materials using both electrode materials. For the ease of understanding, these models were given a specific code (e.g. D2NiBr\_MRR refers to the model for machining Inconel 718 using brass electrode with diameter of  $\text{\O}2$  mm for prediction of MRR output).

Each model has been trained using training data consisting of 31 experiments. The number of these experiments and their machining conditions were specified by design of experiments with central composite design technique. The type and number of membership functions were identical for training of all models. After training stage, all models have been validated by means of 5 additional experiments that were not included within experimental training data. This way, the effectiveness of models was tested in accordance with a number of validation experiments which were unknown to the system. Therefore, the accuracy of developed models was checked by comparison of experimental results with outputs from models. Moreover, linear regression analyses were done in order to test the reliability of models.

## **6.2 Conclusions**

The highlights and concluding remarks of this study are as follows:

- Neuro-fuzzy models developed in this study using ANFIS methodology with hybrid learning algorithm can be used to define input-output relationships in hole drilling EDM process. Such models can predict the values of process outputs for given input parameters within the lowest error range.
- There are some errors between experimental results and results obtained from models. This is caused by several reasons related to experimental aspects. The errors within experimental data may arise from experimental setup and apparatus such as improper or insufficient electrode rotation, the problems in alignment of specimens on the vise, incorrect choice of type of dielectric fluid, insufficient pumping pressure of dielectric fluid. Such errors may also come from unknown or uncontrollable environmental factors as well as the irregularities in microstructure of workpiece and electrode materials. Furthermore, erroneous measurements performed by the operator during and after operation are existent.
- Due to use of design of experiments, seven experiments out of 31 experiments were repeated under the same machining conditions. However, the results of these experiments were different due to the reasons explained above. This is called repeatability error that is inevitable in experimental studies, and it has been introduced into the system during training of models.

- From modeling viewpoint, some errors are introduced by selection of method of inference system (i.e. grid partitioning versus subtractive clustering), inappropriate choice of type and number of membership functions which may result in faulty or insufficient number of rules, use of incorrect epoch number during training, etc.
- In conclusion, this study provides a hybrid approach by adapting learning algorithm of neural networks into advanced modeling capabilities of fuzzy logic technique. The reliability and accuracy of models developed in this study can be improved by aspects in the following section.

### **6.3 Future Studies**

The recommendations on potential future works are as follows:

- It is evident that training and validating models without any errors is not possible. However, the efficiency of models can be improved by refining the experimental data and eliminating/minimizing the errors mentioned in the previous section.
- The models can also be enhanced by selecting different modeling options such as using different type and number of membership functions, using subtractive clustering method, training parameters and epoch numbers, etc. as well as increasing the number of training and validation data.
- The methodology in this study can be used with different workpiece and electrode materials, various electrode diameters, different machining conditions, and so on.
- Furthermore, the other advanced and AI techniques can be adapted so that the efficiency and accuracy of models can be improved. Such techniques can also enable the optimization of process outputs.

## REFERENCES

Behrens, A., and Ginzel, J. (2003). Neuro-fuzzy process control system for sinking EDM. *Journal of Manufacturing Processes*, **5**(1), 33-39.

Bozdana, A.T. (1999). Development of an expert system for the determination of injection moulding parameters of thermoplastics. *MSc thesis in Mechanical Engineering*, University of Gaziantep, Turkey.

Bozdana, A.T., Yılmaz, O., Okka, M.A., and Filiz, İ.H. (2009). A comparative experimental study on fast hole EDM of Inconel 718 and Ti-6Al-4V. *5<sup>th</sup> International Conference and Exhibition on Design and Production of MACHINES and DIES/MOLDS*, Kuşadası, Turkey.

Çaydaş, U., Hasçalık, A., Ekici, S. (2009). An adaptive neuro-fuzzy inference system (ANFIS) model for wire-EDM. *Expert Systems with Applications*, **36**, 6135-6139.

Fuzzy Logic Toolbox in Matlab – User's Guide (<http://www.mathworks.com>)

Guiqin, L., Fanhui, K., Wenle, L., Quingfeng, Y., and Minglun, F. (2007). The neural fuzzy modeling and genetic optimization in WEDM. *IEEE International Conference on Control and Automation*, 1440-1443.

Ho, K.H., and Newman, S.T. (2003). State of the art electrical discharge machining. *International Journal of Machine Tools and Manufacture*, **43**, 1287-1300.

Jameson, E.C. (2001). *Electrical Discharge Machining*. Michigan: Society of Manufacturing Engineers, ISBN: 087263521X.

Jang, J.-S. R. (1993). ANFIS: Adaptive-Network-Based Fuzzy Inference System. *IEEE Transactions on Systems, Man, and Cybernetics*, **23**(3), 665-685.

Jang, J.-S. R. (...). Frequently Asked Questions - ANFIS in Fuzzy Logic Toolbox (<http://www.cs.nthu.edu.tw/~jang/anfisfaq.htm>)

Jiann Sheng Machinery & Electric Industrial Co. Ltd. (<http://www.jsedm.com>)

Jung, J.W., Ko, S.H., Jeong, Y.H., Min, B.-K., Lee, S.J. (2007) Estimation of Material Removal Volume of a Micro-EDM Drilled Hole Using Discharge Pulse Monitoring. *International Journal of Precision Engineering and Manufacturing*, **8**(4), 45-49.

Kaneko, T., and Onodera, T. (2004) Improvement in machining performance of die-sinking EDM by using self-adjusting fuzzy control. *Journal of Materials Processing Technology*, **149**, 204-211.

Kao, C.C., Shih, A.J., and Miller, S.F. (2008). Fuzzy logic control of microhole electrical discharge machining. *Journal of Manufacturing Science and Engineering (ASME)*, **130**, 064502:1-6.

Kao, C.C., and Shih, A.J. (2008). Design and tuning of a fuzzy logic controller for micro-hole electrical discharge machining. *Journal of Manufacturing Processes*, **10**, 61-73.

Kao, J.Y., Tsao, C.C., Wang, S.S., and Hsu, C.Y. (2010). Optimization of the EDM parameters on machining Ti-6Al-4V with multiple quality characteristics. *International Journal of Advanced Manufacturing Technology*, **47**, 395-402.

Kumar, S., Singh, R., Singh, T.P., Sethi, B.L. (2009). Surface modification by electrical discharge machining: A review. *Journal of Materials Processing Technology*, **209**, 3675-3687.

Lazarenko, B.R. (1943). To invert the effect of wear on electric power contacts. *Dissertation of the All-Union Institute for Electro Technique in Moscow* (in Russian).



Leao, F.N., and Pashby, I.R., Cuttell, M., Lord, P. (2005). Optimisation of EDM fast hole-drilling through evaluation of dielectric and electrode materials. *18<sup>th</sup> International Congress of Mechanical Engineering (COBEM)*, 6-11 November, Ouro Preto, Brazil.

Lee, W.M., and Liao, Y.S. (2007). Adaptive control of the WEDM process using a self-tuning fuzzy logic algorithm with grey prediction. *International Journal of Advanced Manufacturing Technology*, **34**, 527-537.

Lin, C.L., Lin, J.L., and Ko, T.C. (2002). Optimisation of the EDM Process based on the Orthogonal Array with Fuzzy Logic and Grey Relational Analysis Method. *International Journal of Advanced Manufacturing Technology*, **19**, 271-277.

Lin, J.L., and Lin, C.L. (2005). The use of grey-fuzzy logic for the optimization of the manufacturing process. *Journal of Materials Processing Technology*, **160**, 9-14.

Maji, K., and Pratihari, D.K. (2010). Forward and reverse mappings of electrical discharge machining process using adaptive network-based fuzzy inference system. *Expert Systems with Applications*, **37**, 8566-8574.

Mamdani, E.H., and Assilian, S. (1975). An experiment in linguistic synthesis with a fuzzy logic controller. *International Journal of Man–Machine Studies*, **7**(1), 1-13.

Montgomery, D.C. (2000). *Design and Analysis of Experiments*. John Wiley and Sons, ISBN: 0471316490.

Negnevitsky, M. (2005). *Artificial Intelligence - A Guide to Intelligent Systems*. (2<sup>nd</sup> ed.). Pearson Education Ltd., ISBN: 0321204662.

Pham, D.T., Dimov, S.S., Bigot, S., Ivanov, A., and Popov, K. (2004). Micro-EDM - recent developments and research issues. *Journal of Materials Processing Technology*, **149**, 50-57.

Pradhan, M.K., and Biswas, C.K. (2010). Neuro-fuzzy and neural network-based prediction of various responses in electrical discharge machining of AISI D2 steel. *International Journal of Advanced Manufacturing Technology*, **50**, 591-610.

Puri, Y.M., and Deshpande, N.V. (2004). Simultaneous optimization of multiple quality characteristics of WEDM based on fuzzy logic and taguchi technique. *5<sup>th</sup> Asia Pacific Industrial Engineering and Management Systems Conference*, Gold Coast, Australia.

Rao, G.K.M., Rangajanardhaab, G., Rao, D.H., and Rao, M.S. (2009). Development of hybrid model and optimization of surface roughness in electric discharge machining using artificial neural networks and genetic algorithm. *Journal of Materials Processing Technology*, **209**, 1512-1520.

Ross, T.J. (2009). *Fuzzy Logic with Engineering Applications*. (3<sup>rd</sup> ed.). McGraw-Hill, USA, ISBN: 9780470743768.

Sugeno, M. (1985). *Industrial Applications of Fuzzy Control*. North-Holland, Amsterdam, ISBN: 0444878297.

Tsai, K.M., and Wang, P.J. (2001a). Predictions on surface finish in electrical discharge machining based upon neural network models. *International Journal of Machine Tools & Manufacture*, **41**, 1385-1403.

Tsai, K.M., and Wang, P.J. (2001b). Comparisons of neural network models on material removal rate in electrical discharge machining. *Journal of Materials Processing Technology*, **117**, 111-124.

Tzeng, Y.-F., and Chen, F.-C. (2007). Multi-objective optimisation of high-speed electrical discharge machining process using a taguchi fuzzy-based approach. *Materials and Design*, **28**, 1159-1168.

Yan, M.T., Li, H.P., and Liang, J.F. (1999). The application of fuzzy control strategy in servo feed control of wire electrical discharge machining. *International Journal of Advanced Manufacturing Technology*, **15**, 780-784.

Yang, Y., Yanghan, M., and Tian, H. (2010). Research of the micro-EDM discharge state detection method based on Matlab fuzzy control. *International Conference on Mechanic Automation and Control Engineering (MACE)*, Wuhan, China.

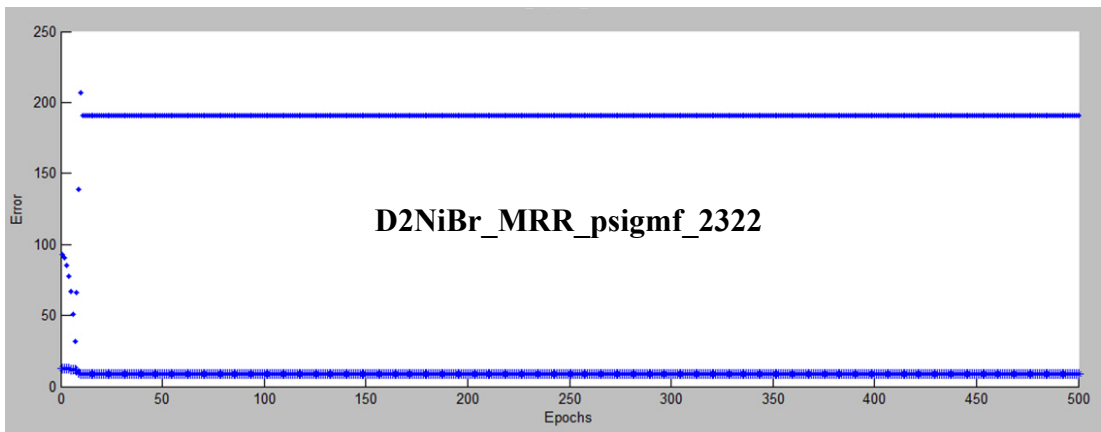
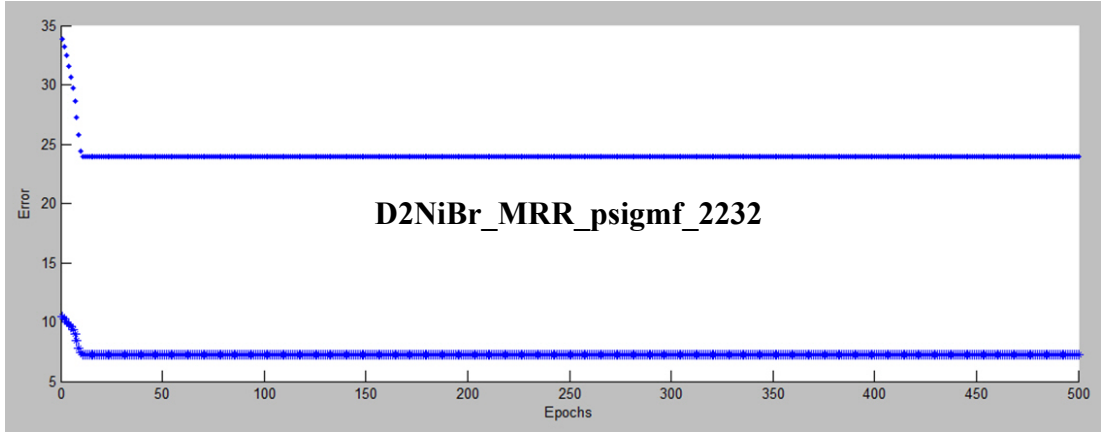
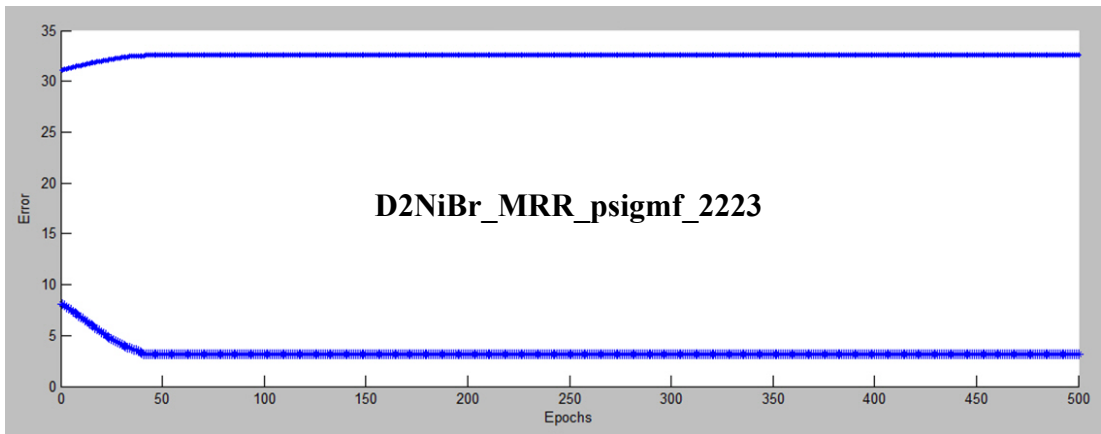
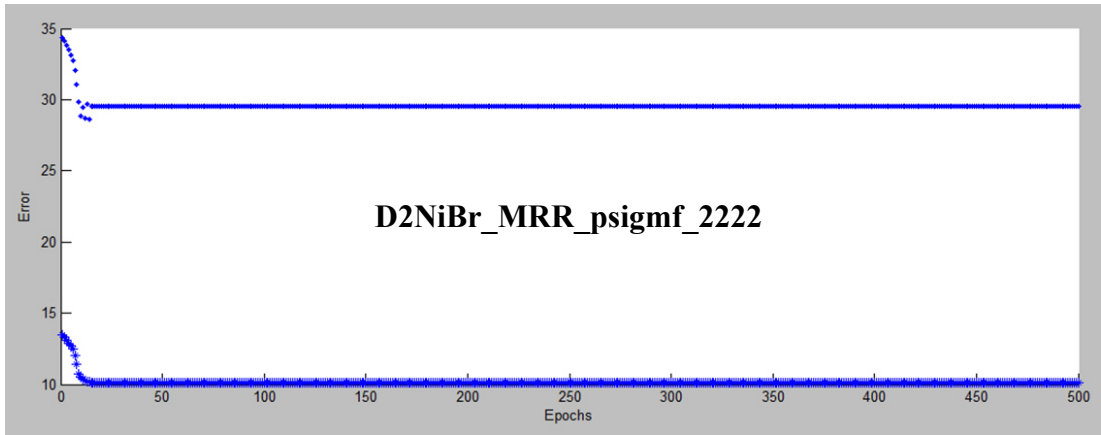
Yılmaz, O., Bozdana, A.T., Okka, M.A., and Filiz, İ.H. (2010). Fast hole drilling of nickel and titanium alloys for aerospace applications using electrical discharge machining. *Research Project supported by Scientific and Technological Research Council of Turkey (TUBITAK)*, University of Gaziantep, Turkey, Project No: 108M022.

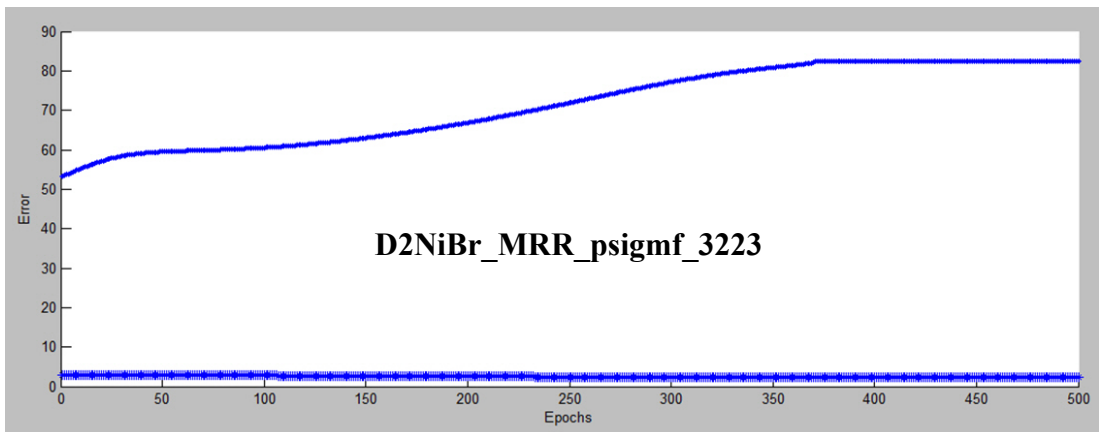
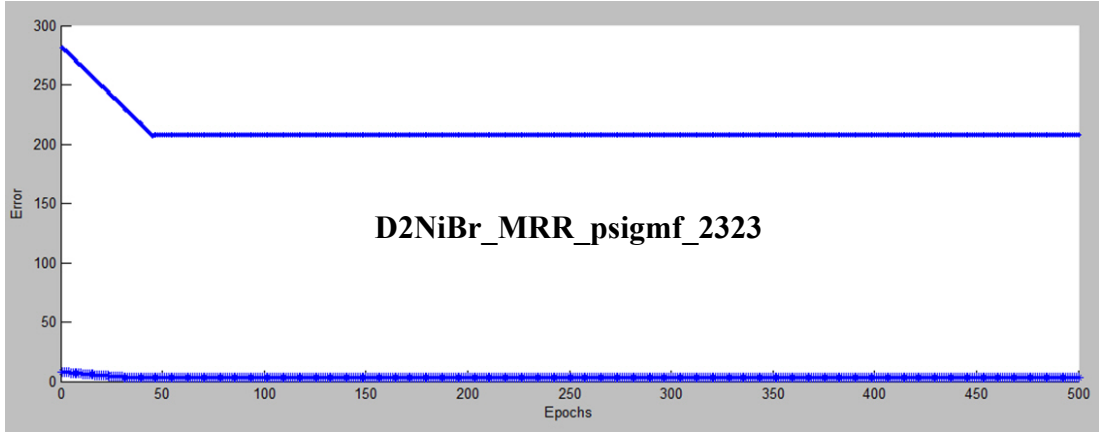
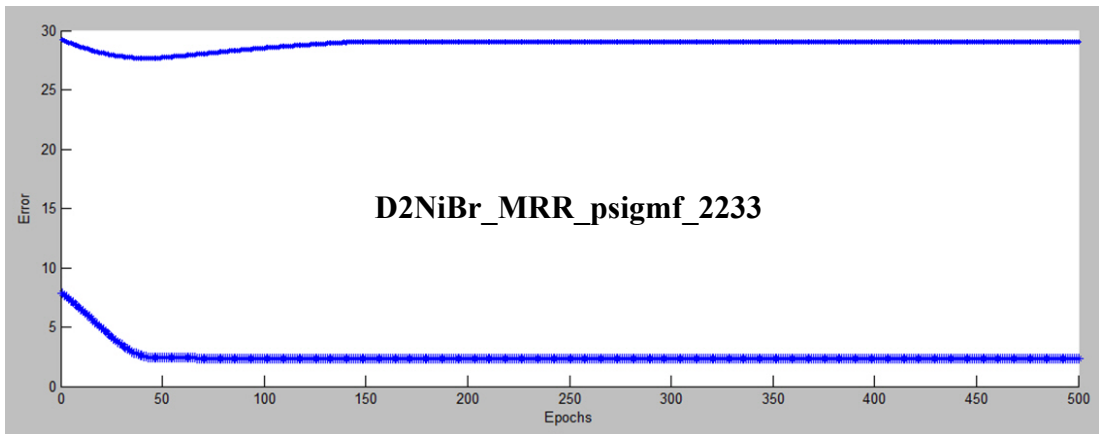
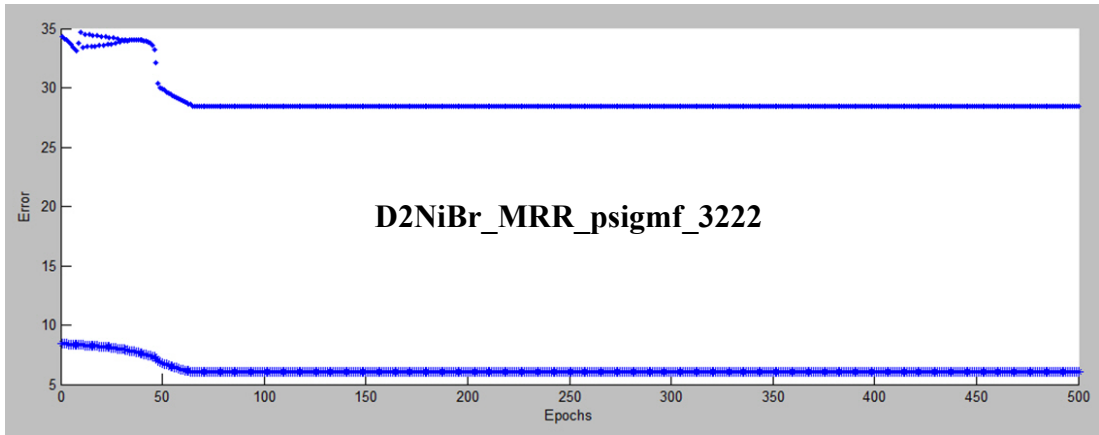
Yılmaz, O., Eyercioğlu, Ö., and Gindy, N.N.Z. (2006). A user-friendly fuzzy-based system for the selection of electro discharge machining process parameters. *Journal of Materials Processing Technology*, **172**, 363-371.

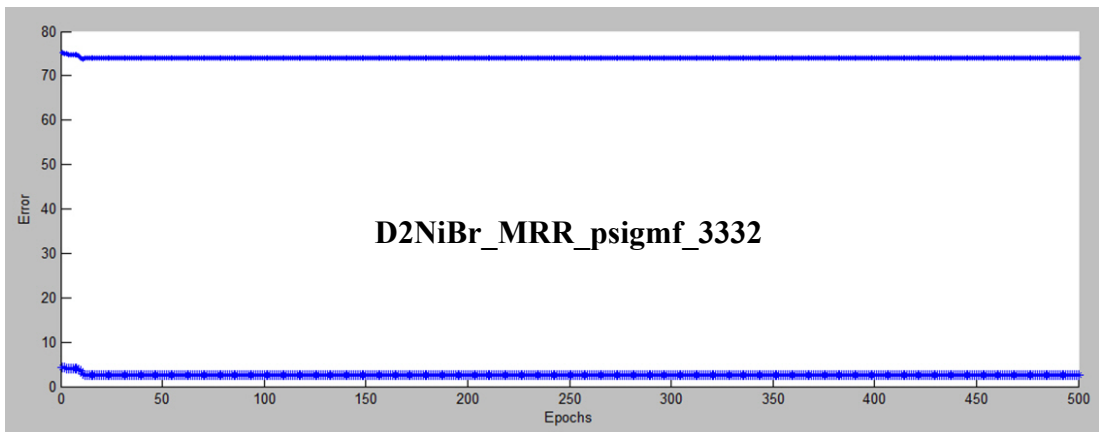
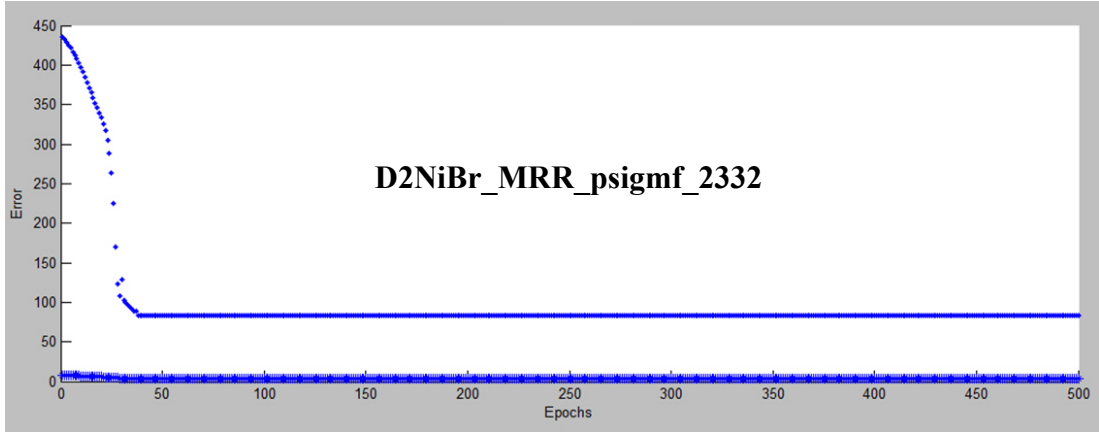
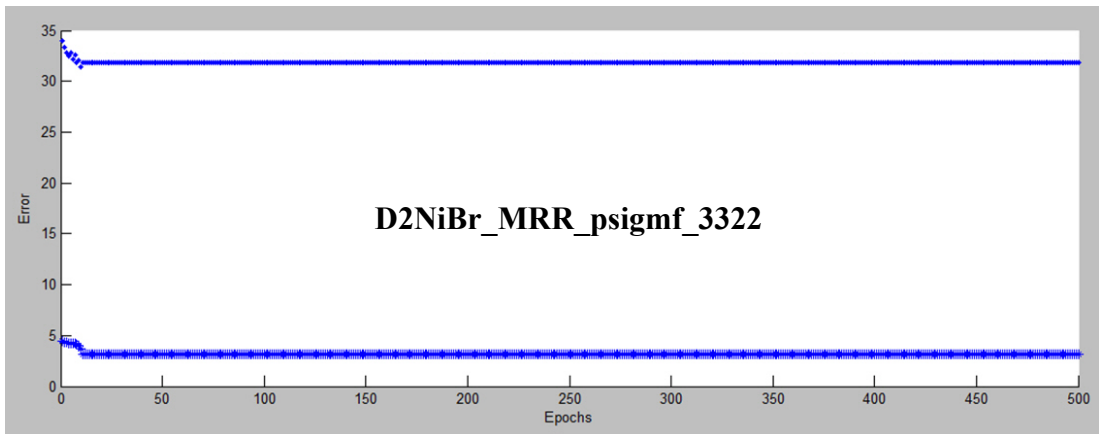
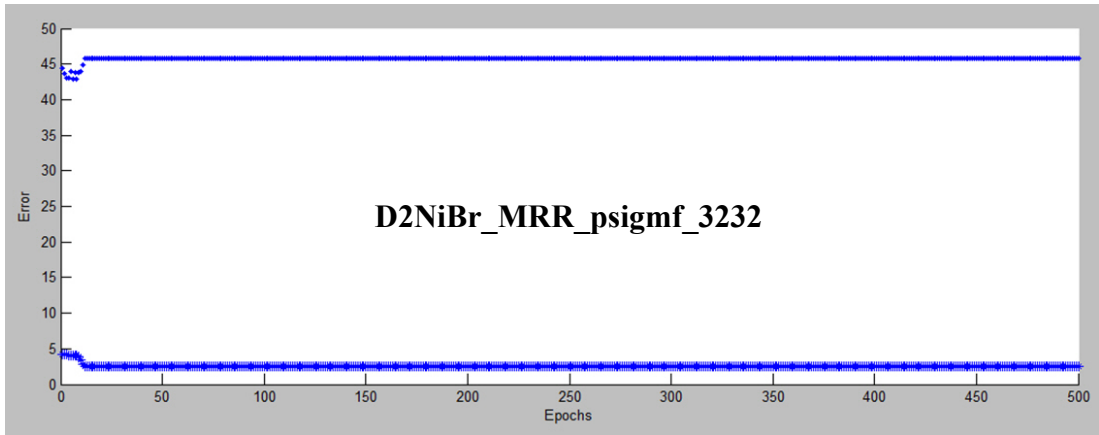
Zadeh, L.A. (1965). Fuzzy sets. *Information and Control*, **8**, 338-353.

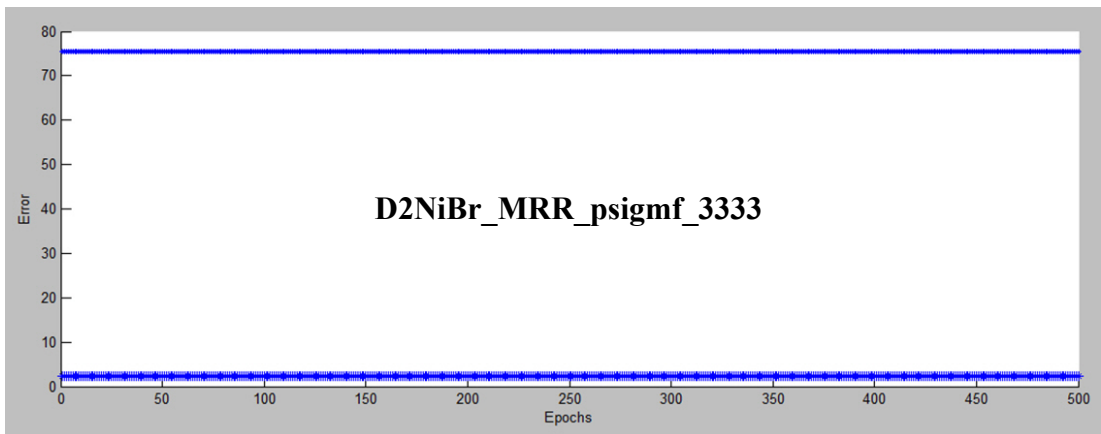
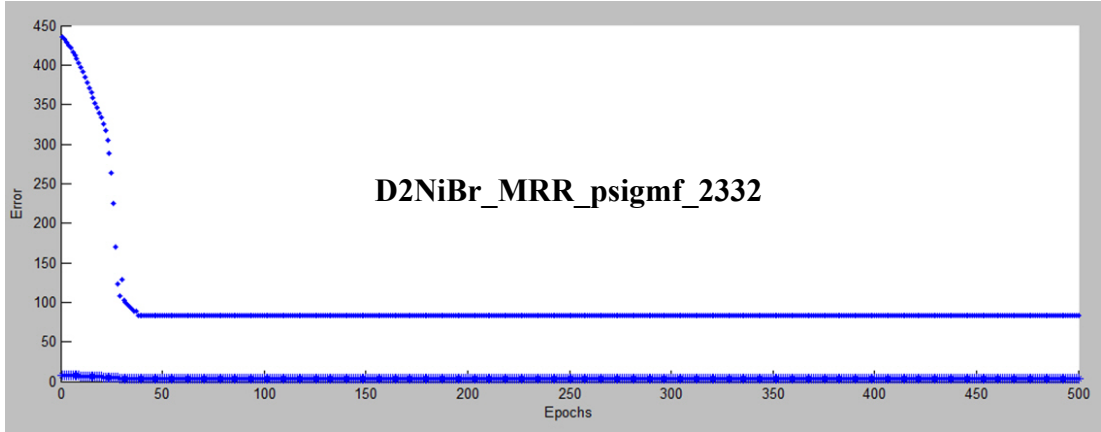
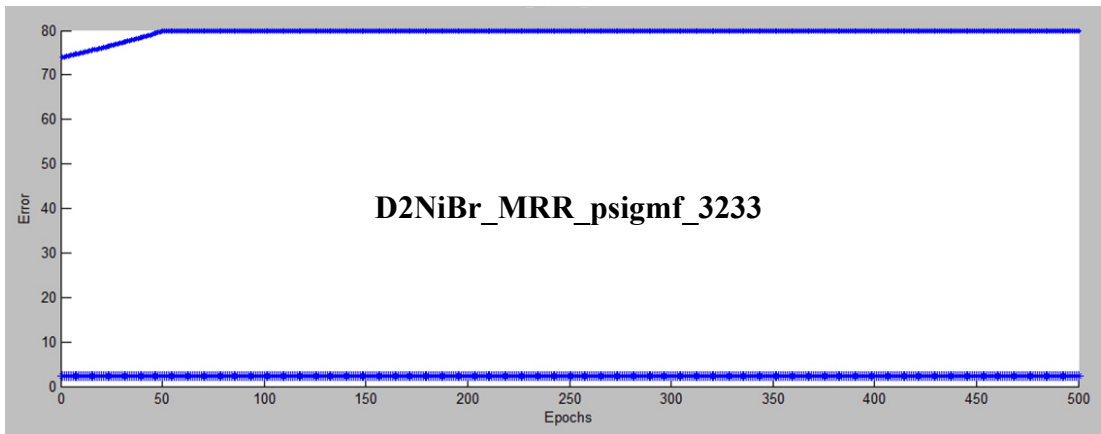
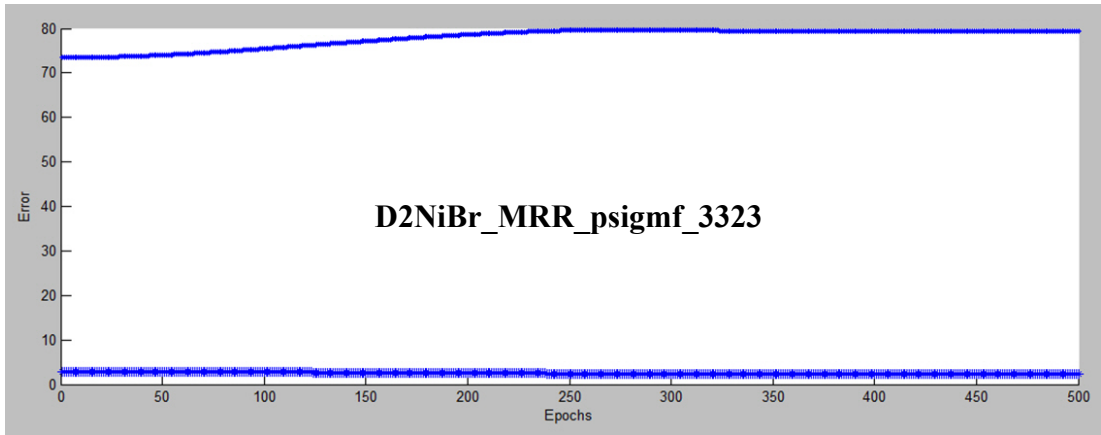
## **APPENDIX A**

### **TRIALS FOR D2NIBR\_MRR**

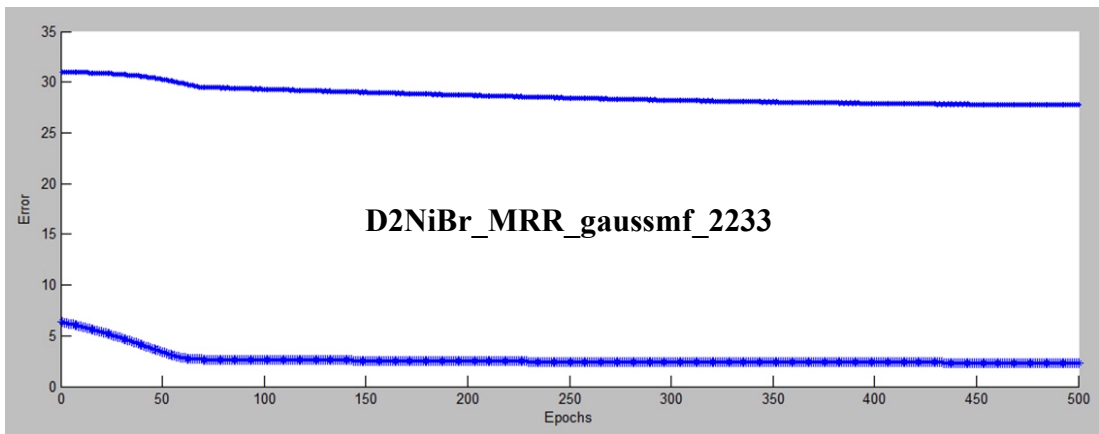
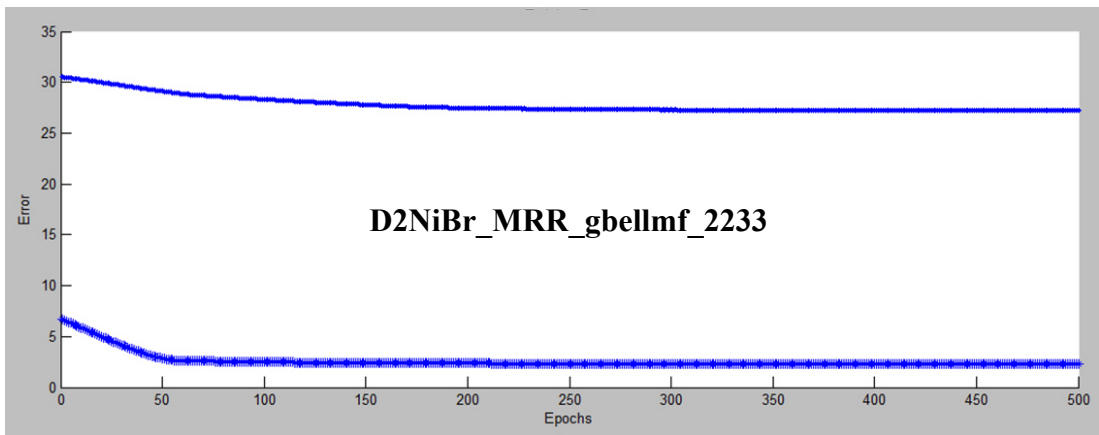
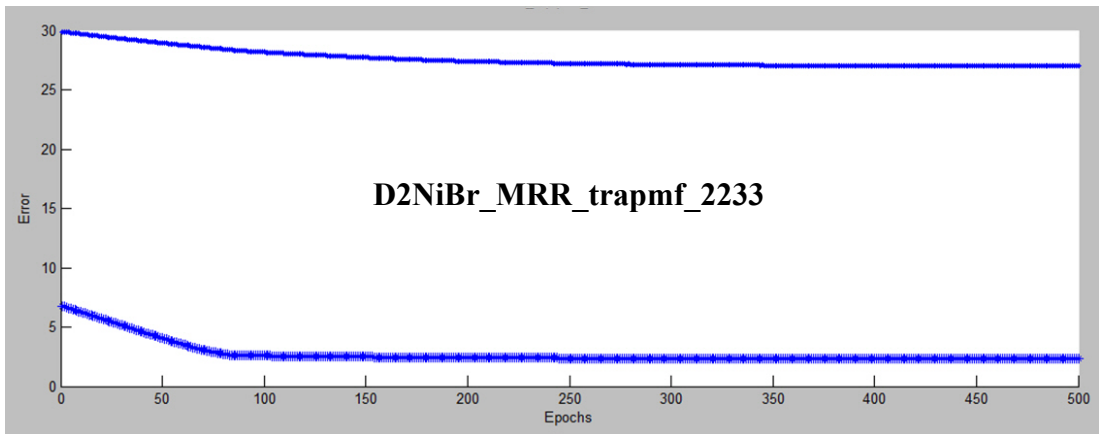
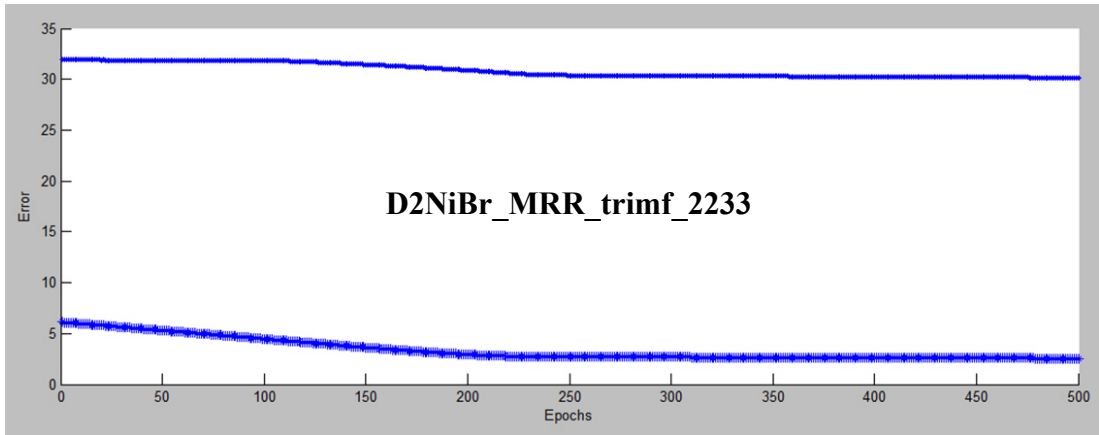






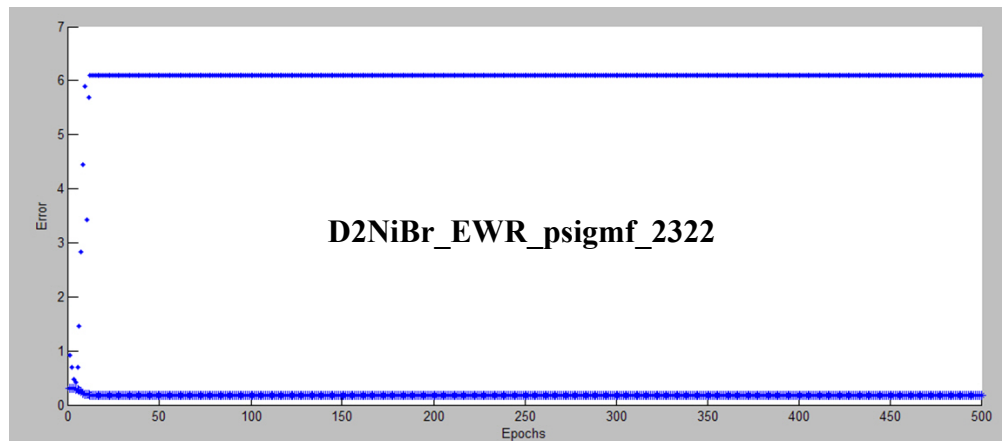
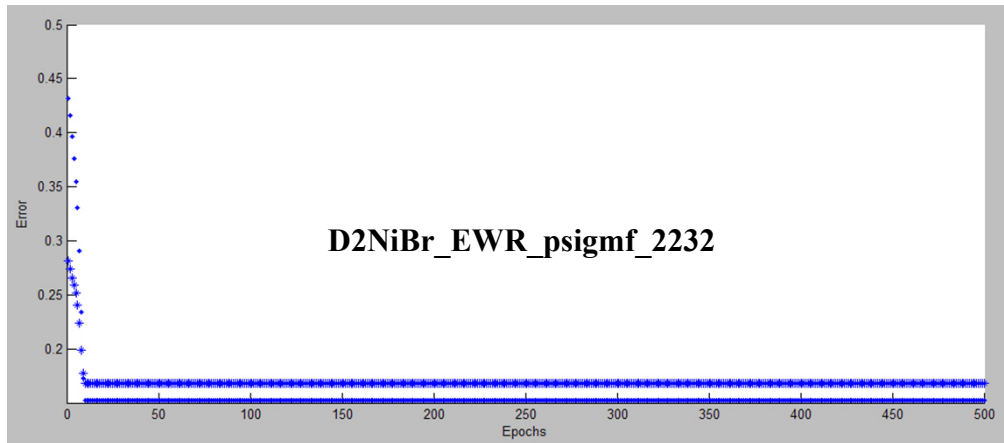
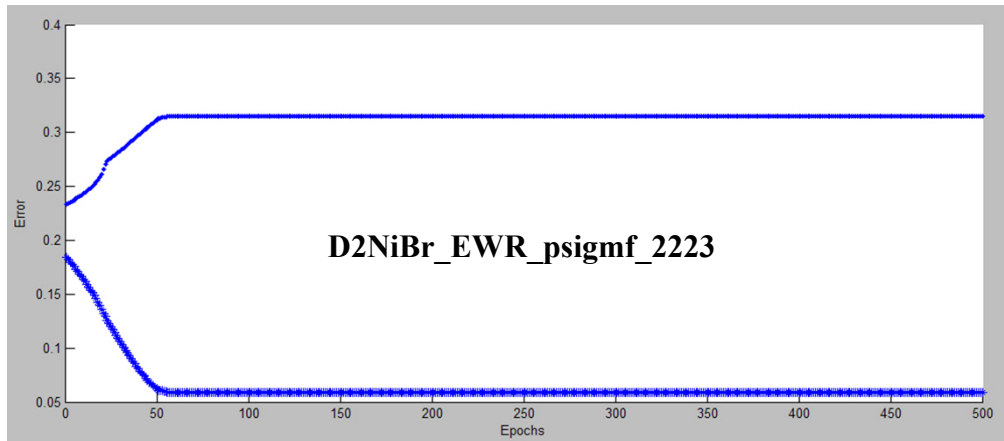
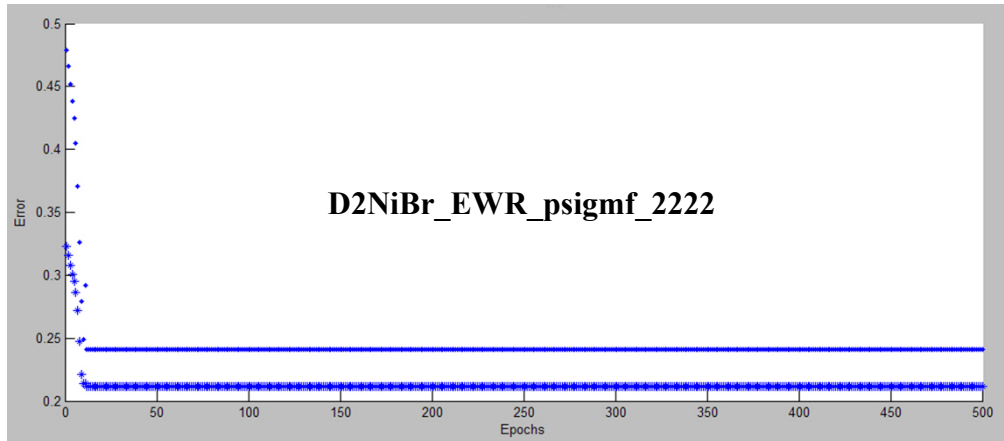


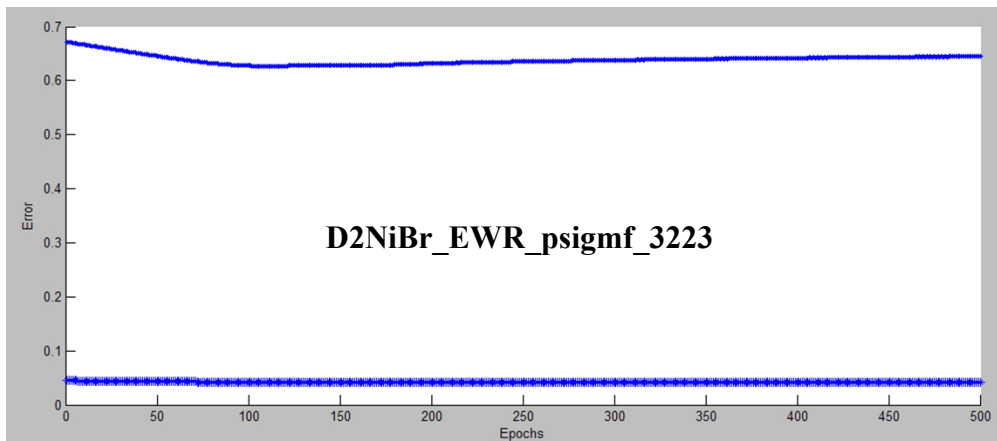
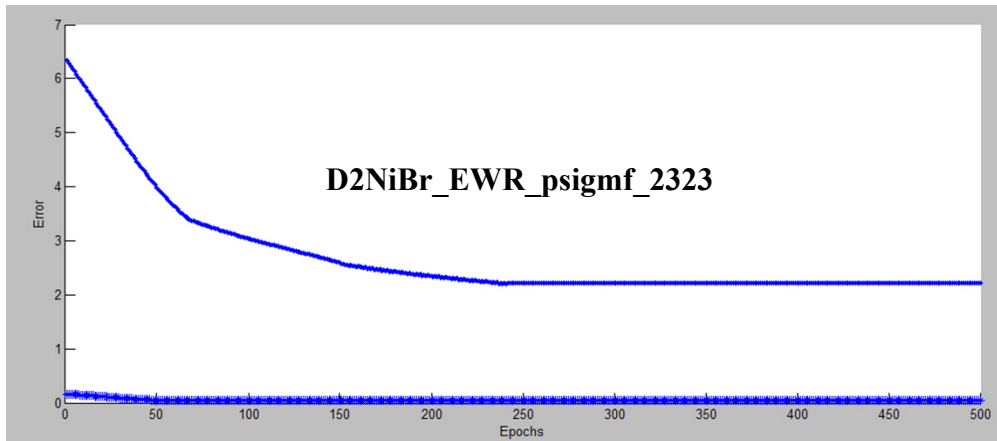
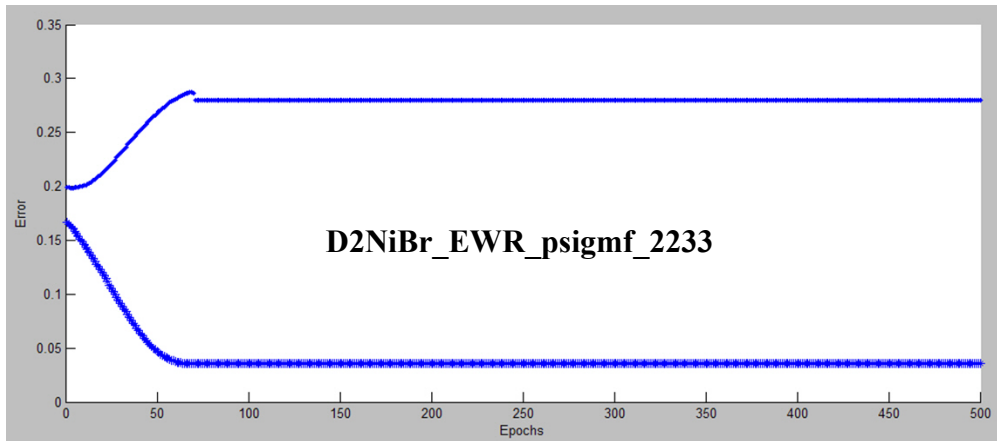
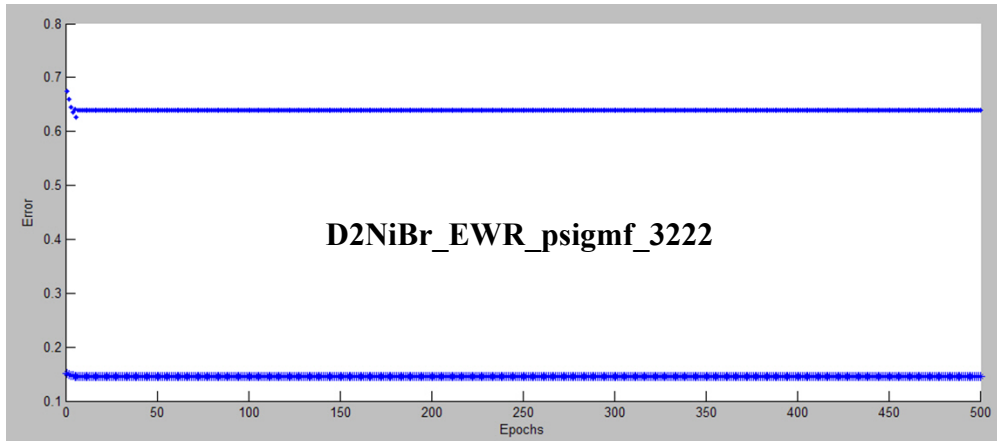


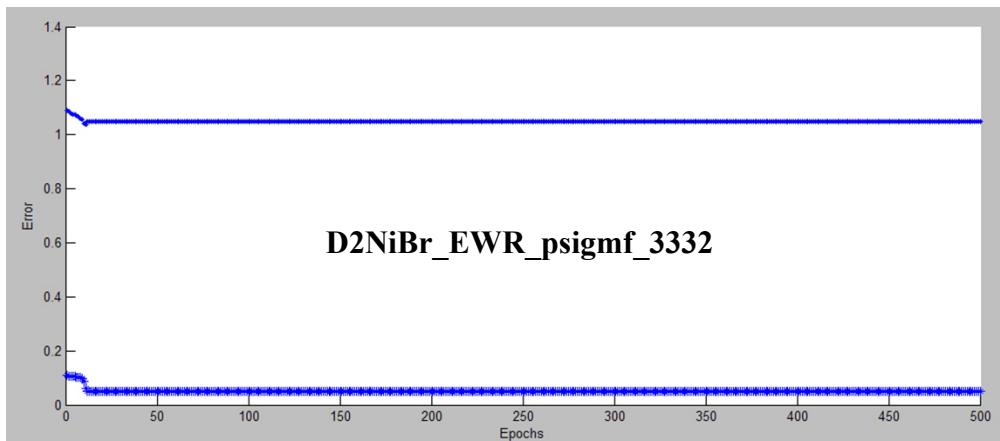
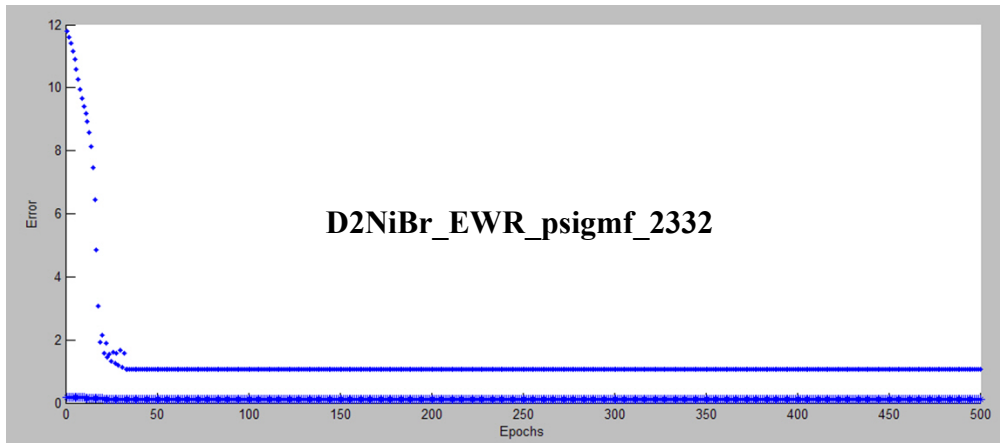
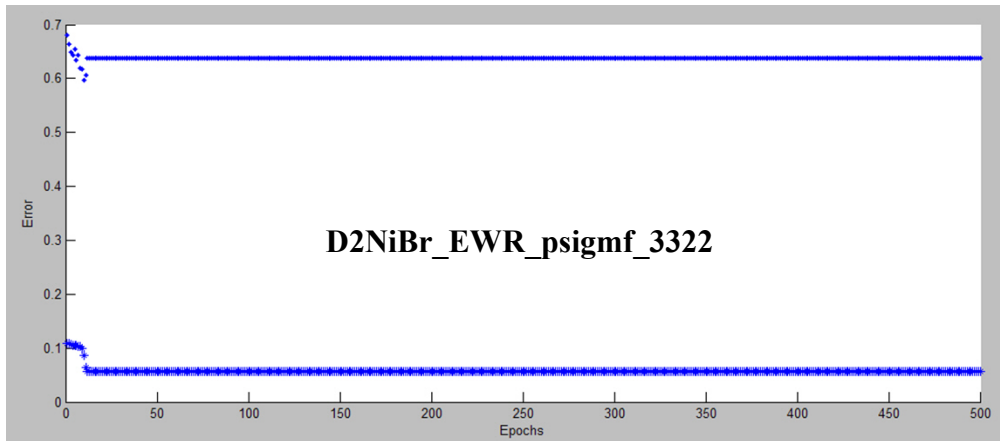
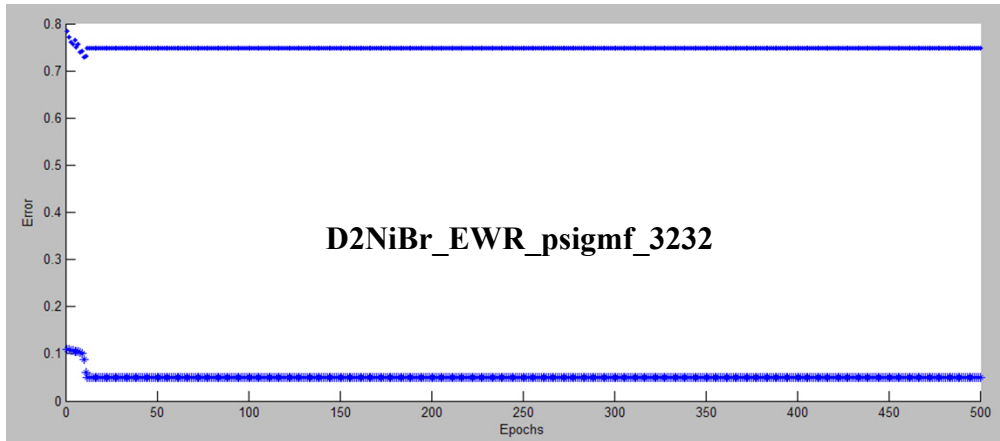


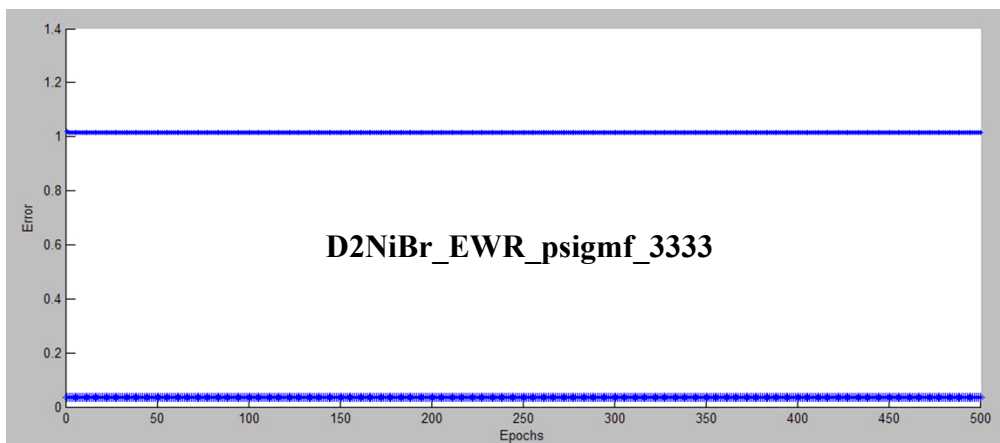
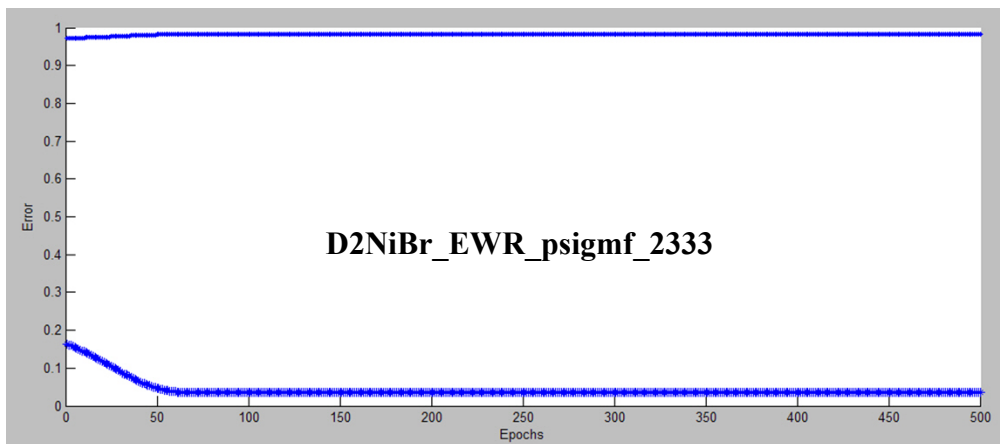
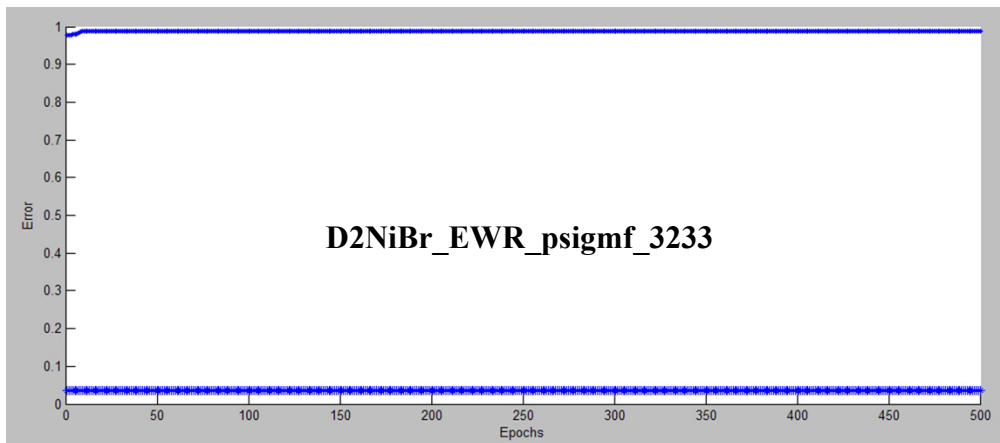
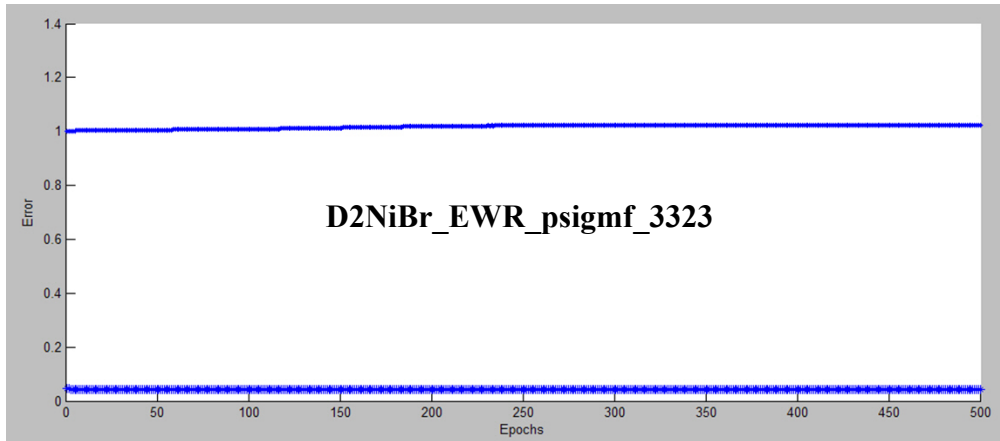
## **APPENDIX B**

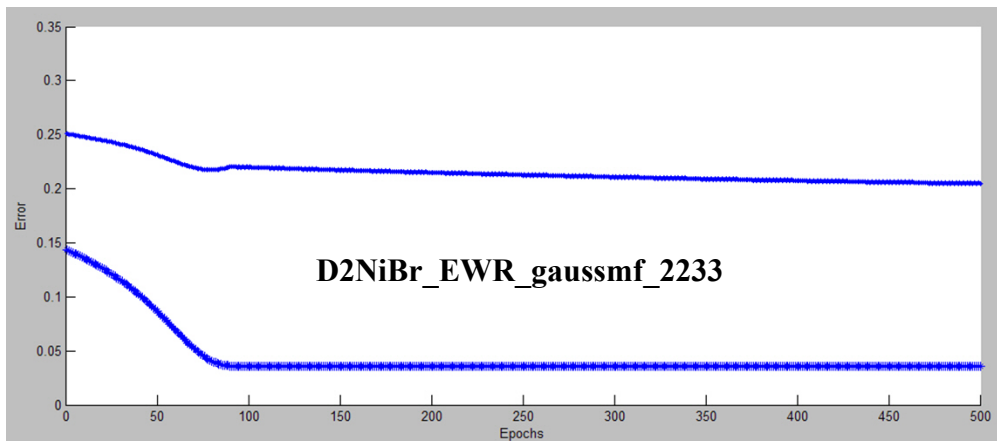
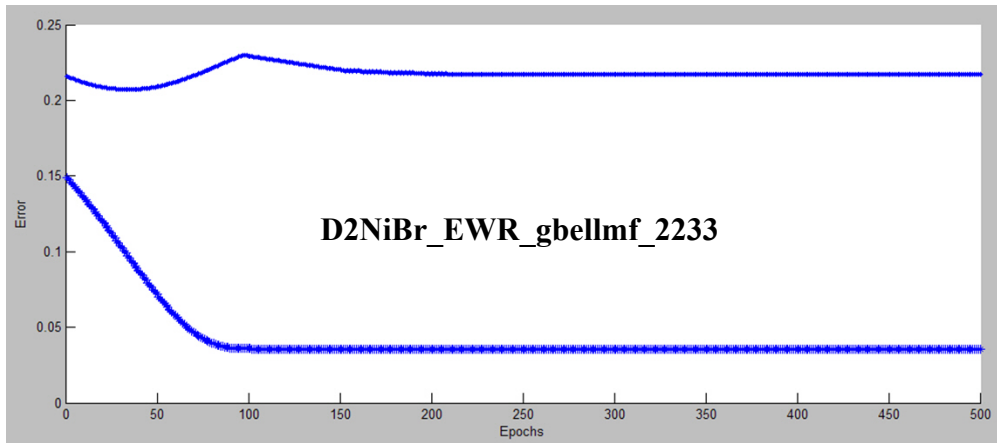
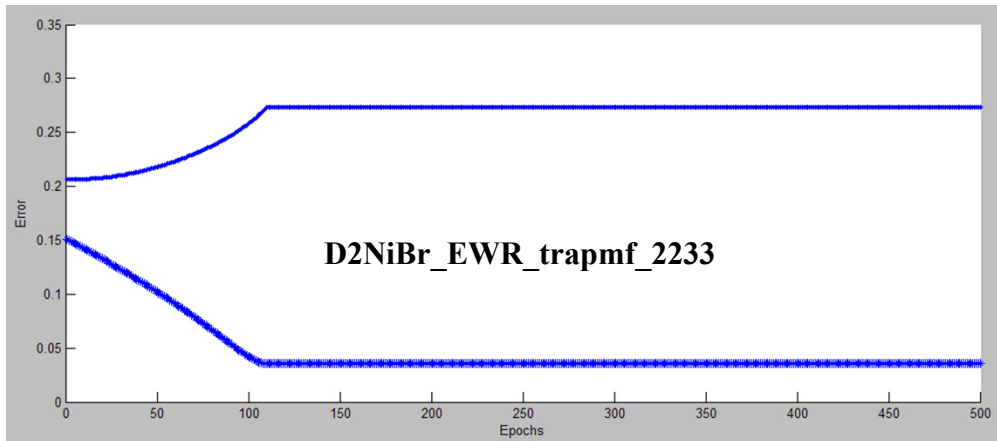
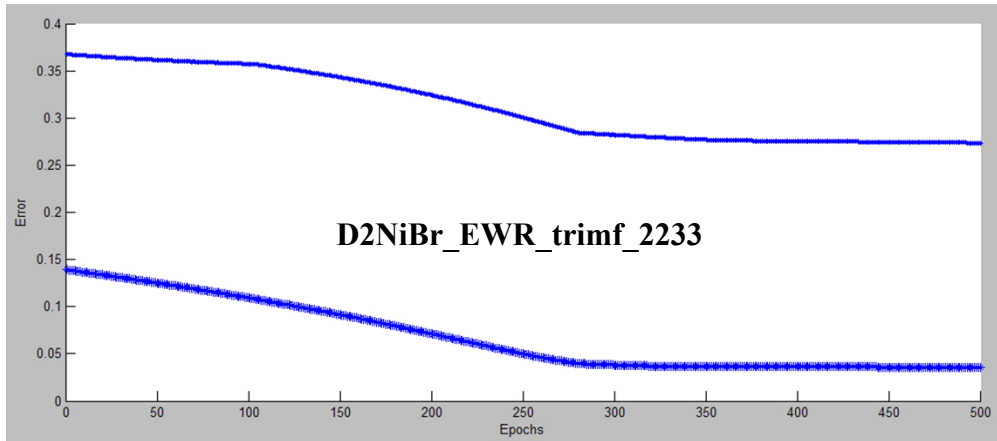
### **TRIALS FOR D2NIBR\_EWR**







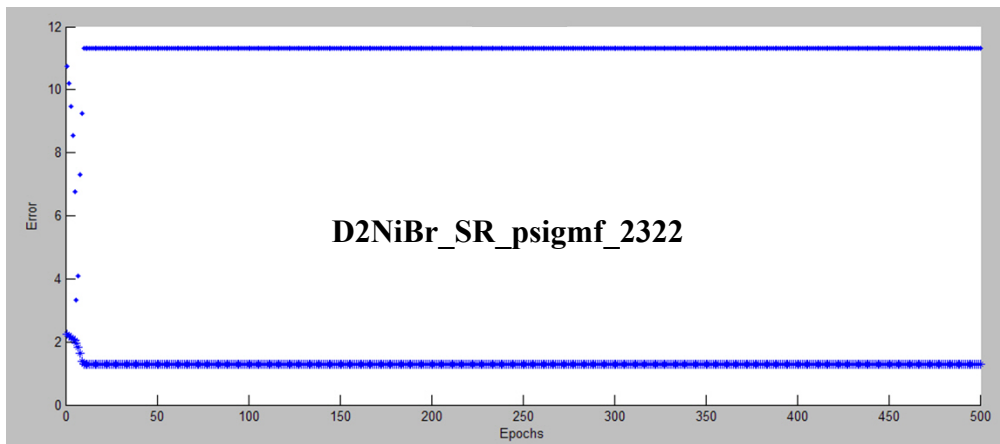
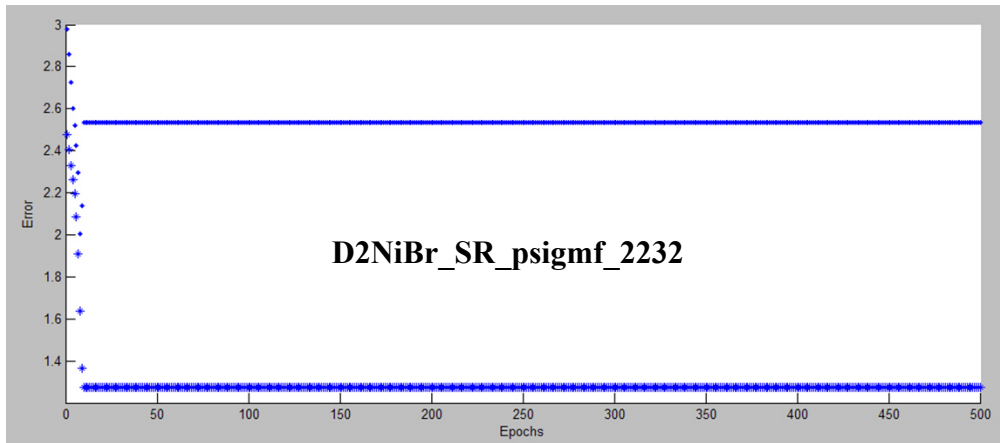
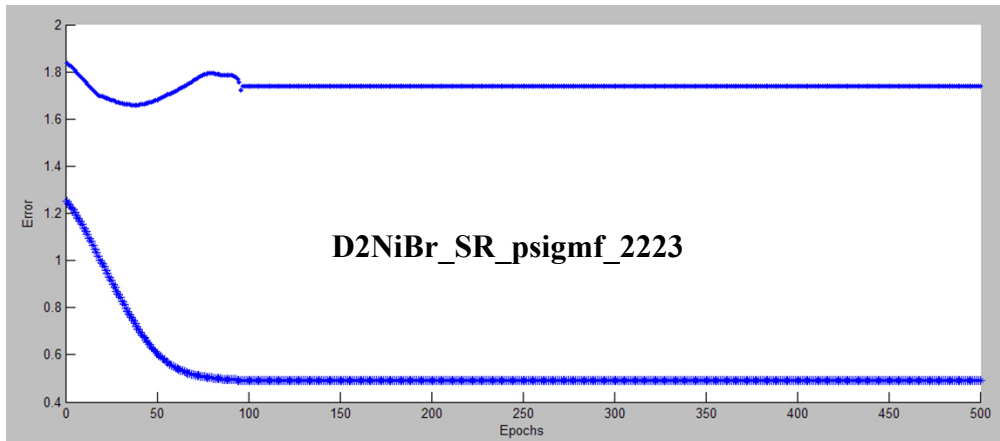
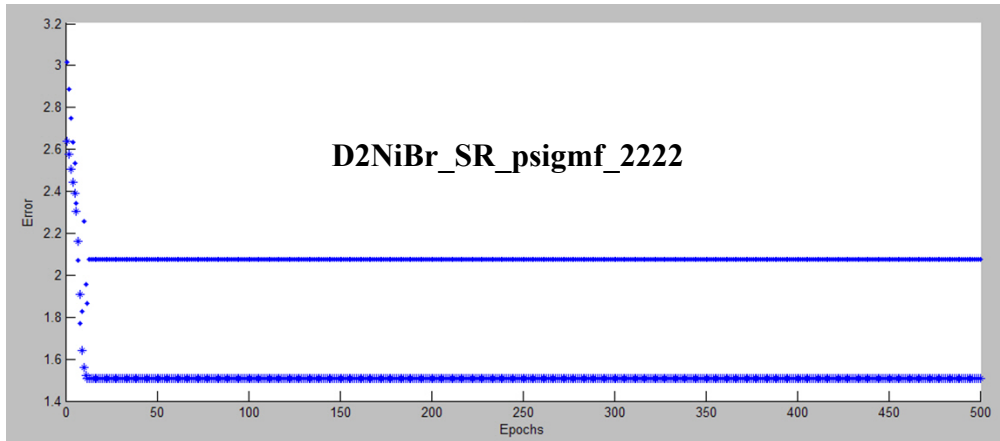


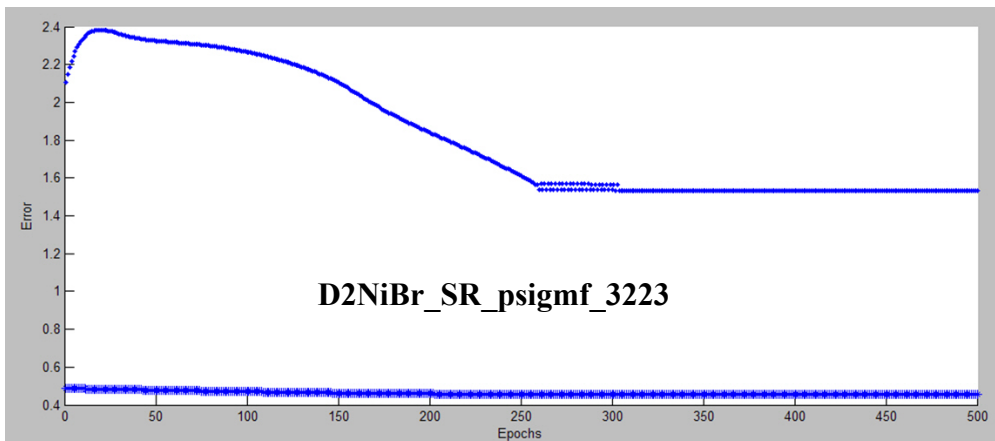
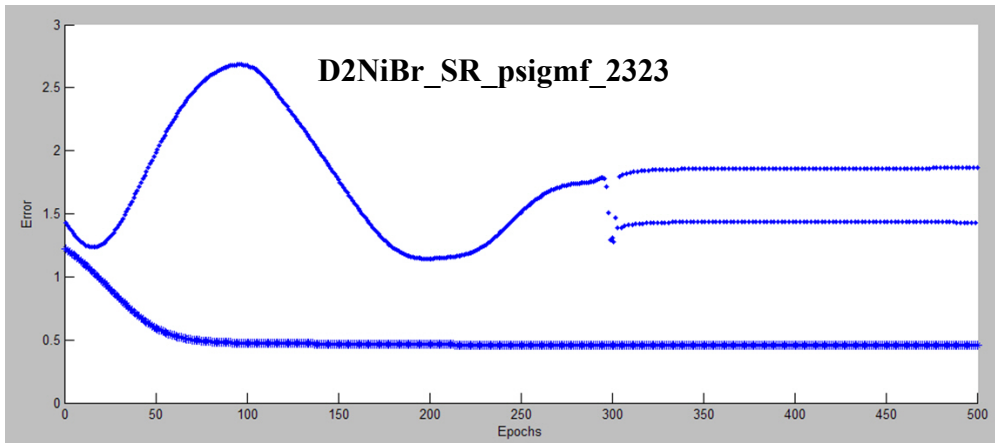
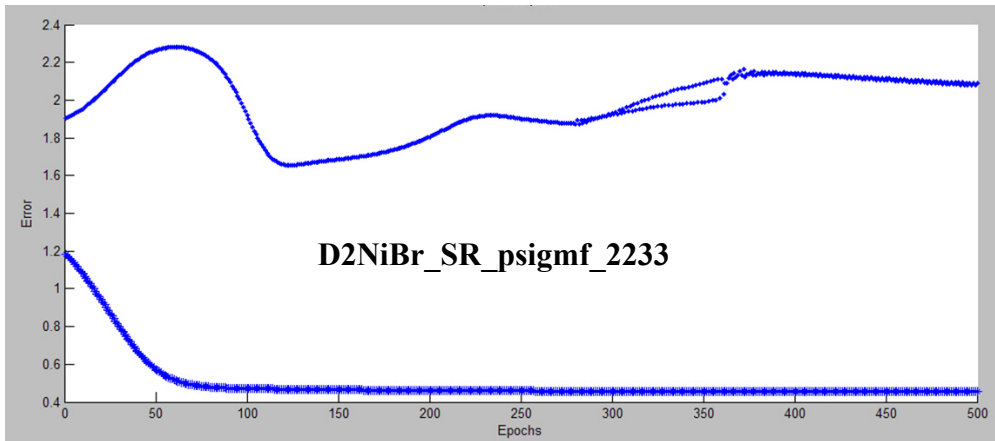
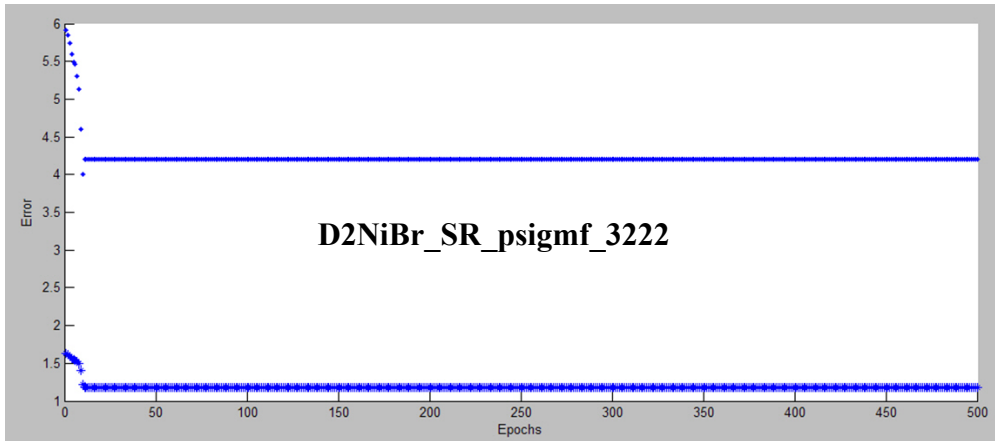


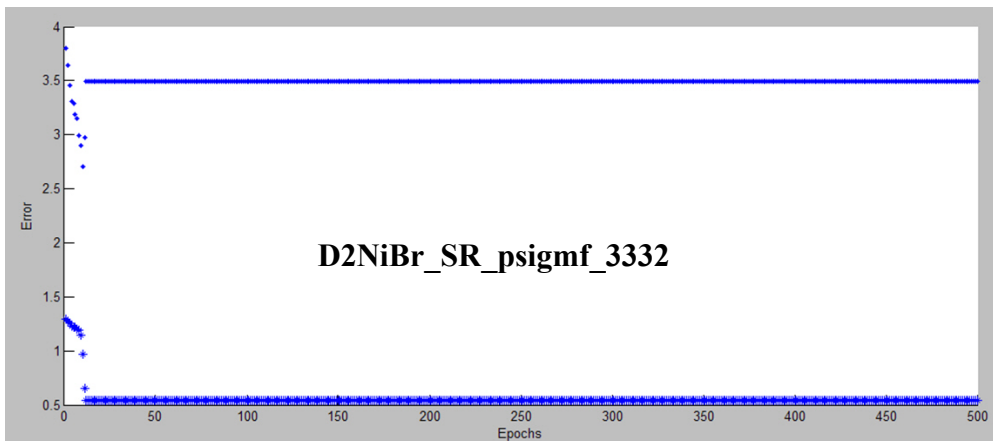
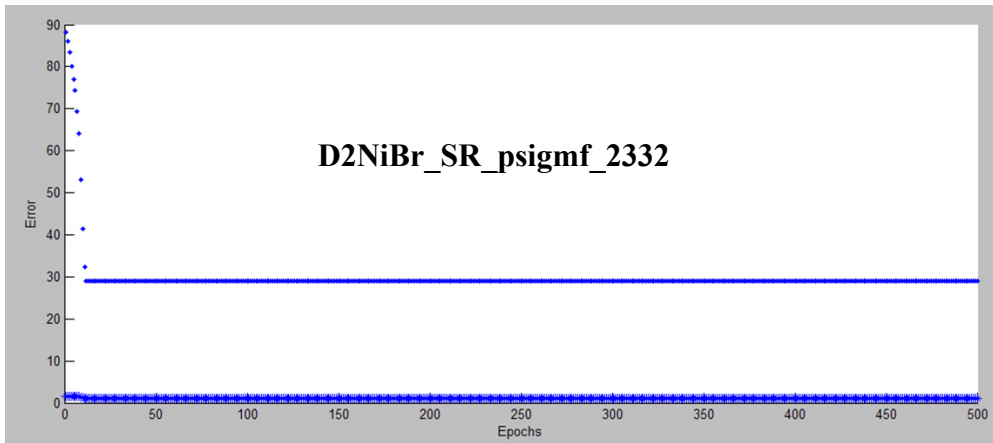
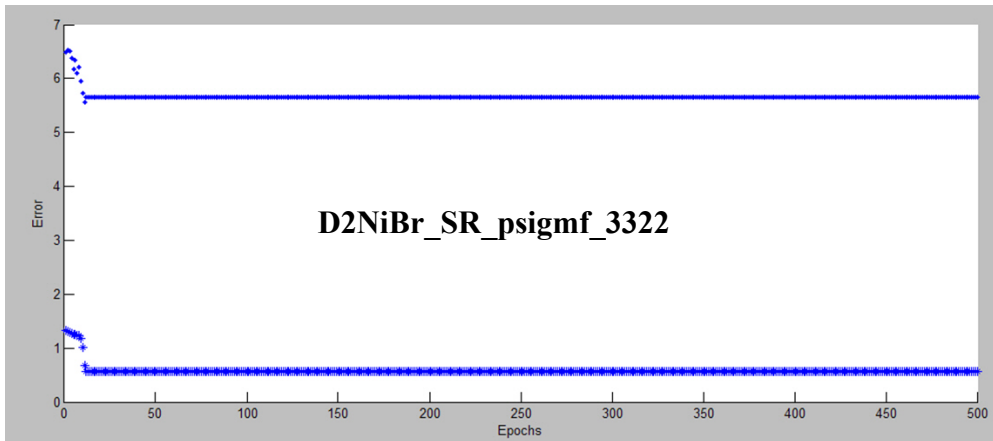
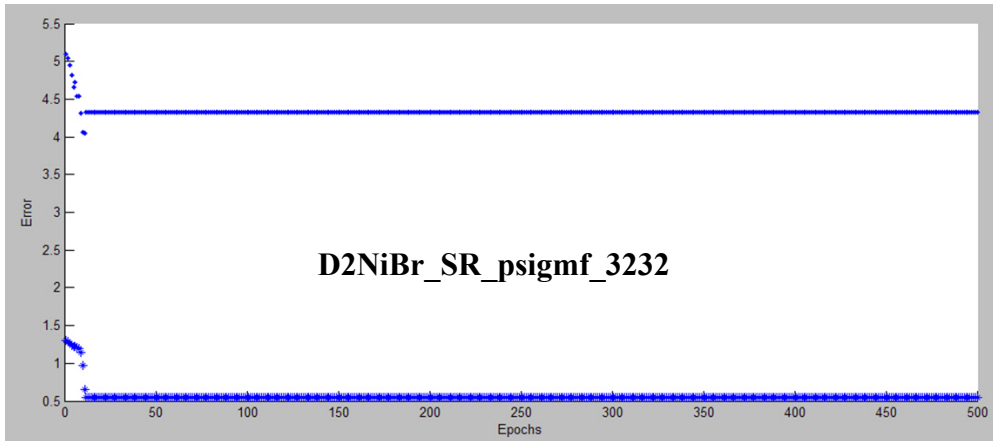
## **APPENDIX C**

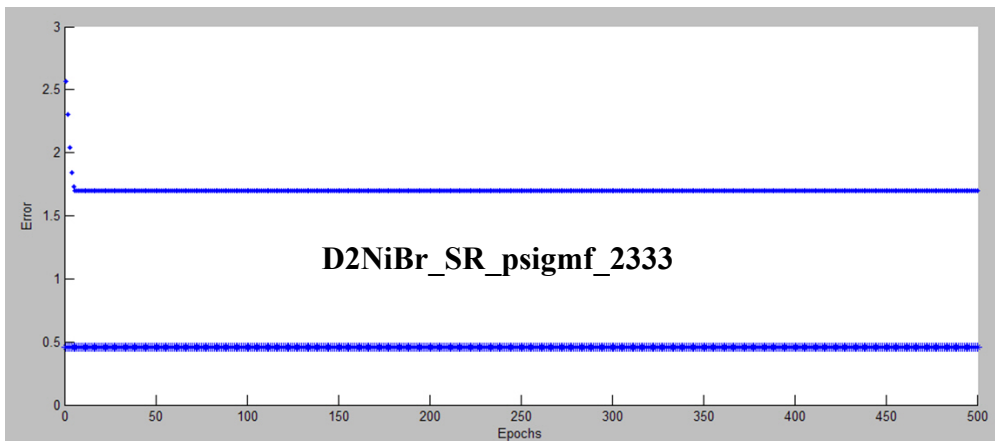
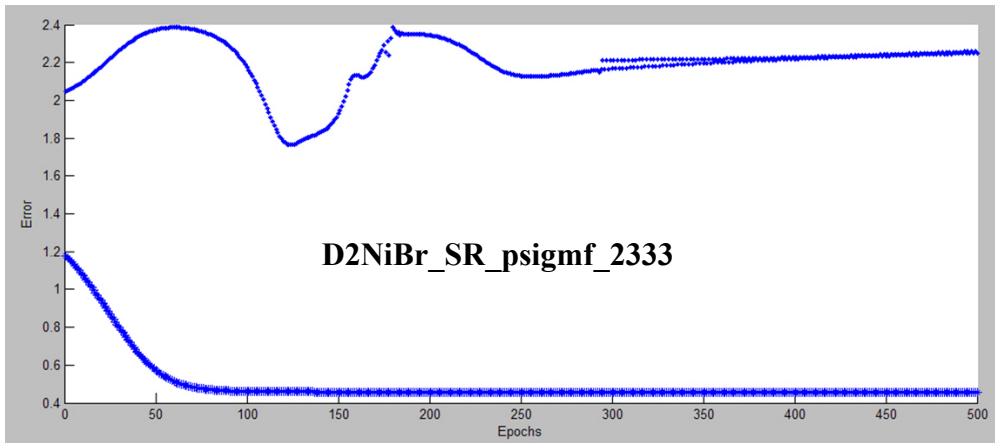
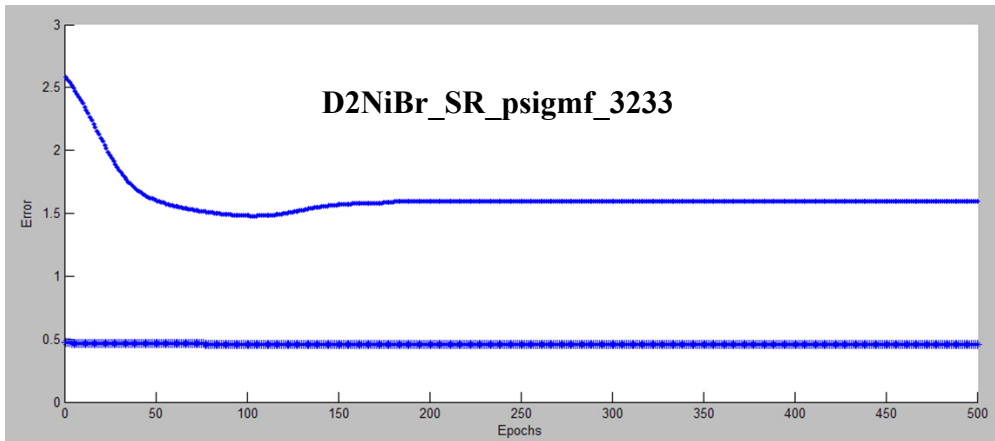
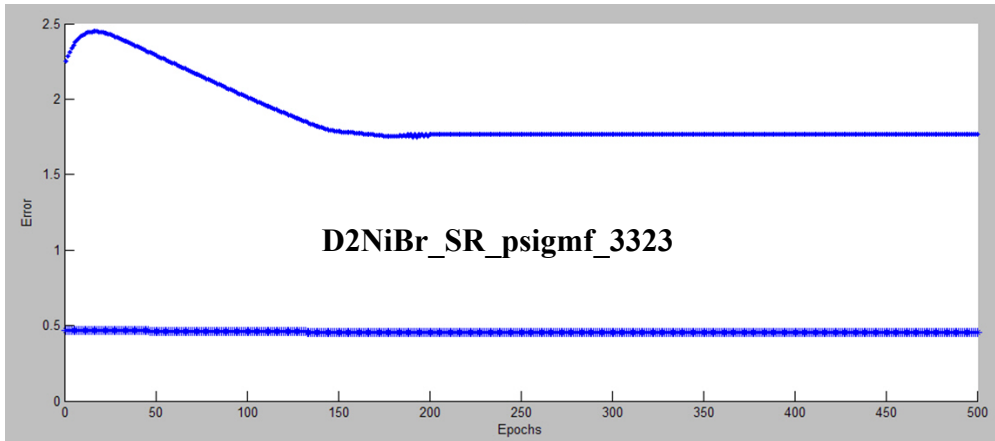
### **TRIALS FOR D2NIBR\_SR**

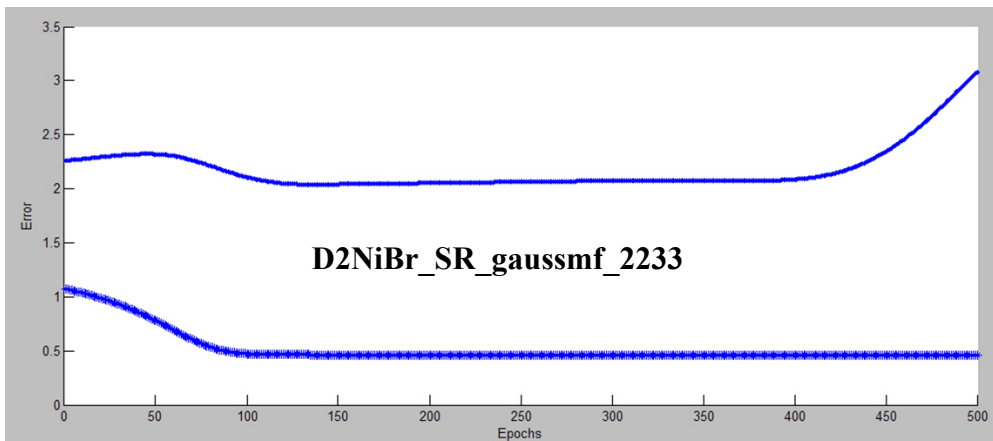
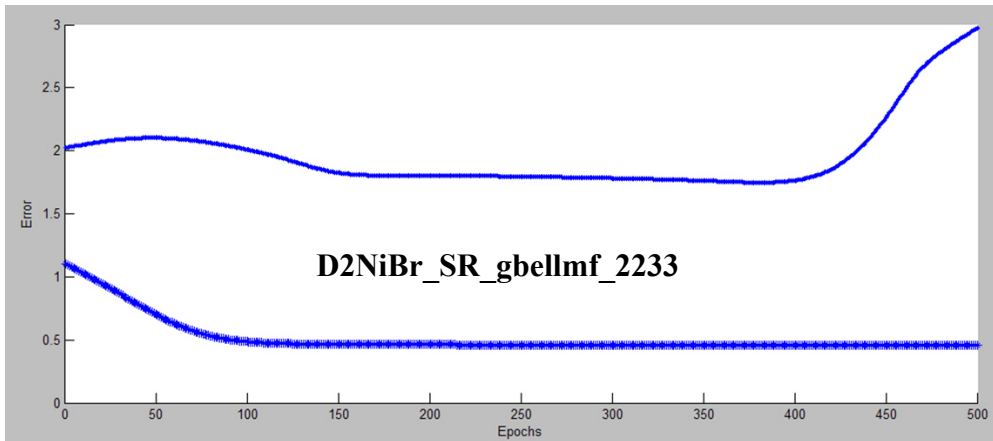
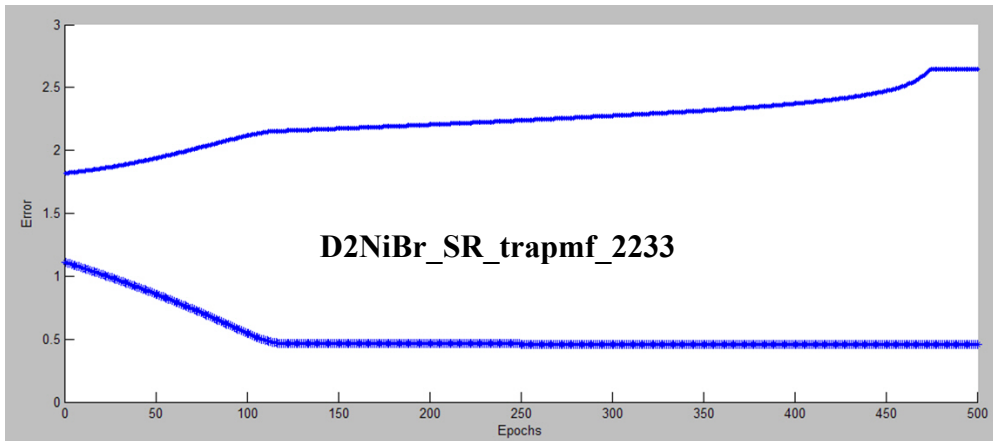
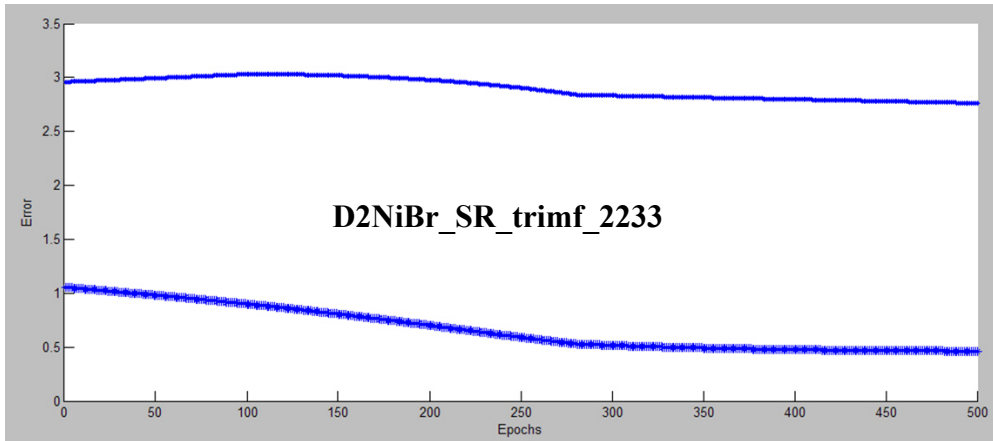










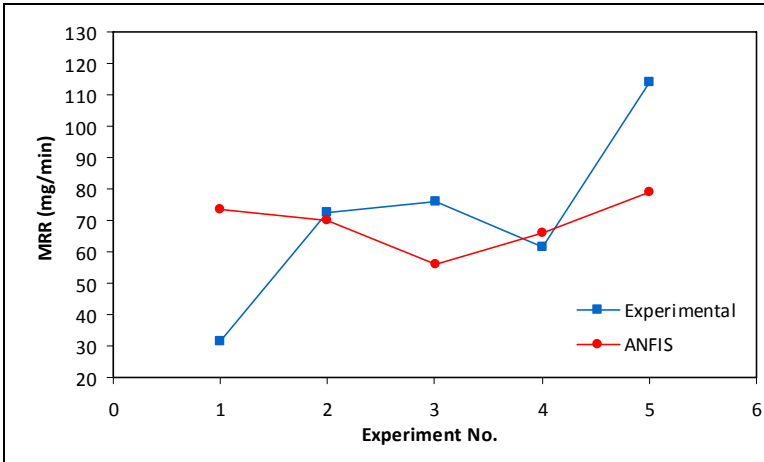


## **APPENDIX D**

### **VALIDATION RESULTS FOR OTHER ANFIS MODELS**

## D2NICU

Exp. No.	MRR (mg/min)			EWR (mm/min)			SR ( $\mu\text{m}$ )		
	Exp.	ANFIS	Error (%)	Exp.	ANFIS	Error (%)	Exp.	ANFIS	Error (%)
1	31.495	73.400	133.055	0.350	0.877	150.444	3.705	3.940	6.357
2	72.667	70.200	3.394	0.547	0.515	5.793	11.368	11.700	2.923
3	76.000	55.800	26.579	0.714	0.397	44.432	8.874	9.790	10.322
4	61.633	66.100	7.248	0.817	0.893	9.256	3.953	3.630	8.163
5	114.000	79.000	30.702	1.962	1.250	36.290	3.359	3.570	6.292
			<b>40.196</b>			<b>49.243</b>			<b>6.812</b>



### Features of ANFIS model (MRR)

Fuzzification method : Grid partitioning

MF type for inputs : psigmf

Number of input MFs : 2 2 3 3

MF type for output : constant

Total number of rules : 36

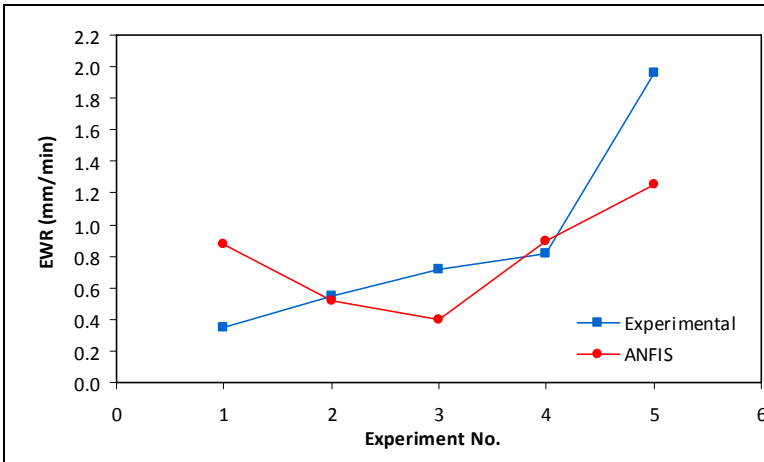
Target error tolerance : 0

Number of epochs : 100

Training error : 1.7575

Checking error : 26.1224

$R^2$  for checking data : 0.045



### Features of ANFIS model (EWR)

Fuzzification method : Grid partitioning

MF type for inputs : psigmf

Number of input MFs : 2 2 3 3

MF type for output : constant

Total number of rules : 36

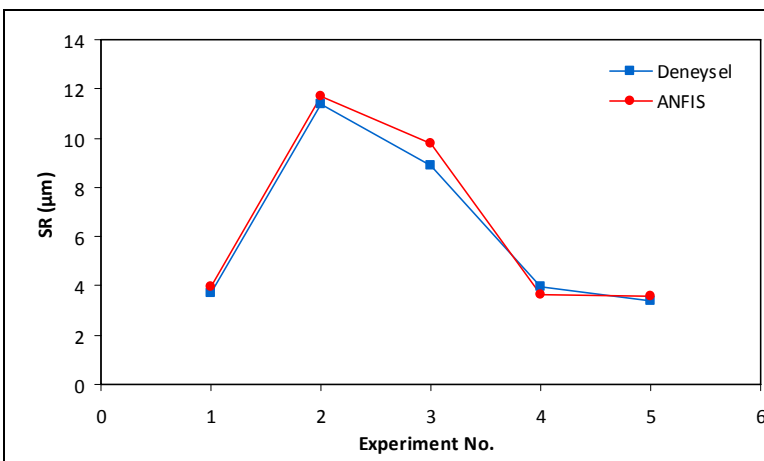
Target error tolerance : 0

Number of epochs : 150

Training error : 0.042409

Checking error : 0.44921

$R^2$  for checking data : 0.4943



### Features of ANFIS model (SR)

Fuzzification method : Grid partitioning

MF type for inputs : psigmf

Number of input MFs : 2 2 3 3

MF type for output : constant

Total number of rules : 36

Target error tolerance : 0

Number of epochs : 100

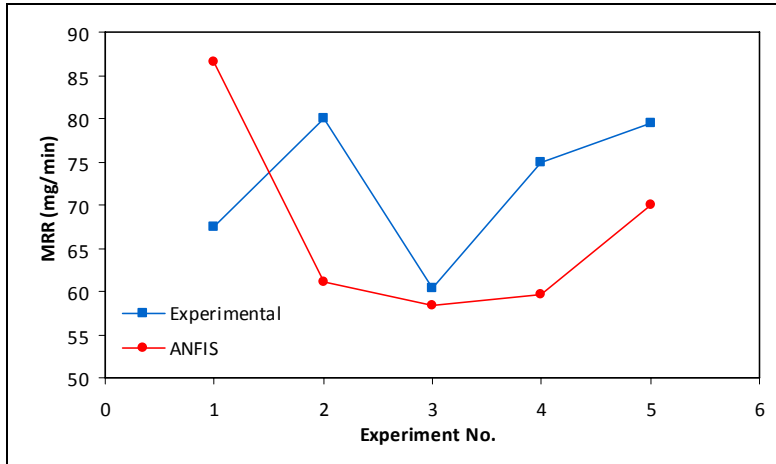
Training error : 0.25252

Checking error : 0.47658

$R^2$  for checking data : 0.9914

## D2TIBR

Exp. No.	MRR (mg/min)			EWR (mm/min)			SR ( $\mu\text{m}$ )		
	Exp.	ANFIS	Error (%)	Exp.	ANFIS	Error (%)	Exp.	ANFIS	Error (%)
1	67.500	86.600	28.296	0.604	0.727	20.331	3.705	4.970	34.155
2	80.000	61.100	23.625	0.675	0.377	44.108	11.333	13.000	14.709
3	60.300	58.300	3.317	0.273	0.403	47.619	10.320	12.500	21.120
4	75.000	59.700	20.400	0.590	0.422	28.475	2.645	3.080	16.468
5	79.500	70.000	11.950	0.668	0.665	0.375	3.204	3.710	15.805
			<b>17.518</b>			<b>28.181</b>			<b>20.451</b>



### Features of ANFIS model (MRR)

Fuzzification method : Grid partitioning

MF type for inputs : psigmf

Number of input MFs : 2 2 3 3

MF type for output : constant

Total number of rules : 36

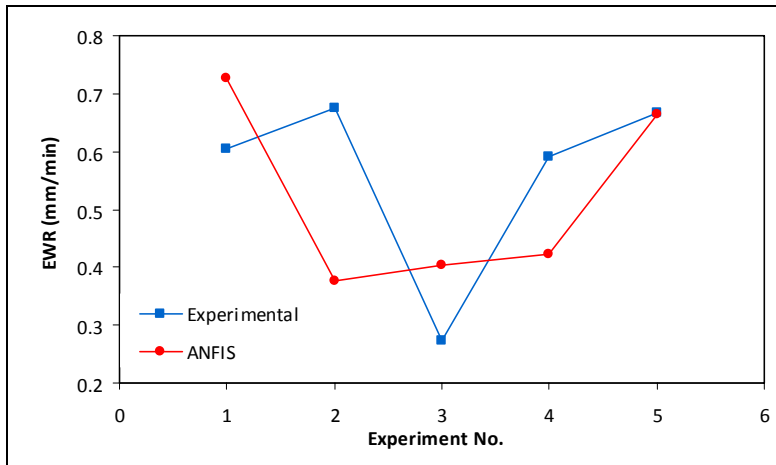
Target error tolerance : 0

Number of epochs : 40

Training error : 3.8845

Checking error : 14.5045

$R^2$  for checking data : 0.007



### Features of ANFIS model (EWR)

Fuzzification method : Grid partitioning

MF type for inputs : psigmf

Number of input MFs : 2 2 3 3

MF type for output : constant

Total number of rules : 36

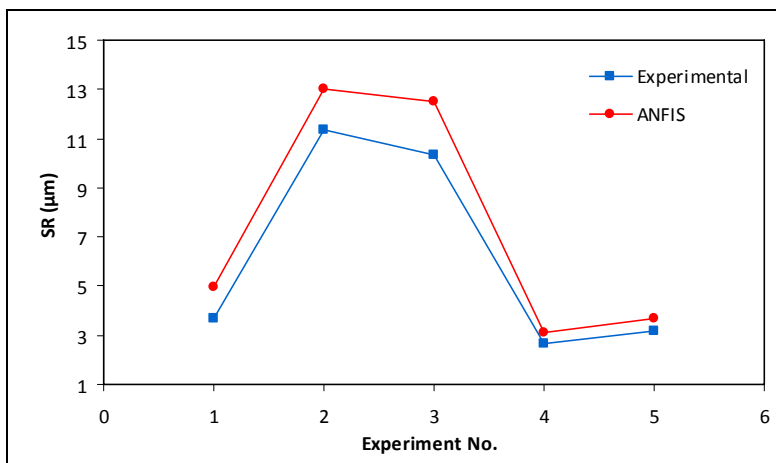
Target error tolerance : 0

Number of epochs : 40

Training error : 0.02922

Checking error : 0.17279

$R^2$  for checking data : 0.1287



### Features of ANFIS model (SR)

Fuzzification method : Grid partitioning

MF type for inputs : psigmf

Number of input MFs : 2 2 3 3

MF type for output : constant

Total number of rules : 36

Target error tolerance : 0

Number of epochs : 250

Training error : 0.4431

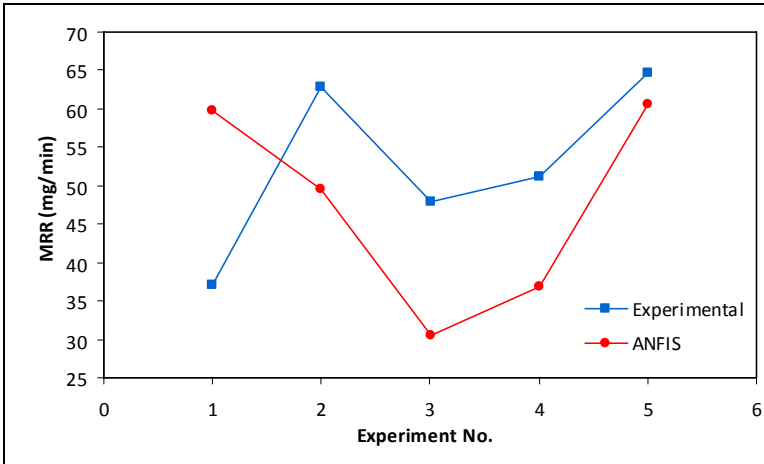
Checking error : 1.373

$R^2$  for checking data : 0.9945



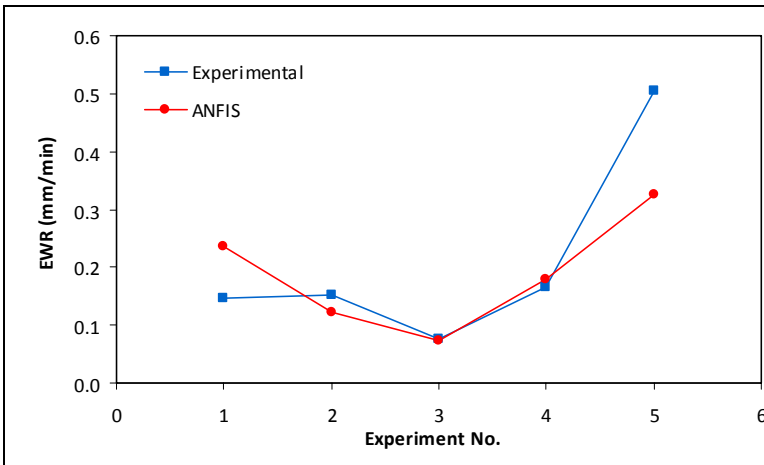
## D2TICU

Exp. No.	MRR (mg/min)			EWR (mm/min)			SR ( $\mu\text{m}$ )		
	Exp.	ANFIS	Error (%)	Exp.	ANFIS	Error (%)	Exp.	ANFIS	Error (%)
1	37.154	59.700	60.683	0.148	0.235	59.115	3.566	4.600	29.008
2	62.933	49.500	21.345	0.153	0.123	19.783	11.843	11.900	0.478
3	47.948	30.500	36.389	0.077	0.075	3.484	10.150	10.100	0.496
4	51.133	36.800	28.031	0.166	0.179	8.146	3.411	4.010	17.549
5	64.675	60.500	6.456	0.505	0.327	35.189	2.987	4.450	48.962
			<b>30.581</b>			<b>25.143</b>			<b>19.299</b>



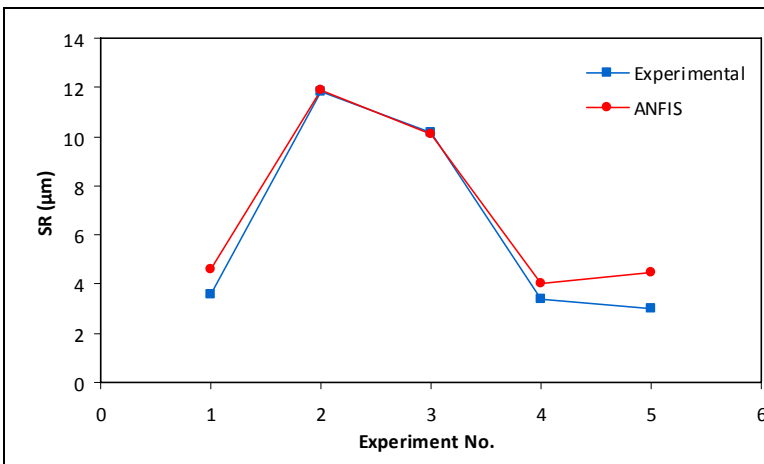
### Features of ANFIS model (MRR)

Fuzzification method : Grid partitioning  
 MF type for inputs : psigmf  
 Number of input MFs : 2 2 3 3  
 MF type for output : constant  
 Total number of rules : 36  
 Target error tolerance : 0  
 Number of epochs : 12  
 Training error : 5.3286  
 Checking error : 15.5938  
 $R^2$  for checking data : 0.0189



### Features of ANFIS model (EWR)

Fuzzification method : Grid partitioning  
 MF type for inputs : psigmf  
 Number of input MFs : 2 2 3 3  
 MF type for output : constant  
 Total number of rules : 36  
 Target error tolerance : 0  
 Number of epochs : 1  
 Training error : 0.021934  
 Checking error : 0.089948  
 $R^2$  for checking data : 0.7439



### Features of ANFIS model (SR)

Fuzzification method : Grid partitioning  
 MF type for inputs : psigmf  
 Number of input MFs : 2 2 3 3  
 MF type for output : constant  
 Total number of rules : 36  
 Target error tolerance : 0  
 Number of epochs : 70  
 Training error : 0.20612  
 Checking error : 0.84656  
 $R^2$  for checking data : 0.993